Graduate School ETD Form 9
(Revised 12/07)

PURDUE UNIVERSITY
GRADUATE SCHOOL
Thesis/Dissertation Acceptance

This is to certify that the thesis/dissertation prepared

By Kyle A. Cissell

Entitled Luminescence-Based MicroRNA Detection Methods

For the degree of Doctor of Philosophy

Is approved by the final examining committee:

Sapna K. Deo
Chair

Eric Long

Garth Simpson

Chengde Mao

To the best of my knowledge and as understood by the student in the *Research Integrity and Copyright Disclaimer (Graduate School Form 20)*, this thesis/dissertation adheres to the provisions of Purdue University's "Policy on Integrity in Research" and the use of copyrighted material.

Approved by Major Professor(s): Sapna K. Deo

Approved by: Martin J. O'Donnell Robert E. Wild 7/12/2010
Head of the Graduate Program Date

Graduate School Form 20
(Revised 1/10)

PURDUE UNIVERSITY
GRADUATE SCHOOL

Research Integrity and Copyright Disclaimer

Title of Thesis/Dissertation:
Luminescence-Based MicroRNA Detection Methods

For the degree of Doctor of Philosophy

I certify that in the preparation of this thesis, I have observed the provisions of *Purdue University Teaching, Research, and Outreach Policy on Research Misconduct (VIII.3.1)*, October 1, 2008.*

Further, I certify that this work is free of plagiarism and all materials appearing in this thesis/dissertation have been properly quoted and attributed.

I certify that all copyrighted material incorporated into this thesis/dissertation is in compliance with the United States' copyright law and that I have received written permission from the copyright owners for my use of their work, which is beyond the scope of the law. I agree to indemnify and save harmless Purdue University from any and all claims that may be asserted or that may arise from any copyright violation.

Kyle A. Cissell
Printed Name and Signature of Candidate

07/28/2010
Date (month/day/year)

*Located at http://www.purdue.edu/policies/pages/teach_res_outreach/viii_3_1.html

LUMINESCENCE-BASED MICRORNA DETECTION METHODS

A Dissertation

Submitted to the Faculty

of

Purdue University

by

Kyle A. Cissell

In Partial Fulfillment of the

Requirements for the Degree

of

Doctor of Philosophy

December, 2010

Purdue University

Indianapolis, Indiana

ACKNOWLEDGEMENTS

I would like to thank my wife for her patience, support, and most importantly her love for me during these last five years. She is my best friend and I am so proud to call her my wife. There were many times when I had to sacrifice time that would be spent with her in order to complete my work, yet she remained patient and understanding. I could not have done it without her. I would also like to thank my parents for all of their hard work to put me through school and for their support through this time. I have been so blessed with two wonderful parents. I would also like to thank my sister and brother-in-law for all of their support as well. I would like to thank my lab mates in the Deo group, for the many conversations we have had these last several years, and for the friendships that we have made as a result of our working together. I would like to thank Suresh Shrestha for helping me out immensely when I first became a graduate student, and throughout the remainder of my time in graduate school. I would like to especially thank my advisor, Prof. Sapna Deo. I am so thankful to have had such a wonderful advisor and it was an honor to have worked for her these past five years. If I had to do it all over again, I would most certainly have chosen her. She has provided me with excellent mentoring, advice on numerous subjects outside of science, as well as excellent oversight during my time in graduate school. I am grateful to have called her my advisor. I only wish so many other graduate students could have had the opportunities which I

have had. Lastly, I would like to thank the National Science Foundation, the National Institutes of Health, as well as the IUPUI School of Science for their monetary support.

TABLE OF CONTENTS

Page

Page

LIST OF TABLES

LIST OF FIGURES

Figure Page

Figure Page

LIST OF ABBREVIATIONS

Abbreviation	Proper Name
miRNA	microRNA
siRNA	small interfering RNA
Rluc	*Renilla* luciferase
Ctz	coelenterazine
CV	coefficient of variation
µmoles	micromoles
nmoles	nanomoles
pmoles	picomoles
fmoles	femtomoles
µM	micromolar
nM	nanomolar
pM	picomolar
fM	femtomolar
PCR	polymerase chain reaction
BRET	bioluminescence resonance energy transfer
FRET	fluorescence resonance energy transfer
QD	quantum dot

ABSTRACT

Cissell, Kyle A. Ph.D., Purdue, December, 2010. Luminescence-Based MicroRNA Detection Methods. Major Professor: Sapna K. Deo.

MicroRNAs (miRNA) are short, 18-24 nucleotide long noncoding RNAs. These small RNAs, which are initially transcribed in the nucleus, are transported into the cell cytoplasm where they regulate protein translation either through direct cleavage of mRNA, or indirect inhibition through binding to mRNA and disrupting the protein translation machinery. Recently, miRNAs have gained much attention due to their implication in numerous diseases and cancers. It has been found that heightened or lowered levels of miRNA in diseased cells vs. healthy cells are linked to disease progression. It is therefore immensely important to be able to detect these small molecules. Current detection methods of Northern blotting, microarrays, and qRT-PCR suffer from drawbacks including low sensitivity, a lack of simplicity, being semi-quantitative in nature, time-consuming, and requiring expensive instruments. This work aims to develop novel miRNA technologies which will address these above problems. Bioluminescent labels are promising alternatives to current methods of miRNA detection. Bioluminescent labels are relatively small, similar in size to fluorescent proteins, and they emit very intense signals upon binding to their substrate. Bioluminescent labels are advantageous to fluorescent labels in that they do not require an external excitation

source, rather, the excitation energy is supplied through a biochemical reaction. Therefore, background signal due to excitation is eliminated. They also have the advantage of being produced in large amounts through bacterial expression.

Four miRNA detection methods are presented which utilize luminescence-based methods. Three employ *Renilla* luciferase, a bioluminescent protein, and one is based on fluorescence. The presented methods are capable of detecting miRNA from the picomole (nanomolar) level down to the femtomole (picomolar) level. These methods are rapid, sensitive, simple, and quantitative, can be employed in complex matrices, and do not require expensive instruments. All methods are hybridization-based and do not require amplification steps.

CHAPTER 1: MICRORNA INTRODUCTION

1.1 Opening Remarks

Few discoveries have had such a large impact on all of science as microRNA has. MicroRNAs (miRNA) are 18-24 nucleotide non-coding RNA molecules involved in RNA interference which regulates protein translation. Within the past few years, miRNA research programs have flourished because of results that were discovered in the laboratory of Dr. V. Ambros at Dartmouth Medical School, where the developmental gene pathway of soil nematode *C. elegans* was being studied. While performing these studies, the researchers discovered that the gene *lin-14* was negatively regulated by the gene *lin-4*, which encoded two small non-coding strands of RNA, one 22 nucleotides and the other, 61 nucleotides [1]. Both *lin-14* and *lin-4* control larval development, and have recently been shown to regulate the life-span of *C. elegans* [2]. The 61 nucleotide strand was predicted to fold into a stem-loop structure believed to be the precursor of the smaller 22 nucleotide strand. This discovery at the time was viewed as an anomaly, unlikely to occur frequently in nature. Less than a decade later, however, another non-coding small RNA molecule was discovered, again in the developmental studies of *C. elegans* [3]. Here, Ruvkun and colleagues discovered that this small, noncoding RNA molecule encoded by the gene *let-7* regulated the transcription of *lin-14*. The discovery of the regulatory gene *let-7* sparked the recent boom in miRNA research. Soon after the

discovery of *let-7,* over one hundred new genes for noncoding small RNAs (miRNAs) were discovered in humans, worms, and *Drosophila* [4-6].

Gene regulation by miRNAs plays a role in cell proliferation, cell death, and tumorigenesis, as well as mammalian cell development [7, 8]. There are thousands of published miRNA sequences located on miRBase [9, 10], a database for miRNAs. Many of these miRNA sequences overlap from species to species; however, there are numerous unique sequences accounted for in nature. The importance of miRNA and its role in gene interference cannot be stressed enough, especially since the 2006 Nobel Prize in Medicine was awarded to Andrew Fire and Craig Mello for their work in RNA interference, in which miRNA plays a vital role. MicroRNA raises questions as to the actual function of genes, in particular, the purpose of noncoding strands of RNA encoded from genes. It has long been thought that most RNA code for the translation of proteins. Could it be possible that there is more to RNA than previously speculated? In fact, a significant amount of RNA in a cell does not code for the translation of protein, rather it regulates gene expression. For example, it has been found that of the 62% of the mouse genome that is transcribed, approximately one-half of the RNA is noncoded [11, 12].

1.2 miRNA Biogenesis

MiRNA biogenesis originates in the nucleus and eventually results in mature miRNA in the cytoplasm (Figure 1.1). Before mature miRNA is formed, primary miRNA (pri-miRNA), a long strand of RNA containing stem-loop structures (up to 1kb in length), is initially transcribed by RNA polymerase II [13], and further excised by the endonuclease Drosha [14]. After excision, the former pri-miRNA, termed pre-miRNA, is exported to the

cytoplasm by the RNA-binding protein Ran-GTP and the exporter receptor Exportin-5 [15-18]. This pre-miRNA consists of a long stem of approximately 25-30 bp along with a small loop structure. After the pre-miRNA is released from the Exp-5, it is cleaved by an RNase III enzyme known as Dicer, to generate mature miRNA. The mature miRNA is further incorporated with the RNA-induced silencing complex (RISC), consisting of proteins from the argonaute family [19], by which the miRNA anneals to the 3' untranslated region of its complementary target messenger RNA (mRNA) [20, 21]. Once bound to the target mRNA, the miRNA can induce cleavage of the mRNA, regulating protein translation directly, or regulating translation indirectly through remaining bound to the mRNA. Due to the similarities between siRNA, miRNA and piwiRNA, it is important to differentiate between each of these small RNAs. While all three are nearly the same length, they are processed differently in the cell. All three are generated by RNase enzymes Dicer and Drosha. The cleavage of exogenous long dsDNA precursors in response to viral infections or artificial introduction generates small interfering RNAs (siRNAs), whereas the processing of genome-encoded stem-loop structures generates miRNAs. A recently uncovered class of small RNAs called PIWI-interacting RNAs (piRNAs) are slightly longer than miRNAs (~26-31 nt) [22]. The proteins required for this pathway are unknown but it is known that the piRNAs function to silence transposons through a complex amplification process that can even modify histones and carry out DNA methylation [23]. Recently, siRNA has found much utility in therapeutics. There have been numerous examples in medical literature in which siRNAs are delivered to diseased cells. Due to the high RNAse activity in serum, great care must be used to avoid siRNA degradation prior to delivery.

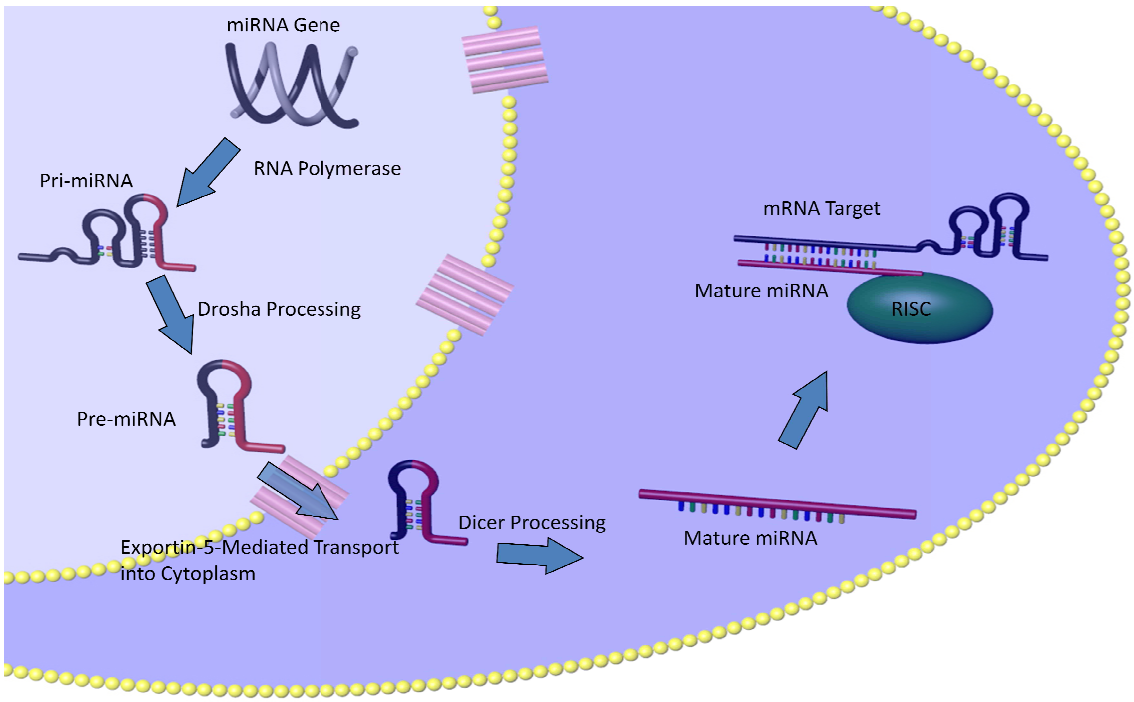

Figure 1.1 miRNA biogenesis. miRNA is initially encoded in genomic DNA. It undergoes transcription, followed by a series of processing steps to produce mature miRNA, which binds to mRNA, inhibiting protein translation. Reprinted with permission from Reference 54. Copyright 2007 American Chemical Society.

Numerous delivery methods have been employed, including liposomal [24], nanoparticle [25], carbon nanotube [26], viral delivery [27], as well as direct injection to target organs. These delivered siRNAs accomplish the task of regulating protein translation through binding to key genes. While siRNA delivery is beyond the scope of this thesis, it is worth introducing due to its important role in therapeutics.

1.3 miRNA Implications in Disease

MicroRNA has been implicated in multiple diseases, including cancer. It can be found freely circulating in bodily fluids such as serum [28], urine [29], sputum [30] and saliva [31].

The utility of circulating miRNA as cancer biomarkers, therefore would be highly advantageous in terms of developing rapid diagnostic tools. Although nascent RNA is unstable in serum due to the very high RNAse activity, miRNA displays remarkable stability, suggesting that miRNA is somehow protected. It has been hypothesized that serum RNA is protected via protein or liposomal encapsulation [32]. It is possible that miRNA is protected in this manner as well. Most likely, miRNA does not freely circulate in serum as naked single-stranded small length RNA.

As the study of miRNA increases, more and more researchers are finding links between miRNA expression levels (the amount of miRNA in the cells), and the onset of cancer and other diseases [33]. Numerous studies have found that miRNA expression levels are increased (upregulated) or decreased (downregulated) in cancer cells. For example, miR-15a and miR-16-1 are downregulated in B-cell chronic lymphocytic leukemia [34]; miR-143 and miR-145 are downregulated in breast, prostate, cervical, and lymphoid cancer cells [35]; while miR-21, miR-373, and miR-520c are upregulated in breast cancer cells [36, 37] and miR-184 is upregulated in prostate cancer cells [38]. There are certainly hundreds more miRNAs which are linked to cancer and the list grows larger as more and more studies are performed. Along with cancer, miRNAs have been shown to play an important role in cardiovascular disease. Hammond and colleagues have found that in the presence of mutated Dicer, the enzyme which cuts pre-miRNA into mature miRNA, the miRNA which is necessary for cardiovascular health cannot be processed. This ultimately results in progressive dilated cardiomyopathy, which leads to heart failure, and eventually death [39]. Due to the significance of miRNA in disease, it is necessary to develop miRNA-based therapeutic methods. Overall, miRNAs are related to several diseases including

neurological [40], cardiovascular [41], cancer, and immunological [42]. Due to their widespread gene regulation and their affects on human health, miRNAs have garnered much attention in the biomedical field.

1.4 miRNAs and Their Applications in Therapeutics

Due to the increasing correlation of miRNA levels with diseases, it is necessary to explore various therapeutic options for miRNA function inhibition or delivery of miRNA in cells where the onset of disease may occur if miRNA level(s) are downregulated. In order to accomplish these tasks, miRNAs must be comparatively studied in both healthy and unhealthy cells. Once a miRNA has been determined to be a viable biomarker, it will be necessary to explore options on how to counteract the disease linked to the specific miRNA or miRNAs. If the miRNA levels are too high, a few options to tackle this problem may be used. Anti-sense oligonucleotides which hybridize with the miRNA can be introduced, preventing the target miRNA from hybridizing with the 3' UTR of the mRNA. By doing this, it is conceivable that aberrant gene regulation will not occur from the target miRNA. A more efficient method to design antisense miRNA is to employ locked nucleic acid (LNA) probes instead of DNA oligonucleotide probes. LNAs contain a 2'-O-4'C methylene bridge on the furanose ring which results in a more rigid double-stranded nucleic acid structure that is more thermally stable as well. This could prevent the dissociation of the hybrid between target miRNA and antisense miRNA. Also, it has been found that antagomirs, anti-sense oligonucleotides which were conjugated to cholesterol to aid in cellular delivery, may be beneficial therapeutic agents for tumors or other diseased cells. In a study by Krutzfeldt and colleagues, it was determined that

cholesterol-modified antagomirs injected into mice inhibit miRNA activity [43]. For over-expressed miRNAs which lead to tumor growth, the delivery of antagomirs or antisense LNA probes, coupled with delivery of miRNAs which lead to tumor suppression are ideal. Lentivirally expressed antagomirs have also been employed for repression of miR18a, miR19b, and miR20a [44]. It is also possible to transfect cells with miRNA in order to inhibit protein translation, rather than to promote protein translation. For example, *let-7* miRNA transfection has been shown to reduce tumor growth in cancer cells [45-47]. Introduction of microRNA miR16 reduces tumor growth in prostate cancer cells [48]. In order to deliver the therapeutic agents, non-invasive delivery is desired, such as liposomal delivery. Recently, single-walled carbon nanotube (SWNT) delivery based on endocytosis has shown promise as a drug delivery alternative [49]. SWNTs have already been shown to deliver siRNA to cells [50, 51], and thus can be applied to miRNA delivery as well. Additionally, the toxicity of SWNT can be substantially decreased by using smaller-length SWNTs which are expelled quickly after use in the urine [52]. Before these therapeutic methods may be used on humans, much research needs to be performed regarding miRNA levels in healthy vs. unhealthy cells to assure that addition of antagomirs and/or miRNAs will not cause harm in the body by inhibiting or promoting expression of proteins which can result in the onset of a different type of disease. While therapeutics is a fascinating facet of miRNA research, they are not the focus of this work.

1.5 Standard miRNA Detection Methods

There are currently multiple miRNA detection methods presented in literature, most of which are based upon hybridization. Mostly all detection methods rely on an

optical label in order to translate the hybridization event into a measureable signal. There are, however, label-free methods such as those employing Raman spectroscopy. In one particular example, silver nanorods are immobilized on a substrate [53]. The target nucleic acids are then adsorbed to the nanorods, resulting in a Raman signal that is sequence-specific. Through measuring the peaks of known oligonucleotides, it is possible to discern the sequence of small RNAs present in a sample. Apart from the small number of label-free examples, most miRNA detection methods are based upon hybridization [54, 55], although this underlying method can be broken down into the following categories: Polymerase chain reaction (PCR)-based methods, blotting methods, microarray-based methods, flow cytometry, and emerging new analytical methods. No matter what the detection method, each assay must have a way to produce a signal upon hybridization; that is, a transducer must be present in order to translate the hybridization event into a measurable signal.

PCR methods utilize the annealing and extension events of complementary primer oligonucleotides to detect miRNA through amplification of miRNA present in the sample. In miRNA profiling, quantitative reverse transcription PCR (qRT-PCR) is widely used due to its ability to quantitate miRNA copy numbers and its high specificity. In this method, reverse transcriptase converts RNA into DNA through the presence of an RT-PCR miRNA-specific primer to form a cDNA library. This cDNA and forward and reverse PCR primers are employed to amplify the cDNA. Because of the small length of the miRNA oligonucleotides, the primer oligonucleotide must also be short in length. This small length primer, with a low melting temperature, can have adverse effects on the efficiency of the polymerase chain reaction. This problem can be combated by detecting

miRNA precursors rather than mature miRNA [56]; however, pre-miRNA may not be homologous with the mature miRNA levels in the cell. Therefore, primer design and small RNA extraction is critical in order to not amplify non-specific regions of RNA.

There are several commercially available kits which employ RT-PCR to detect miRNA. Among them are the miR-Vana kit available from Ambion [57] and the miRCURY LNA PCR kit from Exiqon, both of which employ SYBR green; and the TaqMan probe assay from Applied Biosystems. In the miRCURY kit, cDNA is created through reverse transcription, followed by PCR amplification. During each amplification, SYBR green, a fluorescent dye which has an affinity for the minor groove of dsDNA, becomes highly fluorescent upon binding to dsDNA. This increase in fluorescence can be quantified and the actual amount of miRNA correlated. In the case of the TaqMan probe, upon cDNA formation, PCR primers are added, along with a hairpin probe containing a fluorophore and quencher which binds to a region downstream of the primer extension. The polymerase, upon contacting the hairpin probe, cleaves the fluorophore, resulting in an increase in fluorescence. The resulting fluorescence intensity can be employed to determine the initial miRNA concentration.

Another widely used miRNA detection method is Northern blotting [3, 5, 34, 58]. In Northern blotting, a complementary labeled oligonucleotide probe binds to a target miRNA captured on a nitrocellulose membrane. This method is time-consuming, often taking days for completion; however, it is considered the gold standard for miRNA detection and validation. A complication is that blotting methods are not sensitive and thus require large amounts of sample (~10-30 μg) for miRNA detection and possess detection limits in the nanomolar range. This sensitivity problem has been minimized

with the addition of locked nucleic acids (LNAs) to the probe sequence, increasing the detection sensitivity 10-fold compared to normal RNA or DNA oligonucleotides [59]. Although PCR and Northern blotting are important tools for miRNA detection, it is of interest to explore simpler, faster, and more sensitive detection methods.

Microarray technology has become an important tool for scientists working on genome analysis. Microarrays are being utilized more and more by scientists seeking ways to decrease sample volume, test multiple samples simultaneously, and decrease assay time. The miRNA microarray chips can contain an array of immobilized oligonucleotide probes which are complementary to a cDNA sequence which is reverse transcribed from mature miRNA. These cDNA probes are labeled with a signal transducer, such as Cy 3, Cy 5, or biotin, to characterize the hybridization event. In some cases, the signal transducer may directly be conjugated to the miRNA present in the sample. The target is then added to each well, followed by wash steps to remove unhybridized molecules. Each well produces a particular color upon staining or yield fluorescence signals. The intensity of these colors or fluorescence is measured to determine the amount of hybridized miRNA in a sample well. Perhaps the greatest advantage of the microarray platform over other detection methods is its high-throughput-screening capability. Due to this advantage, microarrays are widely utilized to characterize the expression profiles of miRNA [60-63]. Although the cost of microarray technology is front-loaded with overhead from the robotics needed for fabrication, in the long run, microarrays are cost-effective in large laboratory settings where thousands of samples are screened daily. However, this is not suitable for small research laboratories. Microarrays have other drawbacks along with their high cost, including low sensitivity

due to minimal sample volume, and the possibility of cross-hybridization, which may occur when samples differ by only one base.

There have been many cited articles utilizing microarrays in the detection and profiling of miRNA [61, 64-67]. In one example, Croce and colleagues designed a microarray for profiling 245 miRNAs from humans, mice, and *Arabidopsis* [68]. In this article, the authors genetically modified target miRNA by reacting it with biotin-containing primers. The biotin-containing target was allowed to hybridize with solid-phase oligonucleotides representing the 245 different miRNA sequences. After wash steps to remove unbound miRNA, the hybridized probes were reacted with streptavidin-Alexa 647 conjugate. The affinity of the biotin-streptavidin conjugate allows the Alexa 647 dye to serve as the signal transducer, detecting hybridization. Fluorescence measurements determined the intensity of each well in order to characterize the expression profile of the target miRNA. This method showed that only 2.5 μg of total RNA sample is needed to detect miRNA compared to ~10 μg for Northern blotting. Multiple other examples of miRNA profiling through microarrays exist in literature. Too many are present to reference here, although perhaps the greatest achievement of microarray profiling of miRNAs is the strong predictions which can be made concerning tumor formation. It has been found that in patient samples with certain types of tumors, expression profiles reveal numerous dysregulated miRNAs. For example, in patient serum with small cell lung carcinoma, the miRNAs miR233 and miR25 are significantly upregulated. In breast cancer patients, the microRNA miR21 is highly upregulated.

Flow cytometry is also another method for miRNA analysis. In flow cytometry-based methods, a sample is hydro-dynamically focused in a sheathing liquid to produce a

narrow stream which allows only one particle through the stream at a time. A laser is focused on this stream with detectors placed along the stream to detect any laser-induced fluorescence. Spikes in fluorescence are indications that the target fluorophore has passed through the flow cell. In terms of miRNA detection, complementary oligonucleotides capture amplified, labeled target, and depending on the fluorophores which are used to modify the targets, the amount of miRNA in a sample can be determined. Recently, a bead-based flow cytometry method has been performed to profile 217 miRNAs [69]. More specifically, complementary oligonucleotide capture probes were coupled with polystyrene beads, which were made up of characteristic fluorescent molecules to produce spectrally distinct polystyrene beads. Each color corresponded to a specific miRNA. In order to determine miRNA abundance, miRNAs were PCR-amplified using a biotinylated primer, hybridized with the complementary oligonucleotide-labeled beads, and stained with streptavidin-phycoerythrin. Parallel experiments with a microarray format revealed that the bead-based flow cytometry method showed increased specificity for single nucleotide mismatches compared to the microarray.

While the previously mentioned methods have been widely used, drawbacks exist for each method. Northern blotting is very time consuming and only qualitative. Microarrays, although capable of high-throughput screening, are very costly and suffer from difficulties with specificity. PCR-based methods require amplification of target, increasing the total number of steps involved in detection. Flow cytometry requires highly expensive equipment and amplification of target, increasing the total assay time. Therefore, methods for miRNA detection are needed which are rapid, do not require amplification of target, are highly sensitive and quantitative, do not require expensive

equipment, and are highly specific. New and emerging methods which address the previously stated drawbacks are described next.

1.6 Overview of New and Emerging Methods of miRNA Detection

Numerous methods have been developed which seek to overcome the drawbacks mentioned above associated with Northern blotting, microarrays, qRT-PCR, and flow cytometry. These new methods employ electrochemical, luminescence-based, and other optical methods of detection. Table 1.1 summarizes the methods of microRNA detection mentioned in this chapter. To overcome the low sensitivity of the above methods, labels such as quantum dots and gold nanoparticles have been evaluated by Ruan and colleagues [70]. In this method, isolated miRNA is oxidized to convert the 3' terminal hydroxyls on the ribose ring into a dialdehyde. The dialdehyde reacts with a biotin-X-hydrazide via condensation to biotinylate the target miRNA (Figure 1.2A). The biotinylated sample miRNA is added to the immobilized capture probe. After a wash step, hybridization is detected using a streptavidin-quantum dot conjugate (Figure 1.2B). When the hybridized probes are excited with light, the quantum dots will fluoresce. This fluorescence, resulting from the hybridization, may be detected with a laser confocal scanner. This method produces a lower detection limit of approximately 0.4 fmoles, much lower than Northern blotting methods.

Table 1.1 Standard and emerging miRNA detection methods

Method	Assay Description	Detection Limit	Reference (s)
Northern blotting	Transfer of miRNA onto nitrocellulose membrane, followed by washing with labeled complementary probe	~nM	3, 5, 34, 58
qRT-PCR	Reverse transcription of miRNA target, followed by real-time PCR detected through fluorescence	aM	57
microarray	Reverse transcription of miRNA target, followed by addition of modifying cDNA with label, which is hybridized to a solid-phase capture probe on a substrate	pM	61, 64-67
flow cytometry	Fluorescent-labeled PCR-amplified miRNA target hybridize with probe conjugated to polystyrene beads. Hydrodynamically-focused sheathing liquid allows for in-line flow of beads. Labeled target detected via fluorescence		69
electro-chemical	miRNA target hybridizes with immobilized capture probe. miRNA target reacts with electrocatalytic nanoparticles which produce an electric current upon addition of an oxidizing agent	80 fM	71
luminescence	Biotinylated miRNA target hybridizes with an immobilized capture probe. Streptavidin-modified quantum dots are added, and detected via fluorescence excitation	39 pM	70
	miRNA target and fluorophore/quencher probe hybridize with different regions of a ribozyme, which results in cleavage of the fluorophore/quencher probe, generating fluorescence upon fluorophore excitation	5 nM	73
	Two fluorophore-labeled probes hybridize adjacently with miRNA target and are detected via fluorescence correlation spectrocsopy	100 fM	74
	miRNA target hybridizes with a hairpin oligonucleotide tethered to a magnetic particle, opening up the hairpin. A CdSe-modified oligonucleotide hybridizes adjacently to the miRNA. Upon addition of silver ions, ligand exchange occurs, releasing Cadmium ions, which bind to a fluorogenic substrate, generating fluorescence	35 fM	75
	RNA-primed array-based Klenow enzyme assay where miRNA target hybridizes with adjacent hairpin probes, releasing a DNA fragment through enzyme cleavage, which hybridizes with another pair of adjacent probes. Another enzyme cleavage reaction results in generation of fluorescence	5 fM	77
optical	LNA-modified capture probes bybridize with miRNA, which is poly-adenylated. Gold Nanoparticle-polyT conjugates added and detected through surface plasmon resonance imaging	50 fM	76
	Biotinylated miRNA target hybridizes with an immobilized capture probe. Streptavidin-modified colloidal gold is bound to miRNA, followed by silver enhancement. Visual detection performed via CCD camera.	10 pM	70

As an alternate to quantum dot probes, gold nanoparticles conjugated to streptavidin were utilized (Figure 1.2B). Once the target miRNA is labeled with the nanoparticle-streptavidin complex, followed by hybridization with the complementary oligonucleotide probe, silver enhancement occurs, resulting in a change in color on the gold nanoparticle. During silver enhancement, colloidal gold, in the presence of a reducing agent and silver ions, catalyzes the reduction of silver ions to metallic silver, which forms on the surface of the gold nanoparticle. This buildup of metallic silver

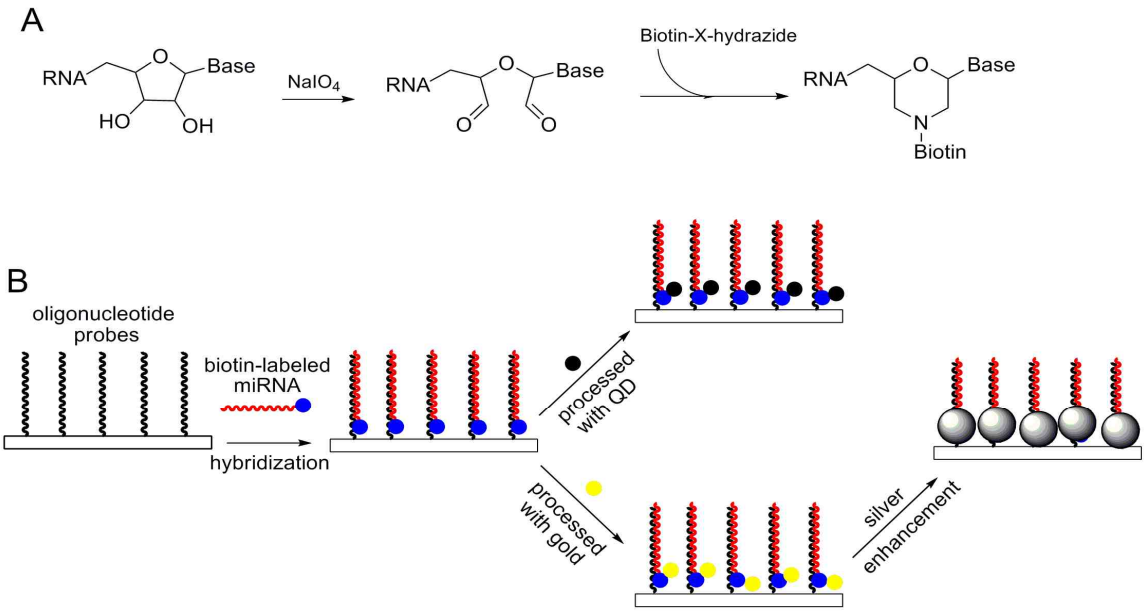

Figure 1.2 Solid-phase quantum dot/ gold nanoparticle miRNA detection. A) Direct labeling of miRNA. B) Fluorescence-based miRNA detection through streptavidin-labeled quantum dots and miRNA detection through silver enhancement on streptavidin-labeled gold nanoparticles. Reprinted with permission from Reference 54. Copyright 2007 American Chemical Society.

changes the color of the nanoparticle which may be detected via a CCD camera mounted to a microscope. This colorimetric method of miRNA detection was found to have a lower detection limit of only 0.1fmol. The quantum dot and gold nanoparticle-based

hybridization methods are both highly sensitive and prove to be viable alternatives to the time-consuming Northern blotting method.

Recently, a novel electrochemical-based solid phase method of miRNA detection was introduced by Gao and Yang utilizing electrocatalytic OsO_2 nanoparticle tags which produces a detection limit in the femtomolar range [71] (Figure 1.3). In this method, complementary oligonucleotide capture probes are immobilized on an ITO-coated glass slide, followed by washing with periodate-treated target miRNA, allowing for hybridization to take place. Upon hybridization, the OsO_2 nanoparticles were added to the reaction chamber. A condensation reaction occurs between the isoniazid and 3' terminal dialdehydes of the miRNA molecules. Once the capped nanoparticles are fused to the miRNA, the hybridization event can be characterized via the electrochemical current

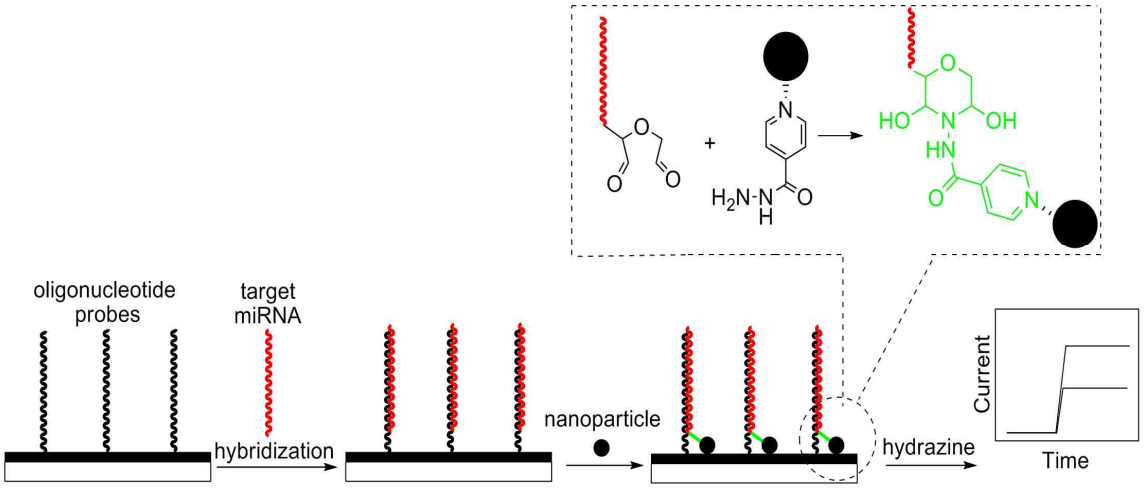

Figure 1.3 Electrocatalytic miRNA detection. Isoniazid-labeled miRNAs are hybridized with tethered capture oligonucleotide probes. Following addition of hydrazine, an increase in current is observed, allowing for quantitation of miRNA. Reprinted with permission from Reference 54. Copyright American Chemical Society.

produced by the nanoparticle-catalyzed oxidation of hydrazine. If a miRNA molecule does not hybridize with the probe, then the nanoparticles cannot conjugate to the miRNA,

thus an electrochemical signal will not result. In this approach, the signal transducer is chemically bound to the target rather than the oligonucleotide capture probe, which increases the sensitivity and selectivity of the assay. This method is simple, sensitive, and rapid for miRNA detection. Another attribute to using electrochemistry is the low cost of the assay, which combats expensive microarray fabrication devices.

Hairpin probes, or molecular beacons (MB), are another tool for miRNA detection. MBs are stem-loop structures consisting of a double-stranded stem approximately 4-5 base pairs in length, containing a donor and quencher fluorophore at the 5' and 3' ends, along with a single-stranded loop complementary to the target DNA or RNA base sequence [72] (Figure 1.4A). In the absence of target the fluorescence of the donor is quenched, whereas in the presence of target, the annealing of the MB leads to separation of the donor and acceptor fluorophore, resulting in fluorescence emission upon excitation. MBs are also very selective, differentiating targets with as little as a single base mismatch. One of the problems of using MBs to detect miRNA is that the small size of miRNA forces the loop of the MB to be small in order to hybridize to the target miRNA. Due to the small size of the loop, the efficiency of the resulting fluorescence signal may be low, since the stems may be unable to dissociate from one another. Another disadvantage with using MBs for direct nucleic acid detection is no signal amplification, which limits sensitivity. To improve the signal amplification researchers have attached multiple fluorophores to the stems of MBs. Due to the ease of design of MBs and their ability to be employed in a mix-and-measure assay, this technique has significant potential in the development of miRNA detection assays. The concept of molecular beacons for miRNA detection has been utilized by Famulok and colleagues [73].

In this article, two separate methods were utilized: direct detection of target miRNA through hybridization of miRNA to MB (Figure 1.4A), or detection of miRNA through signal-amplifying ribozymes (Figure 1.4B). Using the ribozyme approach, a hairpin probe labeled with a donor and quencher fluorophore was utilized as a signal transducer. The basis of this assay is that a ribozyme, iHP-*let-7* will catalyze the cleavage of the hairpin probe upon hybridization of the miRNA *let-7* with its target. Once cleavage results, a fluorescent signal is obtained. A detection limit of 50 fmol miRNA was observed, which was an improvement over Northern blotting techniques that yield detection limits in the pmol range. For detection utilizing the MB without docking to a ribozyme, results were an order of magnitude lower in sensitivity compared to that using signal-amplifying ribozymes. There are drawbacks to the ribozyme method, however, when applied *in situ*. The ribozymes are subject to digestion through ribonuclease activity. In order to be applied *in situ*, the designed ribozymes must be engineered such that they are stable in the presence of ribonucleases.

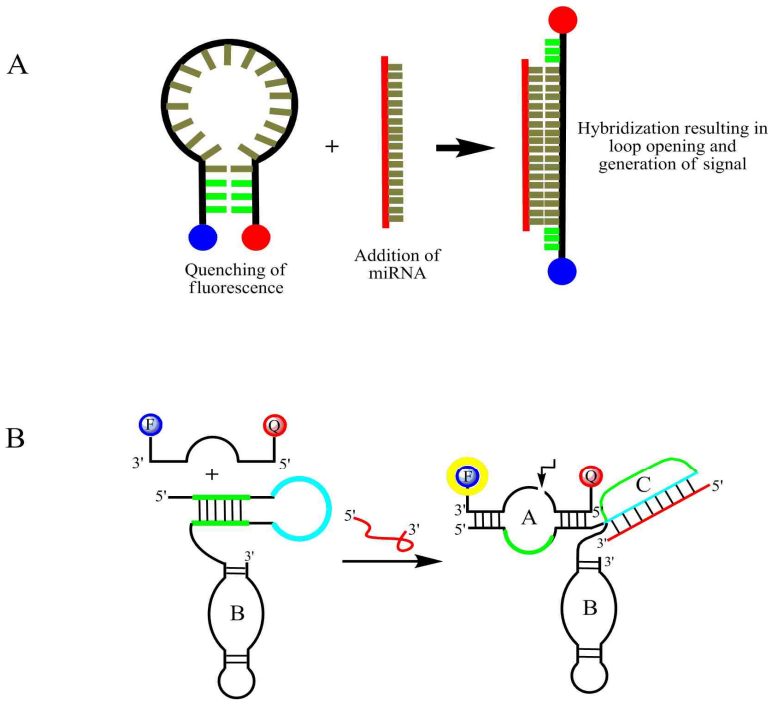

Figure 1.4 Hairpin-probe miRNA detection. A) Molecular beacons consisting of a stem and loop in absence and presence of miRNA target. The target hybridizes with the loop, separating the stem, resulting in an increase in fluorescence intensity. B) Signal-amplifying ribozyme approach in which target miRNA and a fluorophore/quencher hairpin probe hybridize with different regions of a ribozyme. The hybridization of miRNA target with ribozyme induces cleavage of the hairpin probe, resulting in an increase in fluorescence. Reprinted with permission from Reference 54. Copyright 2007 American Chemical Society.

A miRNA detection method utilizing fluorescence correlation spectroscopy has been developed [74]. In this method, oligonucleotide probes composed of DNA and LNA complementary to the 5' and 3' ends of target miRNA were labeled with Oyster 556 and Oyster 656, fluorescent probes which each produce spectrally distinct signals upon laser excitation (Figure 1.5). Once these probes react and hybridize with 50-100 ng total tissue miRNA, unbound probes are hybridized with fluorescent quenchers to minimize background. The resulting probe/miRNA hybridized molecule is passed through a

capillary where probes are excited via a series of lasers and fluorescence emission is recorded on a CCD (charge coupled device) camera. A defining attribute of this method is its ability to differentiate between single-base mismatches, as shown through the studies of the *let-7* gene family members. *Let-7a* and *let-7c* differ by only one base, yet produce a three-fold difference in the number of coincident events counted by the CCD camera upon hybridization of *let-7a* labeled probe to *let-7a* and *let-7c*. Another positive result from this method lay in the ability to detect miRNAs in tissues which were previously not detected via microarrays or Northern blotting due to their low sensitivity.

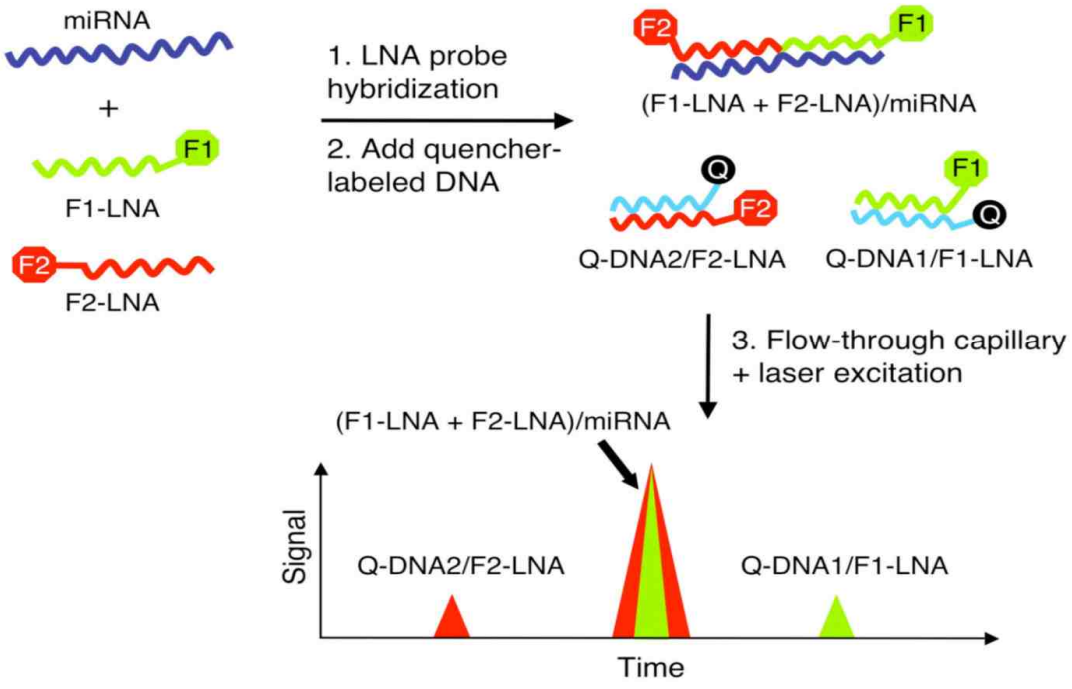

Figure 1.5 Fluorescence correlation spectroscopy-based miRNA detection. Two partially complementary fluorophore-labeled oligonucleotide probes hybridize with miRNA target, followed by laser excitation of fluorophores. The fluorescence confocal microscope detects miRNA based on the emission of the two fluorophores hybridized with miRNA target. Reproduced with permission from reference 55. Copyright 2008 Wiley-VCH Verlag GmbH & Co. KGaA.

In a method by Li and colleagues, cation exchange-based fluorescence is employed as a signal amplification method for miRNA detection [75] (Figure 1.6). In this particular method, the target miR21 was hybridized with a portion of an oligonucleotide capture probe, followed by hybridization of the capture probe with a CdSe ionic crystal-labeled oligonucleotide probe adjacent to the miRNA target. Following ligation, silver ions are introduced to the system. Cation exchange occurs between the Cd^{2+} and the Ag^{+} ions. The Cd^{2+} ions then bind to a fluorogenic molecule Rhod-5N, resulting in enhanced fluorescence emission. This method produced a detection limit of 35 fM. This method also possessed single-nucleotide specificity, and was capable of detecting differential miR21 expression patterns between healthy and diseased cells.

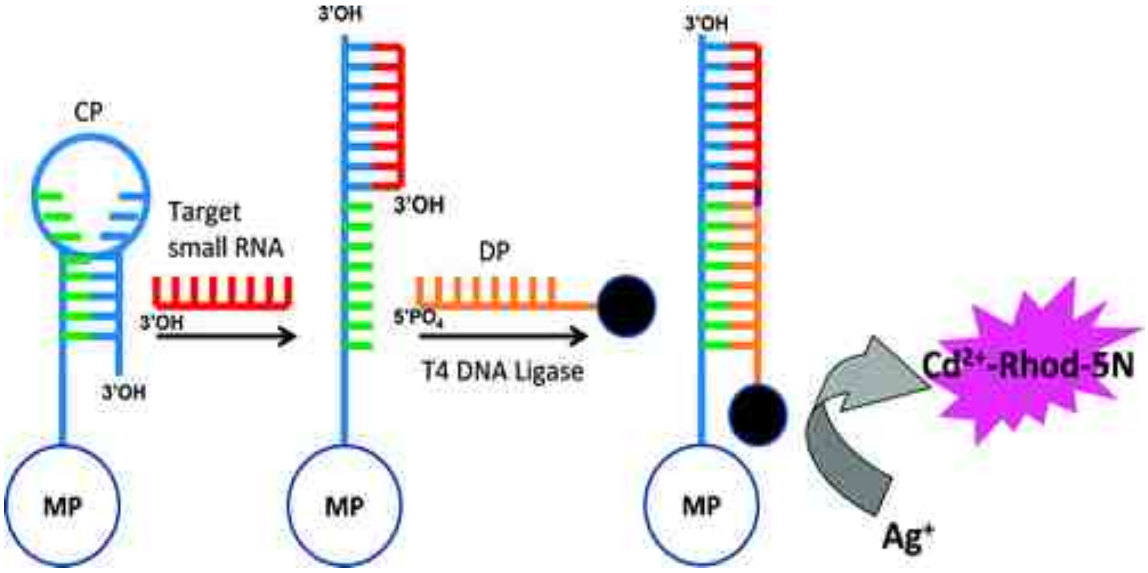

Figure 1.6 Cation exchange-based miRNA detection. Target miRNA hybridizes with a hairpin probe, separating the stem, which allows for CdSe-modified oligonucleotide to hybridize with the probe. Cation-exchange occurs upon addition of silver ions, releasing Cadmium ions. Cadmium ions bind to a fluorophore causing activation of the fluorophore, resulting in an increase in fluorescence signal. Reproduced with permission from Reference 75. Copyright 2009 American Chemical Society.

Another signal amplification-based method is displayed by Fang and colleagues. In this method, gold nanoparticles are employed for the detection of miRNA by surface plasmon resonance imaging [76] (Figure 1.7). First, LNA-modified capture oligonucleotides are immobilized on a gold film, followed by addition of miRNA target. The miRNA is

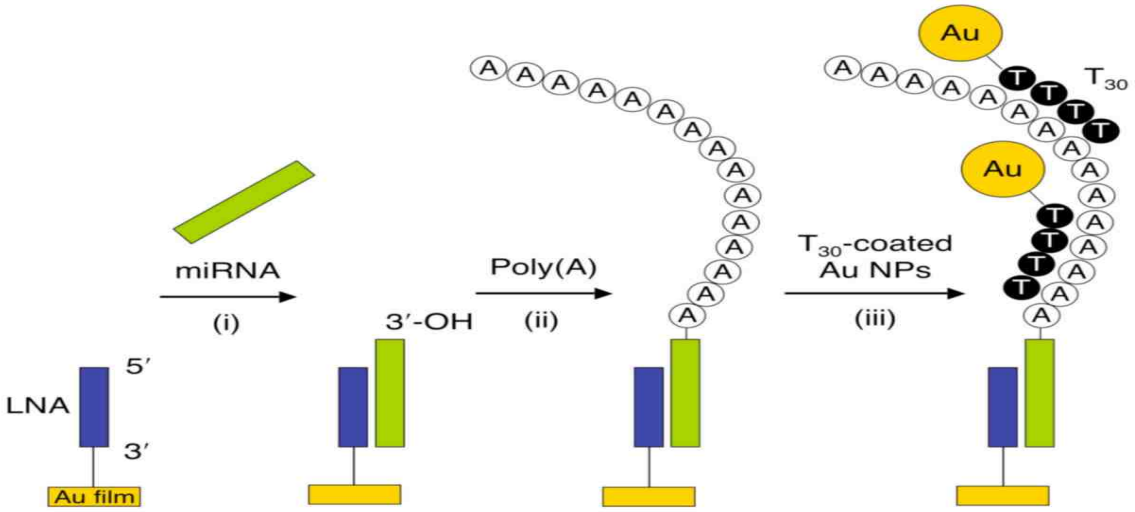

Figure 1.7 Gold nanoparticle-based miRNA detection. miRNA target hybridizes with a tethered oligonucleotide capture probe. miRNA is directly modified through poly(A) polymerase-mediated addition of a poly-adenine tail. Thymine-modified gold nanoparticles are added to the miRNA target, followed by surface plasmon resonance imaging to detect the miRNA. Reprinted with permission from Reference 76. Copyright 2006 American Chemical Society.

directly modified through poly-adenylation by poly(A) polymerase. Next, thymine-modified gold nanoparticles are added to the poly-adenylated miRNAs to result in multiple gold nanoparticles bound to each miRNA. This method resulted in a detection limit of 10 fM.

Another solid-phase amplification-based enzymatic miRNA detection method is displayed in the RAKE (RNA-primed array-based Klenow enzyme) assay [77]. In this method, two probes partially complementary to the miRNA target are utilized (Figure 1.8). One probe, known as the invasive oligo, hybridizes with a portion of the miRNA,

and forms a hairpin shape, partially hybridizing with itself. The secondary oligo probe is also partially complementary to the miRNA target, flanking the invasive oligo. The secondary oligo contains an overlapping section, which hangs off of the miRNA target (Figure 1.8A). This overhang provides a substrate for a structure-specific 5' nuclease. This nuclease enzyme cleaves the overhang portion of the secondary probe. Following cleavage, another reaction template with partial complementarity to the cleaved flap, hybridizes with the reaction template (Figure 1.8B). Next, an oligonucleotide probe containing a terminal fluorophore and internal quencher hybridize with the reaction template. This oligo probe has a small overhang which will serve as a substrate for nuclease cleavage. The cleavage releases the fluorophore, allowing for an increase in fluorescence intensity upon excitation. This method reported a detection limit in the attomole range, and is capable of selectively detecting mature miRNA, while not detecting precursor miRNA.

The new and emerging methods have all addressed the potential difficulties with Northern blotting, qRT-PCR, microarrays, and flow cytometry; however, all of the potential detection methods have not been explored for miRNA detection. The following sections will provide insight into future directions in miRNA research and the gaps that still exist in miRNA analysis.

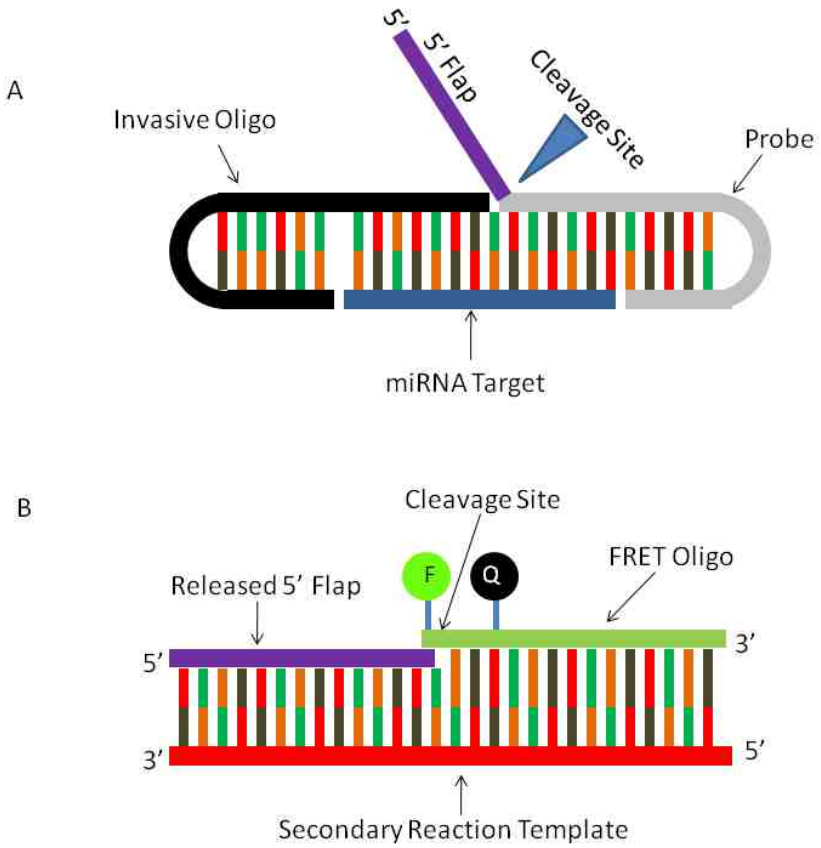

Figure 1.8 RAKE-based miRNA detection. A) The miRNA target partially hybridizes with two oligos: the invasive oligo, and the probe, both of which form hairpin structures and flank the miRNA target. Cleavage results in the release of a 5' flap single-stranded oligo. B) A secondary reaction template partially hybridizes with two oligos: the released 5' flap from the initial cleavage reaction, and a FRET oligo, which contains a fluorophore and an internal quencher. Prior to cleavage, the fluorophore fluorescence is suppressed by the quencher. Upon cleavage, the fluorophore is released, and therefore out of the quenching range of the quencher which remains hybridized with the secondary reaction template. Fluorescence intensity is observed upon excitation of the free fluorophore. Figure adapted from reference 77. Copyright 2004 Oxford University Press.

1.7 Future Developments in miRNA Research

The characterization of the role of miRNA in biology and medicine is now at the forefront of its research. This tiny molecule, through its gene regulation activity, is responsible for diverse physiological functions from cancer suppression to keeping the latent Herpes-Simplex Virus cells infected. More and more, researchers are looking into

roles of miRNA in different cellular processes; however, this activity is not supported at the same pace by new detection technologies. A time-consuming Northern blotting method is the gold standard for accurate determination of miRNA. Microarray methods are rapid and provide for high throughput analyses, but are costly and have limited quantitation ability. Hybridization methods are promising but need further improvement in terms of ease of use and sensitivity. There is much room for progress in detection methods that are sensitive, accurate, and simple to use.

Cellular regulations are dynamic processes, which can be affected by simple perturbations. Therefore, an ideal method for studying gene regulation by miRNA would provide for single cell direct monitoring of miRNA with high spatial and temporal resolution. Advances in microscopy techniques and availability of reporters with high quantum yield should make such detection possible. One of the issues that need to be solved is direct labeling of miRNA in living systems. Researchers have been working in the field of direct labeling in the living system [78]; however, this task remains difficult. Another problem in single cell dynamic detection of miRNA that needs attention is the ability to detect changes in the level of miRNA, on top of the existing background level of miRNA.

The development of computational programs to determine binding between miRNA and their respective mRNA targets is another open area of research. One example of such a program is *MicroInspector* [79]. Using this program, miRNA binding sites are found based on a database of known miRNA/mRNA binding sites, binding strength of hybridization, examination of secondary structures, and the organism the miRNA originated from. With this information, the binding sites on mRNA for unknown

target miRNAs can be predicted. Other bioinformatics methods utilizing different demarcation criteria have been developed as well [80, 81]. Although the binding between miRNA and its target mRNA occurs through base-pairing interactions, in mammals, it is not completely complementary. Other factors may assist in this binding such as various ligands and proteins. In addition, symmetric binding and strong interaction at the 5'end is preferred for miRNA-mRNA binding. Research efforts need to be targeted toward the development of computational methods that allow prediction of miRNA-mRNA binding followed by their experimental validation. In addition, these computational studies would prove highly beneficial in the design of novel therapies that target miRNA-mRNA binding interactions.

MicroRNA expression levels are gaining popularity as signatures for clinical diagnostics. Existing miRNA detection methods are mainly used for research purposes and are not ideal for diagnostic use. In order for miRNA detection methods to be employed for diagnostic use, they need to be rapid, sensitive, specific, and require small sample size. In addition, these methods should be able to detect several miRNAs simultaneously yielding an expression profile. Establishing criteria for validation of these methods is also important before these methods can be used practically. Miniaturization and microfluidics have played a significant role in diagnostic field. There are many papers published on DNA and RNA detection based on microfluidics, some of which have been applied to microchips. For example, Baeumner and colleagues developed a microchip which could detect pathogens based on target mRNA sequences using fluorescence [82]. Detection methods for miRNA could be easily adapted to microchip

platforms. The small sample volume and minimal assay time make the use of microfluidics a desirable method for miRNA-based diagnostics.

Currently, miRNAs are studied only in terms of their biological role. Studies targeting their structure and mechanism of binding may shed light on their activity. In addition, the effects of small ligands as well as macromolecules on miRNA activity have not been studied. These types of fundamental evaluation can be performed through analytical techniques. We have reached a point where hundreds of different miRNAs have been discovered. It is well accepted that these tiny molecules are synthesized in cells for a purpose; however in order to decipher the role of these miRNAs in human health and in plant and animal biology, it is essential that the development of miRNA detection methods continues to progress.

1.8 Gaps in miRNA Analysis

Although methods for miRNA analysis are growing every day, there is a concern that these new methods are not standardized. Standardized methods must be reproducible, accurate, and robust. Also, standardized methods must have established normal levels of miRNA in the cell to determine whether the miRNA is upregulated or downregulated. Therefore, in order for miRNA detection methods to be reliable for medical diagnostics, standardization is necessary. Currently, Northern blotting is considered the gold standard for miRNA detection. This method, however, is time consuming, and has limited sensitivity. In order to detect miRNA with more sensitivity and apply these methods of analysis to practical applications, we must standardize newer, more sensitive miRNA detection methods by measuring a particular miRNA in multiple samples and comparing

the observed miRNA levels with known standards as provided by Northern blotting. Once standardized, these newer, more sensitive methods can be applied to measure lower concentrations of miRNAs which may not be detectable with Northern blotting. By further developing the newer analysis methods, it will be possible to replace time-consuming methods with more time-efficient ones.

In order to develop more sensitive detection methods, it is imperative that the marker which measures the miRNA levels has a very low detection limit. Both electrochemical methods and bioluminescence-based methods are highly sensitive and attractive alternatives to fluorescence-based methods. Bioluminescence-based methods are advantageous compared to fluorescence-based methods due to the fact that bioluminescence labels do not require an external energy source, and lack background noise, yielding higher sensitivity. Many bioluminescent proteins are comparable in size to commonly used fluorescent proteins such as GFP. Fluorescence-based methods utilizing quantum dots are also attractive due to high sensitivity and strong photostability of quantum dots, which is an advantage over commonly used small organic fluorophores.

Another gap in miRNA analysis is the ability to perform multiplex analysis, or detect multiple miRNA molecules simultaneously. While microarrays can already accomplish this [83], many of the more recent miRNA analysis techniques have only reported on detecting a single miRNA. It is thus necessary to further develop these miRNA analysis methods to be capable of multiplex detection.

1.9 miRNA Detection Technologies Developed in This Dissertation

While numerous methods for microRNA detection have been reported, there are virtually no examples in the literature employing bioluminescent labels outside of luciferase reporter bioassays [84, 85]. Bioluminescence-based labels have multiple advantages, including the ability to emit light with no external energy source. In bioluminescent systems, the excitation energy is provided by a biochemical reaction resulting in emission of a photon. In the case of *Renilla* luciferase (Rluc), Rluc catalyzes the oxidative decarboxylation of coelenterazine to coelenteramide, which results in emission of photons of light at ~480 nm with native coelenterazine as a substrate [86] (Figure 1.9). The advantage of no external energy source is an absence of background associated with the external source, a problem encountered with fluorescence-based applications. Along with an internal excitation source, bioluminescent labels have the advantage of being highly sensitive in terms of light output. It has been found that chemiluminescent and bioluminescent labels can detect biomolecules down to the attomole level [87]. Bioluminescent labels also have the advantage of lack of toxicity. Bioluminescent proteins are routinely used in pharmacokinetic assays as reporters and do not result in altered cell activity. Due to the high sensitivity of bioluminescent-based labels, it is proposed that bioluminescence-based systems can be applied to miRNA detection for quantitative analysis. Conjugation of oligonucleotides which are specific to miRNA detection can be performed to allow for hybridization-based assays in both the solid phase and the solution phase. Incorporation of bioluminescent labels for miRNA detection will result in novel component technologies which can form a multifaceted toolkit for miRNA analysis.

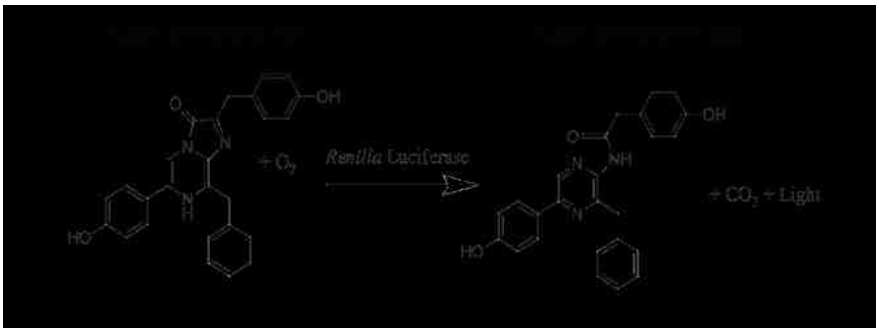

Figure 1.9 Coelenterazine reaction. *Renilla luciferase* catalyzes the oxidative decarboxylation of coelenterazine to coelenteramide. This oxidation reaction releases CO_2 and light.

The work that follows describes the component technology for miRNA detection employing Rluc as a bioluminescent label for quantitative analysis of miRNA in a sensitive, specific, rapid manner. A solid-phase method is introduced which employs Rluc as a label for competitive hybridization between a biotinylated capture probe and two complementary strands: miRNA target, and a complementary Rluc-labeled probe [88]. This method was applied to miRNA detection in cancer cell extracts. In another method, bioluminescence resonance energy transfer (BRET)-based detection is described which employs Rluc as a BRET donor and quantum dot as a BRET acceptor [89]. A third detection method is introduced which employs hybridization-triggered protein complementation between two fragments of Rluc [90]. Each of these three methods has not been employed for miRNA detection. A final, fluorescence-based method is developed which is employed to detect dual miRNA targets. These new technologies will expand current miRNA detection technologies and can potentially be translated to the clinical setting for diagnostic purposes.

CHAPTER 2: SOLID-PHASE MICRORNA DETECTION

2.1 Introduction

MicroRNAs are considered useful diagnostic and prognostic markers, candidates for therapeutic intervention, and targets for basic biomedical research. The tremendous activity in the miRNA research field has fueled the need for experimental methods that are capable of quantifying miRNAs [91]. Because of the emerging diagnostic value of miRNA it is critical that the methods for its detection are simple to use and highly sensitive. In that regard, a competitive solid-phase hybridization-based method has been developed for the detection of the microRNA, miR21 (UAGCUUAUCAGACUGAUGUUGA) using the bioluminescent protein *Renilla* luciferase (Rluc) as a label and employed the method in the detection of miR21 in breast cancer cells.

The solid-phase hybridization assays currently employed for miRNA detection have employed organic fluorophores, quantum dots, and gold nanoparticles as labels [70]. These methods have provided a detection limit in the femtomole range and prove to be viable alternatives to the time-consuming Northern blotting method. One limitation of these methods, however, is that they require miRNA enrichment followed by labeling of miRNA isolated from the sample under study prior to detection. Therefore, there remains

a need for a miRNA detection method that is simple, rapid, and provides for measurement of miRNA directly from a cellular extract in a sensitive manner.

The bioluminescent enzyme, Rluc, employed as a label in the following chapters, is a small, ~36 kDa protein that requires only the addition of coelenterazine for light generation [86, 92-94]. Rluc catalyzes the oxidative decarboxylation of coelenterazine in the presence of molecular oxygen to coelenteramide [86]. This process leads to emission of light that follows glow-type kinetics and has an emission wavelength maximum of 485 nm [86]. Several coelenterazine analogs have been synthesized with different properties in terms of emission wavelength, quantum efficiency, and cell permeability, thus enhancing the applications of Rluc [93]. Since light generation occurs due to a chemical reaction there is no requirement for external excitation light, providing for the detection of Rluc activity with a high signal-to-noise ratio range [95]. Additionally, due to availability of the Rluc gene for cloning, the protein can be reproducibly produced in unlimited amounts and fused to any desired molecule.

In this study, an assay was developed for the detection of the microRNA, miR21, which has been linked to several cancers [96, 97]. For example, levels of miR21 have been found to be elevated in breast, liver, ovarian, pancreatic, and brain tumors compared to their respective normal tissues [36, 96-99]. Furthermore, blocking of miR21 using an antisense oligonuclotide resulted in the reduction of cancerous cell growth *in vitro* and in cell lines [96, 97]. Therefore, availability of a sensitive assay for the detection of miR21 will be useful in diagnostics, basic research, and in designing drug therapy.

In this study, the enzyme Rluc was obtained using genetic engineering tools and conjugated to an oligonucleotide probe corresponding to the sequence of miR21. A

competitive assay was performed between miR21 from the sample and the Rluc-labeled miR21 probe to bind biotinylated anti-miR21 oligonucleotide probe (Figure 2.1). The signal was measured after the addition of the Rluc substrate coelenterazine, and was correlated with the amount of free miR21 in the sample. The assay developed was also utilized to determine the level of miR21 expression in extracts of cancerous and non-cancerous cells.

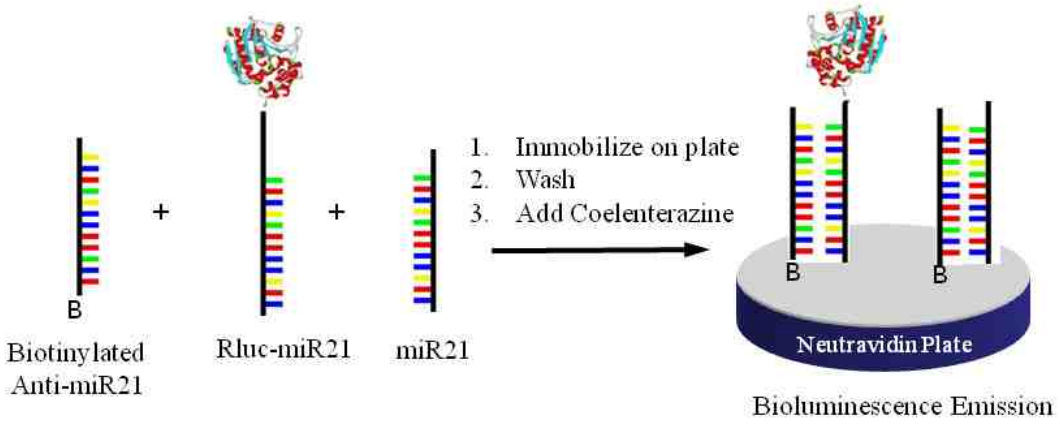

Figure 2.1 miRNA solid-phase assay design. The Rluc-miR21 and miR21 from the sample competitively hybridize with the anti-miR21. The luminescence signal can be measured after a wash step followed by adding coelenterazine. Reprinted with permission from Reference 88. Copyright 2008 American Chemical Society.

2.2 Materials and Methods

Reagents: Luria Bertani (LB) broth and agar were purchased from DIFCO Laboratories (Detroit, MI). Ampicillin, bovine serum albumin (BSA), and Coomasie Brilliant Blue R250 stain were obtained from Sigma Laboratories (St. Louis, MO). The high performance Ni^{+2}-sepharose beads were purchased from GE Healthcare (Uppsala, SE). Coelenterazine (ctz) was purchased from Prolume (Pinetop, AZ). Chemically synthesized oligonucleotide probes were obtained from Operon Technologies (Huntsville, AL).

Ninety six-well neutravidin coated white microtiter plates and Sulfo-SMCC (Sulfosuccinimidyl 4-[*N*-maleimidomethyl]cyclohexane-1-carboxylate were purchased from Pierce Technology (Rockford, IL). TRIZOL reagent and Trypsin-EDTA were purchased from Invitrogen (Carlsbad, CA). All of the buffers used for miRNA work were autoclaved and DEPC treated to protect from RNAse degradation.

Apparatus: Bacterial cell cultures were grown in an orbital shaker, and centrifuged using a Beckman J2-MI centrifuge (Palo Alto, CA). Luminescence emission scans were obtained using the Varian Cary Eclipse Fluorescence Spectrophotometer (Palo Alto, CA). Luminescence intensity measurements were recorded using a Genios workstation luminometer (TECAN, NC). All luminescence intensities reported are the average of three replicates, and have been background corrected. UV-Visible absorbance measurements were performed using a Perkin Elmer UV/Vis/NIR LAMBDA spectrophotometer.

Rluc Plasmid Construction: The gene for Rluc was isolated from the plasmid phRl-CMV (Promega, WI) using polymerase chain reaction employing primers (RlucFor-5'-GGTGGTGGATCCGATGGCTTCCAAGGTGTACGACCCCGAG-3', RlucRev-5'-GGTGGTGAATTCTTACTGCTCGTTCTTCAGCACGCGCTCC-3') that also code for the restriction enzymes BamHI and EcoRI. The sequence coding for BamHI is underlined in the Forward primer, while the sequence coding for EcoRI is underlined in the Reverse primer. The plasmid pRsetB and the gene for Rluc isolated by PCR were digested with restriction enzymes BamHI and EcoRI and cloned into pRSetB (Invitrogen, Carlsbad

CA.) to construct the plasmid pSKD2. The ligated plasmid was transformed into *E. coli* cells strain 2566 (NEB Biolabs, MA). Gene sequencing and restriction analysis were performed to confirm the presence of the gene for Rluc. Gene sequencing results are shown in Appendix A.

Rluc Expression: The cells containing the plasmid pSKD2 were grown in Luria Bertani (LB)-broth containing ampicillin (100 μg/mL) at 37^{o}C to an optical density of 0.5 measured at 600 nm. Protein expression was induced using IPTG (0.5 mM final concentration) and the cells were grown for an additional 3 h at 37^{o}C. The cells were harvested by centrifugation at 16^{o}C, 8600 x g, for 15 min and were sonicated for 5 min with a 20 s on and 20 s off cycle. The crude protein was obtained by centrifugation at 16^{o}C, 8600 x g, for 15 min.

Rluc Purification: High performance nickel-bound sepharose column was prepared by washing with distilled water followed by equilibration with binding buffer (100 mM potassium phosphate buffer containing 250 mM NaCl, 0.6 mM NaN_3, and 20 mM imidazole, pH 7.6). The crude Rluc protein in binding buffer was loaded onto the nickel-bound sepharose column and incubated overnight at 4^{o}C. The column was then washed with 20 mL of binding buffer followed by 20 mL of wash buffer (100 mM potassium phosphate buffer containing 250 mM NaCl, 0.6 mM NaN_3, and 50 mM imidazole, pH 7.6). Purified Rluc was then eluted with 5 mL of elution buffer (100 mM potassium phosphate buffer containing 250 mM NaCl, 0.6 mM NaN_3, and 100 mM imidazole, pH 7.6). Eluted fractions which showed luminescent activity were collected and the purity

was determined by SDS-PAGE using Coomassie staining solution. Protein concentration was determined by measuring absorbance at 280 nm employing an extinction coefficient of 62520 $M^{-1}cm^{-1}$ (www.luxbiotech.com/Docs/Nanolight/Renilla_luciferase.pdf).

Labeling of Oligonucleotide Probes: The oligonucleotide probe complementary to miR21 (anti-miR21) was designed containing a biotin moiety at the 3' end (5'-TAGCTTATCAGACTGATGTTGA-biotin-3'). An oligonucleotide probe that has a sequence the same as miR21 was designed to contain an amino modification at its 3'end (5'-TCAACATCAGTCTGATAAGCTA-NH_2-3'). This oligonucleotide probe was reacted with equimoles of sulfo-SMCC (1:1). The reaction was performed at room temperature for 30 min. Rluc was reduced by adding 80 mM TCEP. The reduced Rluc was added to the probe-linker mixture such that the ratio of Rluc to probe was 1:5. The reaction was performed for 30 min at room temperature and BSA was added to the reaction mix to achieve a final amount of 0.1% BSA. The unconjugated probe and sulfo-SMCC was removed by dialysis against 100 mM potassium phosphate containing 250 mM NaCl, 0.1% BSA, 0.6 mM NaN_3 pH 7.4 to eliminate interference from unlabeled oligonucleotide. Removal of unconjugated probe is also necessary for the determination of concentration of Rluc-miR21 concentration. The concentration of Rluc-miR21 conjugate was determined spectrophotometrically at 260 nm by following established protocol [100]. A volume of 200 µL of miR21-Rluc probe was placed into a microtiter plate, and the emission scan of the protein was obtained after the addition of 0.5 µL of ctz (1 mg/mL).

Hybridization Study: A 20 pmole/µL concentration of biotinylated-anti-miR21 probe was prepared in Rluc buffer (100 mM phosphate buffer containing 250 mM NaCl, 1 mM EDTA, and 0.1% BSA, pH 7.4). Serial dilutions of Rluc-miR21 probe were prepared using the Rluc buffer. A volume of 50 µL of biotin-anti-miR21 probe and 50 µL of varying concentrations of Rluc-miR21 probe were mixed together and incubated at 37^{o}C for 30 min. At the end of 30 min, the probe mixture was placed in a neutravidin-coated microtiter plate pre-washed three times with a wash buffer (100 mM phosphate buffer containing 250 mM NaCl, 1 mM EDTA, and 0.5% BSA, pH 7.4) and incubated with shaking at room temperature for 1 h. A three-time wash step was performed using wash buffer. Next, 200 µL of Rluc buffer and 0.5 µL of coelenterazine (ctz) were added to the plate and luminescence measurement was performed with a 100 ms integration time.

Hybridization Time Study: The mixture of 50 µL biotinylated-anti-miR21 probe (20 pmoles) and Rluc- miR21 probe total volume 50 µL (20 pmoles) was incubated at 37^{o}C for 30 min and was immobilized on a neutravidin-coated microtiter plate for different periods of time. A wash step was performed to remove unbound probes. Luminescence intensity was measured after the addition of Rluc buffer and ctz.

Dose-Response Curve for miR21: A mixture of biotinylated-anti-miR21probe (50 µL, 20 pmoles), Rluc-miR21probe (25 µL, 20 pmoles), and 25 µL of varying concentrations of unlabeled miR21 DNA probe was incubated at 37^{o}C for 30 min. Next, the mixture was added to the neutravidin coated plate and the immobilization step was performed at room temperature for 1 h with shaking. After 3-times wash step, 200 µL of Rluc buffer and 0.5

µL of ctz was added to the wells and luminescence measurement was performed. A dose-response curve was generated for miR21 by plotting luminescence intensity against the concentration of miR21. Intra-assay precision was estimated by analyzing six replicates of three different miR21 concentrations (0.1, 1, 10 pmoles/well) in a single assay. Inter-assay precision was determined by measuring three miR21 concentrations (0.1, 1, 10 pmoles/well) in three separate assays. Next, a dose-response curve was generated using miR21 RNA probe. The procedure performed was the same as when using the miR21 DNA probe.

Recovery Study of miR21 in MCF-10A Cells: Cells from the human mammary epithelial cell line (MCF-10A) were obtained from the laboratory of Prof. Pamela Crowell's at Indiana University Purdue University Indianapolis. Adherent cells were released by trypsin treatment and washed with autoclaved and DEPC treated 100 mM potassium phosphate buffer containing 100 mM NaCl, pH 7.4. The cellular extract was prepared using previously published protocol [101, 102]. All of the buffers used for cellular extraction were autoclaved and DEPC treated to protect miRNA from RNAse degradation. The cell pellet was washed with buffer A (10 mM HEPES, pH 7.9 containing 1.5 mM $MgCl_2$, 10 mM KCl, and 0.5 mM DTT). The cells were resuspended in buffer B (20 mM HEPES, pH 7.9 containing 25% (v/v) glycerol, 0.42 M NaCl, 1.5 mM $MgCl_2$, 0.2 mM EDTA, 0.5 mM phenylmethylsulfonyl fluoride (PMSF), 0.5 mM DTT, and 0.1% Nonidet P-40) and incubated on ice for 15 min. The cell suspension was vortexed and centrifuged for 10 min at 4^{o}C. The supernatant was diluted with buffer C (20 mM sodium phosphate, pH 7.5 containing 20% (v/v) glycerol, 0.1 M KCl, 0.2 mM

EDTA, 0.5 mM PMSF, and 0.5 mM DTT) and stored at -80^{o}C until used. The cell extract after thawing was directly subjected to analysis in triplicate. For the recovery studies, 0.1, 1, and 10 pmoles/well of miR21 was added to MCF10A total RNA. The concentration values of added miR21 were determined using the dose-response curve generated concurrently using standard amounts of miR21. Detection of miR21 was also performed from the same cell samples using extracted RNA. The total RNA was extracted using a previously published protocol (www.sanger.ac.uk/Projects/Microarrays/arraylab/protocol1.pdf). Briefly, the cell pellet was vortexed to break open cells. TRIZOL reagent was added to the cell pellet followed by incubation at room temperature for 5 min. RNA extraction was performed using chloroform followed by precipitation using isopropanol. A total of 10 µg of isolated RNA was employed in the assay. The amount of miR21 in MCF10A RNA was determined by generating a dose–response curve using standard amounts of miR21 probe.

2.3 Results and Discussion

Detection methods for microRNA that are highly sensitive and simple are in demand due to the emerging role of miRNA in several diseases and its significance in medical diagnostics. MicroRNAs can serve as early markers of cancer and hence have become a target of biomedical research. In this work, a sensitive detection method for the miRNA, miR21 based on the bioluminescence of *Renilla* luciferase has been developed. High signal-to-noise ratio achieved using the bioluminescence detection provides an advantage for the detection of miRNA *in vitro* and other sample matrices such as a cellular extract.

For this study, the gene for Rluc was cloned into the expression vector pRSetB and was expressed in *E. coli* cells. The protein was purified using nickel affinity chromatography. The amine-modified miR21 oligonucleotide probe was conjugated to Rluc through the sulfhydryl groups of cysteines present on Rluc. The conjugation was performed using a hetero-bifunctional linker SMCC containing succinimide and maleimide functional groups. The conjugation of probe to Rluc did not affect the activity of Rluc as the luminescence emission profile and intensity was found to be similar to the unmodified Rluc. A biotinylated-oligonucleotide probe (anti-miR21) complementary to the miR21 sequence was synthesized chemically. First the hybridization study was performed to determine if labeling of miR21 probe with Rluc interferes with the hybridization to the anti-miR21 probe. For the hybridization study, various concentrations of Rluc-miR21 probe were mixed with biotinylated-anti-miR21 probe and incubated at 37^{o}C for 30 min. The hybridized probe mixture was then added to a neutravidin coated plate to immobilize the probe on the wells of the plate through biotin-neutravidin interactions (Figure 2.2). After a wash step to remove unbound probes, coelenterazine was added and luminescence intensity was monitored.

Figure 2.2, depicting luminescence intensity against the concentration of miR21-Rluc probe, shows that using a fixed concentration of the anti-miR21 probe and increasing the concentration of miR21-Rluc probe, resulted in a linear increase in intensity. This result indicates that the Rluc labeled oligonucleotide probe can hybridize effectively with its complementary probe. A hybridization time study was performed to determine the minimum time sufficient for hybridization to occur and the optimal temperature for the hybridization. From this study the hybridization time of 30 min and

incubation at 37°C followed by immobilization on the plate for 1 h were chosen as the optimal conditions for the study.

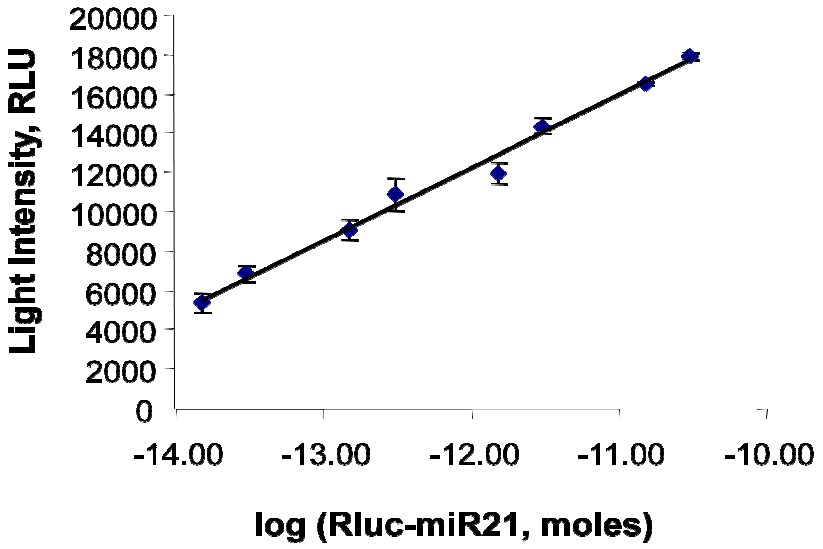

Figure 2.2 Binding curve between miR21-Rluc probe and biotinylated anti-miR21 probe. The data are based on an average response of three samples +/- the standard deviation. Reprinted with permission from Refernce 88. Copyright 2008 American Chemical Society.

A dose-response curve was generated based on competition between miR21-Rluc and free miR21 DNA probe to hybridize with biotinylated-anti-miR21 probe (Figure 2.3). A synthetic DNA target was employed first due to its enhanced stability compared to RNA. The assay is designed such that the competitive reaction between Rluc-miR21 and free miR21 from sample to bind biotin-anti-miR21 occurs in a solution phase. After the hybridization the sample mixture is added to the neutravidin coated plate where hybridized DNA binds through biotin-neutravidin interactions. Therefore, it is expected that the hybridization between probes can occur more efficiently compared to the assay design where hybridization occurs on a solid phase. The dose-response curve (Figure 2.3)

shows that with an increasing concentration of free miR21 probe, the luminescence intensity decreases. From this curve a linear range from 1 x 10^{-11} - 5 x 10^{-15} moles was obtained, with the ability to detect 5 femtomoles (25 pM) of miR21. An estimate of intra-assay precision was obtained by analyzing six replicate samples within a single assay (Table 2.1). The calibration curve was generated and the concentrations of six replicates of samples containing 0.1, 1, and 10 pmoles of miR21/well were estimated.

The inter-assay precision was evaluated from the measurement of 0.1, 1, and 10 pmoles of miR21/well from three experiments performed on three different days (Table 2.1). The precision of the assay was satisfactory with levels of variability below 10%. A dose-response curve was also generated using a miR21 RNA probe instead of a DNA probe (Figure 13). The dose-response curve as shown in Figure 2.4 correlates well with the dose-response curve generated using the miR21 DNA probe (Figure 2.3).

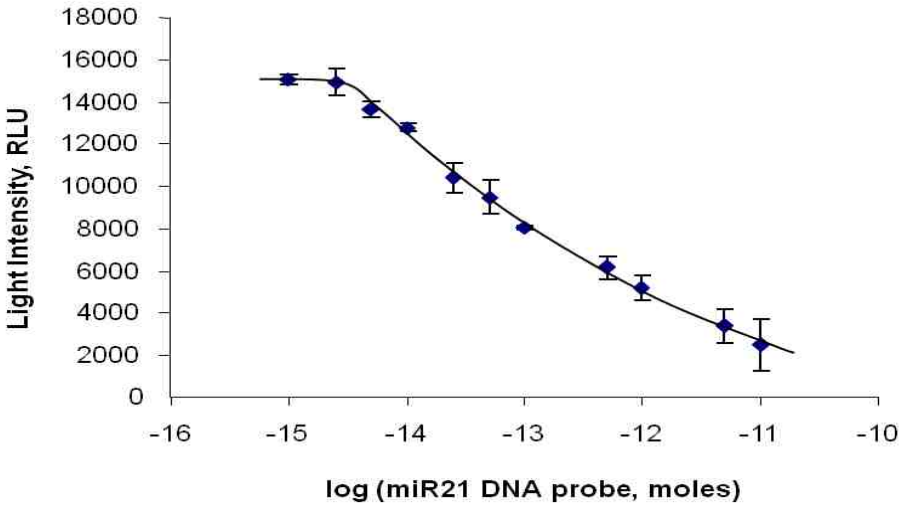

Figure 2.3 Dose-response curve for miR21 DNA target. The dose-response curve was generated by incubating a fixed amount of biotinylated anti-miR21 probe and miR21-Rluc probes with varying concentrations of miR21 DNA target probe. The data are based on an average response of three samples +/- the standard deviation. Reprinted with permission from Reference 88. Copyright 2008 American Chemical Society.

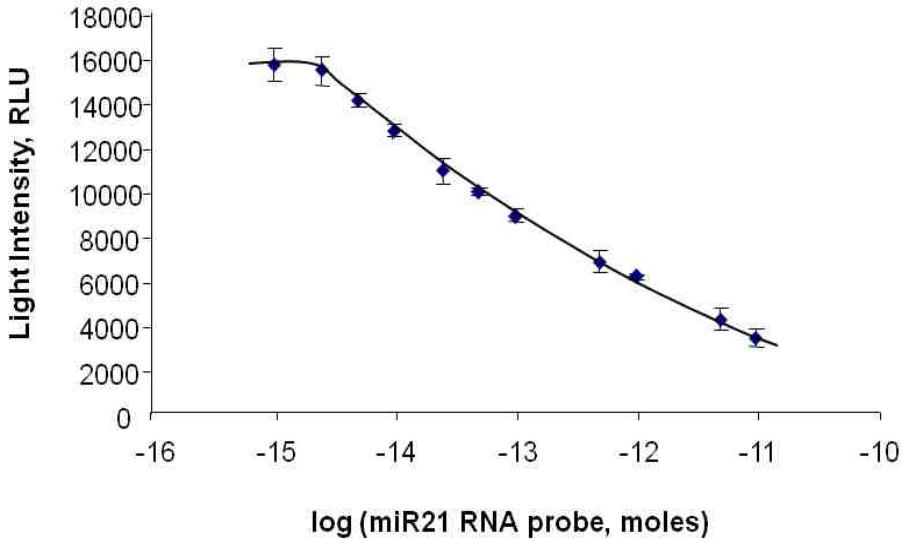

Figure 2.4 Dose-response curve for miR21 RNA. The dose-response curve was generated by incubating a fixed amount of biotinylated anti-miR21 probe and miR21-Rluc probes with varying concentrations of miR21 RNA target. The data are based on an average response of three samples +/- the standard deviation. Reprinted with permission from Reference 88. Copyright 2008 American Chemical Society.

Table 2.1 Solid-phase intra- and inter-assay precision. For intra-assay precision, the values are the means of six determinations, and for inter-assay precision, the values are the means of three determinations.

Intra-assay	added (pmol/well)	found (pmol/well) ± SD	%CV
1	0.1	0.1 ± 0.002	2.0
2	1	1.0 ± 0.02	2.0
3	10	10.1 ± 0.6	5.9
Inter-assay			
1	0.1	0.1 ± 0.004	3.6
2	1	1.1 ± 0.04	3.6
3	10	10.3 ± 0.8	7.7

To demonstrate suitability of the assay developed in the detection of miR21 in real samples, analysis was performed in a cellular extract. For this study, extracts from a non-tumorigenic human mammary epithelial cell line (MCF-10A) were utilized. The

level of miR21 in the MCF-10A cell extract was found to be 50 fmoles. It should be also noted that the bioluminescence signal obtained in the cell extract study was comparable to the *in vitro* assay, indicating no effect of the matrix on the signal. The accuracy of the method was also determined by measuring the recovery of known amounts of miR21 spiked into the cellular extract. Data reported in Table 2.2 shows that the recovery was found to be between 97 and 103% for 0.1, 1, and 10 pmoles of miR21 spiked per well. This study demonstrates the feasibility of the assay developed in the detection of miR21 directly from a cellular extract thereby reducing the sample preparation time.

MCF-7 cells are a well-characterized estrogen receptor (ER) positive control cell line and therefore are a useful *in vitro* model of breast cancer. Levels of miR21 have been shown to be increased in breast cancer. Therefore, MCF-7 cells were employed to determine their levels of miR21 and compared these levels with that in MCF-10A cells which are primary epithelial non-tumorigenic cells. Two separate MCF-7 cultures were utilized and compared to MCF-10A samples (Figure 2.5). A 3-4 fold increase in the concentration of miR21 was observed in MCF-7 cells compared to MCF-10A cells. A %CV (coefficient of variation) for the miR21 determination ranged from 2-8%. This study demonstrates that the developed assay can be employed as a simple test to monitor expression of miRNA in cancerous vs. non-cancerous cells. Therefore, the method developed can be potentially employed as a diagnostic test for breast cancer that utilizes miR21 as a biomarker.

Table 2.2 Solid-phase miR21 detection accuracy. Synthetic miR21 RNA was added to MCF-10A cellular extract containing 50.0 pmoles of miR21, as previously determined, and the recovered amount of miR21 was determined from the dose-response curve.

added miR21 (pmol/well)	recovered (pmol/well)	mean recovery (%)	bias (%)
0.1	0.097 ± 0.003	97.0	-3.0
1	1.03 ± 0.04	103.0	3.0
10	10.14 ± 0.50	101.4	1.4

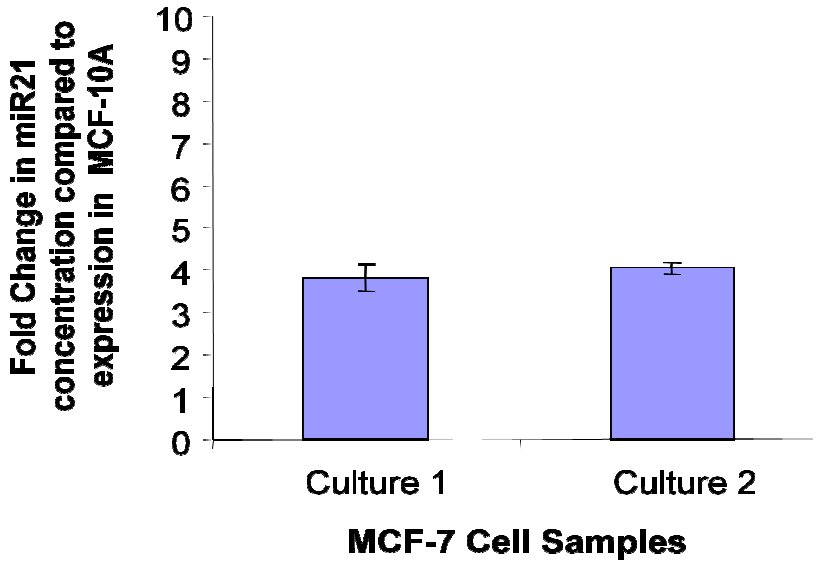

Figure 2.5 Comparison of miR21 levels in MCF-7 cells vs. noncancerous MCF-10A miR21 levels. Error bars indicate the +/- standard deviation values. The solidphase method was employed with the total RNA extracted from MCF-10A and MCF-7 cells to quantify the miR21 miRNA that was present in each culture. Reprinted with permission from Reference 88. Copyright 2008 American Chemical Society.

2.4 Conclusions

A rapid and highly sensitive hybridization assay for microRNA, miR21 based on the bioluminescence of *Renilla* luciferase has been developed. This is the first study to employ Rluc as a direct label for hybridization assays for miRNA detection. Others have employed Rluc mainly as a reporter for gene expression analysis. The bioluminescence emission, small size, and the requirement for the addition of only coelenterazine make

Rluc an efficient label for hybridization assays. The hybridization method developed was applied for the determination of miR21 in both MCF-10A and MCF-7 cellular extract. The method developed was able to discriminate levels of miR21 in cancerous vs non-cancerous cells, which can be a significant advantage in early cancer diagnosis. The need for the detection of early molecular markers in cancer diagnosis is immense, which can be potentially fulfilled by the availability of methods that are rapid and sensitive such as the one developed in this work. The method allowed sensitive, accurate, and precise measurement of miR21 *in vitro* as well as in cells. The availability of simple, rapid, and sensitive assays for microRNAs that provides for determination directly from a cell extract should prove valuable because of their potential as diagnostic markers for a variety of diseases including cancer. Furthermore, the method developed offers the advantage of parallel analysis in a 96-well microtiter plate and makes it suitable for application in clinical diagnostics and drug discovery. The advantages of the method developed in this work such as high signal intensity afforded by Rluc and minimal sample preparation enhances the suitability of this method for adapting to miniaturized analytical platforms providing for high sample throughput. Furthermore, recent findings in miRNA research areas indicate that miRNAs can be isolated from biofluids such as serum, plasma, saliva, and urine [103]. The assay developed in this work can be easily applied to determination of miRNAs in these sample matrices if desired since bioluminescent proteins have been employed previously in saliva and blood analysis of physiological molecules [104, 105].

CHAPTER 3: BIOLUMINESCENCE RESONANCE ENERGY TRANSFER (BRET)-BASED DETECTION

3.1 Introduction

Thus far, a solid-phase method for miRNA detection has been described which is capable of detecting miRNA in the femtomole range. Due to the washing steps required to remove unbound probe inherent to solid-phase assays, the total assay time is increased. In order to develop a more rapid, simple method for miRNA detection, and to increase the available component technologies for nucleic acid detection employing Rluc, a solution-phase method has been developed incorporating Rluc and quantum dots as labels. Like all hybridization-based detection assays, a change in signal must result from the hybridization event. Due to the fact that Rluc signal will not change in the solution-phase when conjugated to a single oligonucleotide probe and hybridized with a complementary oligonucleotide probe, an alternative method must be developed which can transfer the hybridization event into a measurable signal. To accomplish this task, bioluminescence resonance energy transfer can be employed such that hybridization leads to a transfer of energy from donor to acceptor. BRET, which is similar to fluorescence resonance energy transfer (FRET), occurs when energy is transferred from a donor to acceptor. What differentiates BRET from FRET, is in the donor. A BRET donor is not excited through an external source, rather energy is generated through a biochemical reaction between the BRET donor and a substrate [106]. The luminescence emission peak of

Rluc in the presence of native coelenterazine is approximately 485 nm, which overlaps well with the absorption of QDs in the 300-500 nm range. Therefore, employing Rluc and quantum dots as a bioluminescence resonance energy transfer (BRET) donor and acceptor, respectively for the detection of miRNA was performed.

The use of QDs as BRET acceptors and their application in hybridization-based miRNA detection can have several advantages. QDs have attracted much interest as labels because of their desirable properties, including high quantum yields, high photostability, and tunable sharp spectral emission [107-109]. However, the requirement of excitation of QDs from an external source can be a disadvantage due to the associated background signal [110]. If excitation of QDs can be achieved using a chemical reaction that occurs in a bioluminescent system as demonstrated in this work, the background problem from an external excitation source can be overcome. The background signal associated with the detection of a bioluminescence signal is insignificant. Additionally, the use of QDs opens the possibility of multiplex nucleic acid detection by taking advantage of their wide array of emission wavelengths which can be excited internally through Rluc. Due to the fact that QD emission wavelengths are sharp, spectral deconvolution will not be a difficult task, as this has been demonstrated previously [110].

The method developed in this work for nucleic acid detection is a rapid method that does not require separation of unhybridized probes. The use of QDs as BRET acceptors also overcomes the problem encountered when using fluorescent proteins as acceptors where the broad emission of fluorescent proteins overlap with the emission of Rluc, reducing the sensitivity of detection. While *Renilla* luciferase has been employed in numerous studies to measure protein-protein interactions [106, 111, 112], only a small number

of methods have employed Rluc as a BRET donor in nucleic acid detection assays [113]. There are no known methods which employ the Rluc and QD as a donor and acceptor for nucleic acid detection.

The presented work utilizes a competitive assay such that in the absence of target nucleic acid, complementary oligonucleotide probes labeled with Rluc and QD hybridize with each other bringing the two labels in close proximity. Upon addition of coelenterazine, the Rluc emits light at 485 nm which is absorbed by the QD, which in turn emits light at 710 nm. In the presence of target DNA, the target and Rluc-labeled probe compete to hybridize with the QD-labeled probe, thus lowering the emission intensity observed at 710 nm. This decrease in signal can be correlated with the amount of target nucleic acid present in the sample (Figure 3.1).

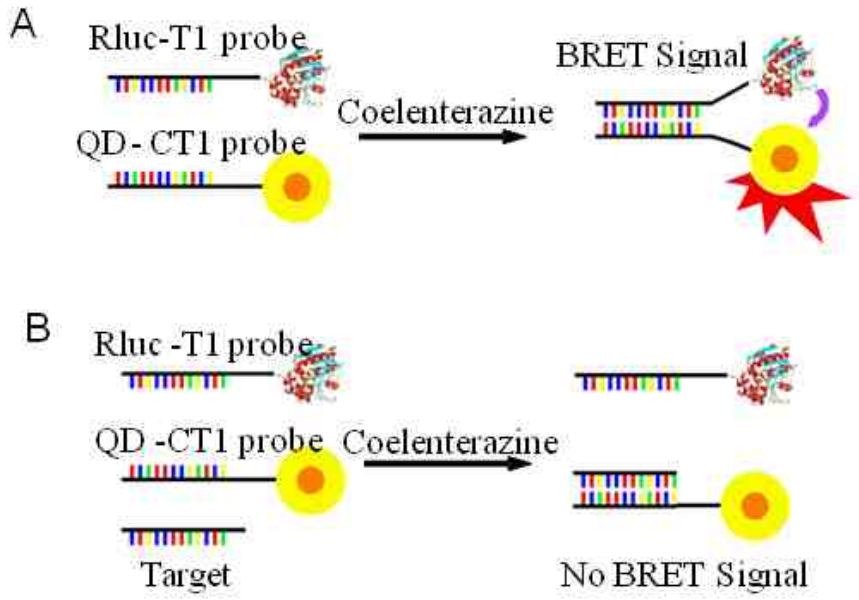

Figure 3.1 Bioluminescence resonance energy transfer (BRET)-based detection assay. A) The result of bringing Rluc and QD within close proximity upon hybridization and addition of coelenterazine. B) The result of the competitive hybridization between target present in the sample and the QD-probe, disrupting the BRET signal. *T1* 5'SH-TAGCTTATCAGACTGATGTTGA-3', *CT1* 5'-TCAACATCAGTCTGATAAGCTA-NH_2 3'. [Reprinted with kind permission from Springer Science + Business Media: Anal Bioanal Chem Vol 391 2008 2577-2581.]

3.2 Materials and Methods

Reagents: Luria Bertani (LB) broth and agar were purchased from DIFCO Laboratories (Detroit, MI). Ampicillin, bovine serum albumin (BSA), and Coomassie Brilliant Blue R250 stain were obtained from Sigma Laboratories (St. Louis, MO). Carboxylated quantum dot, QD705, was obtained from Invitrogen (Carlsbad, CA). The high performance Ni^{+2}-sepharose beads were purchased from GE Healthcare (Uppsala, SE). Native coelenterazine (ctz) was purchased from Prolume (Pinetop, AZ). Chemically synthesized oligonucleotide probes as well as site-directed mutagenesis primers were obtained from Operon Technologies (Huntsville, AL). 96-well microtiter plates,

Sulfosuccinimidyl 4-[N-maleimidomethyl]cyclohexane-1-carboxylate (Sulfo-SMCC) and 1-Ethyl-3-(3-dimethylaminopropyl)-carbodiimide (EDC) were purchased from Pierce Biotechnology (Rockford, IL). *E. coli* strain ER2566 was purchased from New England Biolabs (Ipswich, MA). The phRl-CMV plasmid was purchased from Promega (Madison, WI).

Rluc plasmid construction: The plasmid phRl-CMV was used for protein expression. In order to perform purification, a 6x histidine was added to the Rluc gene via site-directed mutagenesis using the following primers: Rluc His Tag Forward and Rluc His Tag Reverse. The bases coding for the histidine tag are underlined. An EcoRI site was added to the 3' end of the histidine coding region for further utility (See Chapter 4). EcoRI site nucleotides are italicized (Table 3.1). The mutated plasmid was transformed into *E. coli* cells strain ER 2566. Gene sequencing and restriction analysis were performed to confirm the presence of the 6x histidine tag (Appendix B).

Table 3.1 *Renilla* luciferase + histidine tag site-directed mutagenesis primers

Rluc His Tag Primers	Primer Sequence
Rluc His Tag Forward	5'-CTAGCCACCATGCATCACCATCACCATCAC*GAATTC*GCTTCCAAGGTGTAC-3'
Rluc His Tag Reverse	5'-GTACACCTTGGAAGC*GAATTC*GTGATGGTGATGGTGATGCATGGTGGCTAG-3'

Rluc expression and purification: The cells containing the phRL-CMV plasmid were grown in Luria Bertani (LB)-broth containing ampicillin (100 µg/mL) at 37^{o}C to an optical density of 0.5 measured at 600 nm. Protein expression was induced using IPTG (0.5 mM final concentration) and the cells were grown for an additional 3 h at 37^{o}C. The

cells were harvested by centrifugation at 16^{o}C, 8600 x g, for 15 min and were sonicated for 5 min with a 20 s on and 20 s off cycle. The crude protein was obtained by centrifugation at 16^{o}C, 50000 x g, for 15 min. For purification of Rluc, a high performance nickel-bound sepharose column was prepared by washing with distilled water followed by equilibration with binding buffer (100 mM potassium phosphate buffer containing 250 mM NaCl, 0.6 mM NaN_3, and 20 mM imidazole, pH 7.6). The crude Rluc protein in binding buffer was loaded onto the nickel-bound sepharose column and incubated overnight at 4^{o}C while shaking. The column was then washed with 20 mL of binding buffer followed by 20 mL of wash buffer (100 mM potassium phosphate buffer containing 250 mM NaCl, 0.6 mM NaN_3, and 50 mM imidazole, pH 7.6). Purified Rluc was then eluted with 5 mL of elution buffer (100 mM potassium phosphate buffer containing 250 mM NaCl, 0.6 mM NaN_3, and 100 mM imidazole, pH 7.6). Eluted fractions which showed luminescent activity were collected. Purified protein was dialyzed against 100 mM potassium phosphate, 250 mM NaCl, pH 7.6 to remove imidazole and NaN_3 for conjugation reactions. Protein concentration was determined by measuring absorbance at 280 nm employing an extinction coefficient of 62520 $M^{-1}cm^{-1}$ (www.luxbiotech.com/Docs/Nanolight/Renilla_luciferase.pdf).

Rluc and QD oligonucleotide probe conjugation: The Rluc was conjugated to the thiol-modified T1 oligonucleotide probe (5'-SH-TAGCTTATCAGACTGATGTTGA-3') using the heterobifunctional linker Sulfo-SMCC. Rluc and Sulfo-SMCC were mixed together and allowed to react for 2 h at room temperature while stirring. Next, the excess Sulfo-SMCC was dialyzed out of solution against PBS buffer (25 mM sodium phosphate,

100 mM NaCl, 1 mM Na_2EDTA, pH 7.4). After dialysis, T1 probes were added to a stirring Rluc-SMCC and reacted at 4^{o}C overnight while stirring, followed by dialysis to remove unbound T1 probe against the same PBS buffer. For the conjugation reaction, mole ratios of Rluc: Sulfo-SMCC: Thiol-probe were 1:80:4, respectively. Due to the low concentration of the Rluc (2.9 µM), a large excess of crosslinker was used. The luminescence scan and intensity measurements were performed using the Rluc-T1 probe employing a Cary Eclipse spectrophotometer (Varian, CA). The carboxy-activated QD705 was conjugated to the amine-modified CT1 probe (5'-TCAACATCAGTCTGATAAGCTA-NH_2-3') in the presence of 1-Ethyl-3-(3-dimethylaminopropyl)-carbodiimide (EDC) and reacted for 2 h at room temperature while stirring in 10 mM borate buffer pH 7.4. The mole ratios of QD705: EDC: Amine-probe were 1: 7.5: 1.5, respectively. The activity of the QD-CT1 was monitored by direct excitation of QD705. The fluorescence was measured using an excitation wavelength of 485 nm while scanning the emission from 650-750 nm.

Non-specific BRET study: Equimoles (4 pmoles) of non-conjugated Rluc in hybridization buffer (50 mM borate buffer pH 8.0 containing 0.1% BSA) and non-conjugated carboxy-activated QD705 in 10 mM borate buffer pH 7.4 containing 0.1% BSA were mixed together to analyze whether BRET can occur from Rluc to QDs in the absence of oligonucleotide hybridization. Solutions of Rluc and QDs were mixed together and ctz (0.5 µL of 1 mg/mL) was added. The luminescence scan was obtained spanning a spectral range of 450-750 nm.

Hybridization study: Initially, BRET from Rluc to a quantum dot was investigated upon probe hybridization. To achieve that, 4 pmoles of the Rluc-T1 probe and the QD705-CT1 probe in 200 µL of hybridization buffer were mixed. The mixture was incubated at 37^{o}C for 30 min and was allowed to cool down to room temperature before the addition of the substrate coelenterazine. A luminescence emission scan was obtained and the light intensity counts were measured at 485 nm corresponding to the Rluc emission and 710 nm corresponding to the QD705 with a 1000 ms signal integration time. Several controls were monitored along with the sample. These controls include, (1) buffer + ctz, (2) buffer + QD705-CT1+ ctz, (3) buffer + RLuc-T1 + ctz, (4) buffer + Target + RLuc-T1 + ctz.

Calibration study: A calibration study was performed using 4.0 pmoles of the Rluc-T1 and QD705-CT1 probes and by changing the amount of the unlabeled target probe 5'-TAGCTTATCAGACTGATGTTGA-3', (4, 8, 12, 16, 20, and 26 pmoles). Probe mixture in 200 µL of hybridization buffer was incubated at 37^{o}C for 30 min and was allowed to cool down to room temperature before the addition of the substrate ctz. Luminescence intensity counts were measured at 485 nm and at 710 nm with a 1000 ms signal integration time. BRET ratio ($Intensity_{485nm}/Intensity_{710nm}$) was plotted against the concentration of the target.

Hybridization in cellular extract: 4 pmoles of Rluc-T1 and QD705-CT1 were premixed with *E. coli* strain ER2566 extract to mimic the cellular environment. The ER2566 cell extract was prepared by growing the strain in LB media up to an optical density of 0.9 measured at 600 nm. The cells were sonicated with a 20 s on and 20 s off cycle for 5 min

in 10 mM borate buffer, pH 7.4. The resulting mixture was directly used as an extract. The sample was hybridized at 37^{o}C for 30 min. A luminescence scan was obtained after the addition of ctz spanning 450-750 nm.

3.3 Results and Discussion

The application of nucleic acid-based assays continues to expand into medical, forensic, and environmental fields. Nucleic acids do not have intrinsic properties that are useful for their direct detection; hence their detection requires the use of a reporter label. A majority of the label-based assays require separation steps, which makes these assays time-consuming. Here, a rapid, single-step nucleic acid detection method based on BRET from Rluc to quantum dots has been developed.

In this proof-of-concept, a model DNA oligonucleotide corresponding to the microRNA miR-21, (5'-TAGCTTATCAGACTGATGTTGA-3') was employed as a target nucleic acid sequence. A probe complementary to the target (CT1) was labeled with carboxy-activated QD705 using EDC chemistry. Another probe (T1), with the same sequence as the target was designed and labeled with Rluc through the heterobifunctional crosslinker Sulfo-SMCC.

In BRET-based assays, the spatial orientation of the BRET donor and acceptor is an important consideration. The efficiency of BRET is dependent on the distance between the donor and acceptor molecules [114]. In particular, BRET efficiency (E) is proportional to the inverse 6th power of the distance between the two molecules (r), as seen in the following equation:

$$E= R_0^6/ (R_0^6 + r^6)$$

Where R_0 is the Förster distance (the distance in which energy transfer between the donor and acceptor is 50%). The Förster distance can be described by the following equation:

$$R_0 = 9.78 \times 10^3 (\Phi_D K^2 n^{-4} J)^{1/6}$$

Where Φ_D is the quantum yield of the donor, K is the orientation factor, n is the refractive index of the medium in which the hybridization is taking place, and J represents the overlap integral obtained from measuring the area beneath the overlapping portion of the donor fluorescence curve and absorption acceptor curve. Therefore, according to the resonance energy transfer efficiency equation, the closer the BRET donor and BRET acceptor (within 1-10 nm), the greater the BRET efficiency [115]. Because of this fact, the labels on the oligonucleotides were placed such that they were adjacent to one another upon hybridization rather than end-to-end.

Upon mixing Rluc-T1 and QD-CT1, it is expected that probe hybridization will occur, bringing the Rluc and QD within close proximity. Upon addition of ctz, the Rluc will emit bioluminescence with a peak at 485 nm, which will excite the QD, resulting in a 710 nm emission referred to as the BRET signal (Figure 3.1A). Upon simultaneous mixing of target DNA with the Rluc-T1 and QD-CT1, a competitive reaction occurs in which the target and Rluc-T1 probe compete to hybridize with the QD-CT1. Using a fixed amount of QD-CT1 and Rluc-T1 probe and adding increasing amounts of target probe, the BRET signal is expected to decrease because of hybridization of target probe to QD-CT1 probe (Figure 3.1B).

To evaluate the generation of BRET upon mixing of labeled probes, equimole amounts (4 pmoles) of Rluc-T1 probe and QD-CT1 probe were hybridized for 30 minutes at 37^{o}C in hybridization buffer. The substrate coelenterazine (ctz) was added, and

luminescence was recorded from 450 to 750 nm. Since there was no target present in the sample, once ctz is added it is expected that a portion of the Rluc-T1 emission will be absorbed by QD-CT1, resulting in two peaks, one at 485 nm, corresponding to the Rluc, and another at 710 nm, corresponding to the BRET signal associated with the emission of QD705. As can be seen in Figure 3.2A, BRET occurs in the absence of target DNA. Several blanks were performed to assure that nonspecific BRET signal did not occur when ctz was added.

Since it is evident that BRET does occur upon QD-CT1 and Rluc-T1 hybridization, a calibration plot was developed in order to determine the relationship between the BRET ratio and the amount of target present in the sample (Figure 3.2B). The BRET ratio was determined by dividing the emission intensity at 485 nm by the emission intensity at 710 nm. To obtain luminescence intensities at 485 nm and 710 nm, point readings at these wavelengths were recorded instead of obtaining full luminescence scans. Figure 3.2B shows that as the amount of target DNA in the sample increases, emission from the QD decreases, resulting in a higher BRET ratio. This agrees with the initial hypothesis that competition from the target probe will prevent the QD-CT1 and Rluc-T1 probes from hybridizing, thus decreasing the emission intensity observed at 710 nm. Through increasing the amount of target in the sample, the QD-CT1 emission will decrease, and since the Rluc-T1 emission energy is not absorbed by the QD-CT1, the Rluc-T1 emission intensity will increase. Therefore, an increase in emission intensity at 485 nm, coupled with a decrease in emission intensity at 710 nm, will result in the increase in BRET ratio with increasing amounts of target probe. The results in Figure

16B show that as little as 4 pmoles of target DNA can be detected in solution with only a 30 min hybridization time.

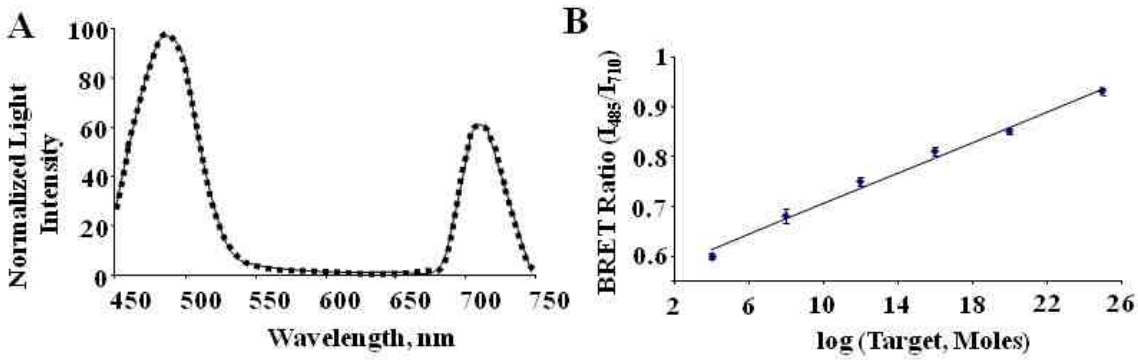

Figure 3.2 BRET luminescence scan and calibration curve. A) The luminescence scan, upon addition of coelenterazine when hybridizing equimole amounts (4 pmoles) of Rluc-T1 and QD-CT1 in solution. B) The calibration curve of the BRET ratio ($I_{485\ nm}$/ $I_{710\ nm}$) vs. the amount of target present in the sample when different amounts of target were mixed with equimole amounts (4 pmoles) of Rluc-T1 and QD-CT1. [Reprinted with kind permission from Springer Science + Business Media: Anal Bioanal Chem Vol 391 2008 2577-2581.]

One of the major applications of any nucleic acid detection method is in the cellular detection of target nucleic acid. Therefore, to show that the BRET strategy will work in a cellular matrix, Rluc-T1 and QD-CT1 probe hybridization was tested in the extract of *E.coli* strain ER 2566. It is expected that the assay will yield similar results to that obtained when performed in the hybridization buffer. After sonicating *E.coli* strain ER 2566 cells in 10 mM borate buffer pH 7.4, equimole amounts (4 pmoles) of QD-CT1 and Rluc-T1 were mixed, hybridized, ctz was added, and an emission scan was obtained from 450 to 750 nm. The results obtained yielded the same emission profile as that seen previously with the hybridization in a buffer matrix. A peak at 485 nm and 710 nm were observed, representing the Rluc-T1 and QD-CT1 emissions, respectively (Figure 3.3).

The relative peak heights in the two sample matrices were nearly the same as well. A comparison of the normalized light intensity ratio of 485 nm/710 nm in the buffer matrix and in the *E. coli* cell matrix showed an approximately 9% decrease from buffer matrix to cellular matrix. Therefore, this detection assay is compatible in more complex cellular matrices.

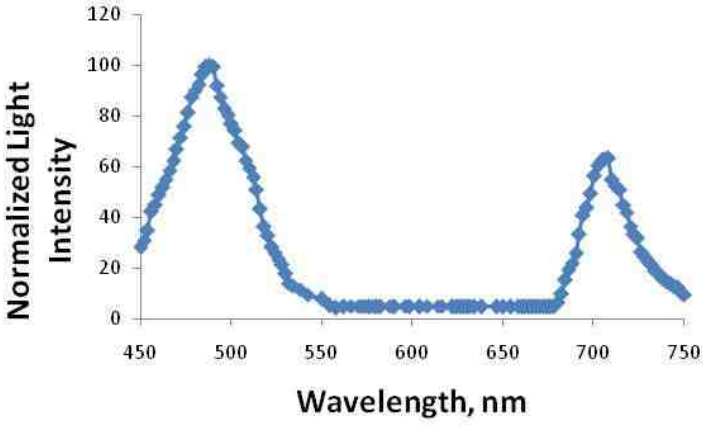

Figure 3.3 BRET luminescence scan in cellular extract. The BRET assay was performed in *E. coli* ER2566 cellular extract to determine if BRET is hindered in a more complex matrix. Equimole amounts of Rluc-T1 and QD-CT1 (4 pmoles) were mixed together at room temperature for 30 min. [Reprinted with kind permission from Springer Science + Business Media: Anal Bioanal Chem Vol 391 2008 2577-2581.]

3.4 Conclusions

The results show that as little as 4 pmoles of target nucleic acid corresponding to miR21 can be detected in solution with only a 30 min hybridization time. This study represents a proof-of-concept for the rapid, sensitive detection of nucleic acids utilizing a quantum dot and *Renilla* luciferase as a BRET acceptor and donor, respectively. This method is an improvement over common solid-phase methods in that no wash steps to eliminate unbound probe are needed. While BRET was shown to work efficiently between the Rluc and QD, it is possible that the BRET efficiency can be improved with

smaller diameter quantum dots due to a decrease in the distance between donor and acceptor. This BRET-based method also has the potential to be employed for the detection of larger nucleic acid sequences through adjacent hybridization of Rluc-T1 and QD-T2 probes. Through adjacent hybridization instead of hybridization of Rluc-probe and QD-probe complementary to one another, an increase in QD signal will be observed upon addition of ctz instead of a decrease in QD signal that is observed in this method.

CHAPTER 4: PROTEIN REASSEMBLY-BASED DETECTION

4.1 Introduction

As demonstrated in previous chapters, the utility of *Renilla* luciferase is quite diverse, from applications as a reporter in gene expression and pharmacokinetics studies, to solid-phase and solution-phase hybridization labels. One area which has not been widely explored with Rluc is a process known as protein complementation. Protein complementation involves the genetic modification of proteins to produce non-luminescent fragments capable of reorganizing into an active bioluminescent protein. In order to expand the component technology available for miRNA analysis, it becomes a logical step to consider the impact of protein complementation of *Renilla* luciferase and its application in miRNA detection. In that light, a method has been developed to detect miRNA based on protein complementation of two genetically modified *Renilla* luciferase fragments.

The split protein complementation method has found applications as a biochemical tool to detect specific protein-protein and protein-nucleic acid interactions [116-123]. In this method, two rationally designed fragments of a reporter protein are fused to proteins which interact with each other. The fragments in isolation are inactive; however, non-covalent biomolecular interactions between fused interacting proteins lead to the formation of an active reporter, allowing for the detection of protein-protein interactions.

This strategy has been successfully utilized in the reassembly of reporter proteins, specifically, dihydrofolate reductase, β-lactamase, β-galactosidase, ubiquitin, aminoglycoside kinase, *Renilla* luciferase, firefly luciferase, red fluorescent protein, green fluorescent protein (GFP), yellow fluorescent protein (YFP), and *Gaussia* luciferase [119, 120, 124-133].

There is only one report on protein reassembly achieved through nucleic acid hybridization using split GFP as the reporter [134]. In this study, reassembly of split GFP upon formation of a hybrid between two complementary oligonucleotides at a 200 nanomolar concentration was accomplished. Design and development of fluorescent proteins such as GFP has revolutionized the biochemical field; however, as discussed in chapter one, these proteins have some limitations because of the requirement of high energy excitation and high background signal, reducing the sensitivity of the signal measurement. In that respect, bioluminescent proteins are a viable alternative since they do not require a high energy excitation source and do not suffer from background noise in signal measurement [87, 135-138]. In a recent paper by Porter et al., these advantages of the bioluminescent enzyme firefly luciferase (Fluc) were utilized to detect proteins, small molecules, RNA, and double stranded DNA, both methylated and nonmethylated [139]; and also have been utilized as a sensor for protease activity [140]. This was accomplished through the expression of the Fluc fragments flanked by expressed protein domains, which when bound to the specific target, brought the split Fluc fragments within close proximity. This allows for protein reassembly to occur, resulting in a luminescent signal upon the addition of luciferin, the substrate for Fluc. In the case of nucleic acid detection, this method is not a hybridization-based assay that works for any target nucleic acid. This

method will work only for targets for which peptide domains that bind to the target can be engineered. Taking this into consideration, a proof-of-concept study was performed to apply *Renilla* luciferase as a label for the detection of nucleic acids through protein reassembly of split Rluc fragments driven by hybridization (Figure 4.1). The usefulness of this method was evaluated with the detection of a target nucleic acid mimicking the sequence of the microRNA miR21.

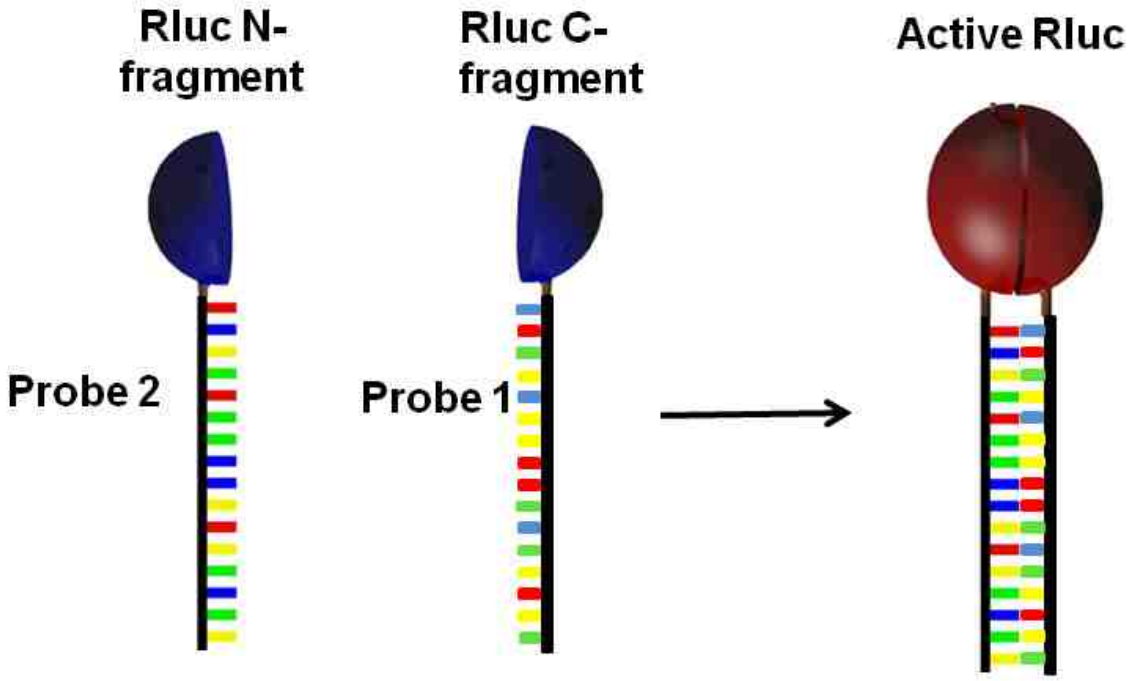

Figure 4.1 Schematic representation of the Rluc fragment reassembly driven through oligonucleotide probe hybridization. Reprinted with permission from Reference 90. Copyright 2009 American Chemical Society.

4.2 Materials and Methods

Reagents: The plasmid containing the gene for Rluc (phRl-CMV) was purchased from Promega (Madison, WI). Chemically synthesized oligonucleotide probes (Probe 1, 5'-Thiol-TAGCTTATCAGACTGATGTTGA-3', Probe 2, 5'-

TCAACATCAGTCTGATAAGCTA-Thiol-3', and free Probe 1, 5'-TAGCTTATCAGACTGATGTTGA-3') were obtained from Operon Biotechnologies (Huntsville, AL). Luria Bertani (LB) broth and agar were purchased from DIFCO Laboratories (Detroit, MI). The Hi-Trap copper chelating columns (1 mL) were purchased from GE Healthcare (Piscataway, NJ). Ampicillin, bovine serum albumin (BSA), and Coomasie Brilliant Blue R250 stain were obtained from Sigma Laboratories (St. Louis, MO). Protein molecular weight marker was purchased from Fisher Scientific. Coelenterazine (ctz) was purchased from Prolume (Pinetop, AZ). 96-well Neutravidin coated white microtiter plates and 1,8-bis-Maleimidotriethylene glycol ($BM(PEO)_2$) were purchased from Pierce Technology (Rockford, IL).

Apparatus: Bacterial cell cultures were grown in a Fisher Scientific orbital shaker, and centrifuged using a Beckman J2-MI centrifuge (Palo Alto, CA). Luminescence emission scans were obtained using the Varian Cary Eclipse Fluorescence Spectrophotometer (Palo Alto, CA). Luminescence intensity measurements were recorded using a Genios workstation luminometer (Tecan, NC). All luminescence intensities reported are the average of three replicates, and have been background corrected.

Construction of Rluc split fragments: The gene for Rluc from the plasmid phRl-CMV was employed as the initial template. Before constructing fragments of Rluc, a non-cleavable N-terminal 6x histidine tag was introduced on the Rluc gene to aid in protein purification, as well as a recognition site for EcoRI restriction enzyme cleavage. The 6-histidine tag and EcoRI site were introduced using site-directed mutagenesis using the

primers Rluc His Tag Forward and Rluc His Tag Reverse, which can seen in Table 3.1. In order to perform site-directed mutagenesis, primers were added to the template phRL-CMV, along with DNA polymerase and deoxynucleotide triphosphates (dNTPs). Next, polymerase chain reaction (PCR) was performed for 25 cycles to copy the new plasmid. Following PCR, the sample was digested with DpnI enzyme to digest plasmids that did not contain the added DNA. The mutated plasmid (pRluc-HisTag) was transformed into *E. coli* cells strain ER 2566, plated on LB agar supplemented with 100 µg/mL ampicillin, and DNA was isolated from the colonies via mini-preparation to perform gene sequencing and restriction analysis.

Table 4.1 Primers for split luciferase plasmid design

N-terminal Fragment Primers	Primer Sequence
Big Lux Forward	5'-GTTAAGGGAGGC*AGTGGAGGTGGAGGTAGTTGT*TAGTAAAAGCCCGACGTC-3'
Big Lux Reverse	5'-GACGTCGGGCTTTTACTA*ACAACTACCTCCACCTCCACT*GCCTCCCTTAAC-3'
C-terminal Fragment Primers	
Small Lux Forward	5'-GTTAAGGGAGGCGAATTC*TGTAGTGGAGGTGGAGGTAGT*AAGCCCGACGTC-3'
Small Lux Reverse	5'-GACGTCGGGCTT*ACTACCTCCACCTCCACTACA*GAATTCGCCTCCCTTAAC-3'

In order to genetically engineer the plasmid to code for the N-terminal Rluc fragment (amino acids 1-229), two stop codons were added between the codons for amino acids Gly229 and Lys230, using the plasmid pRluc-HisTag as the template DNA. Along with the stop codons, the DNA coding for a flexible linker (Ser Gly Gly Gly Gly Ser) and for a cysteine residue was added via site-directed mutagenesis as described

previously. The primers which coded for the stop codons, flexible linker, and cysteine to construct the N-terminal fragment are referred to as Big Lux Forward and Big Lux Reverse. The primer sequences are shown in Table 4.1. The bases coding for the stop codons are underlined, and the flexible linker and cysteine codons are italicized. After site-directed mutagenesis, the mutated plasmid was transformed into ER 2566 competent cells, followed by minipreparation, restriction analysis, and gene sequencing to confirm the presence of the stop codons, flexible linker, and cysteine codons (Appendix C). The purpose of the flexible linker was to allow the oligo-Rluc fragments to come into close proximity, while decreasing the amount of strain on the Rluc fragments caused by the oligonucleotide hybridization. The cysteine residue is present to provide an accessible thiol moiety through which conjugation to thiol-modified oligonucleotide probes can occur. A diagram explaining the steps of N-terminal fragment engineering can be seen in Figure 4.2A.

In order to genetically engineer the plasmid coding for the C-terminal fragment (amino acids 230-311), a recognition site for EcoRI cleavage was added via site-directed mutagenesis between the codons coding for amino acids Gly229 and Lys230, using plasmid pRlucHisTag as the template. Also, a flexible linker and cysteine residue were added adjacent to the EcoRI cleavage site, on the N-terminal side of the C-terminal fragment (Figure 4.2B).

The primers were used for the addition of the EcoRI cleavage site, linker, and cysteine, referred to as Small Lux Forward and Small Lux Reverse, are seen in Table 4.1. The bases coding for the EcoRI site are underlined, and the linker and cysteine-coding DNA is italicized. After site-directed mutagenesis was performed, followed by Dpn1

digestion, the new plasmid transformed into ER 2566 cells. Minipreparation was performed to isolate the plasmid, followed by restriction analysis with EcoRI, and gene sequencing in order to confirm the addition of the EcoRI site, the linker, and the cysteine residue. Upon verification of the mutated plasmid, digestion with EcoRI was performed to cut the plasmid, resulting in two DNA fragments, one fragment representing the N-terminal fragment, and the other representing the linker, cysteine, and C-terminal fragment. After gel extraction, the C-terminal fragment was ligated to form the plasmid coding for C-terminal split Rluc (Figure 4.2B). Gene sequencing and restriction analysis with EcoRI were performed again to verify that the C-terminal fragment plasmid did not contain the N-terminal fragment gene (Appendix C). Once verified, the plasmid was transformed into ER 2566 competent cells for protein expression.

A

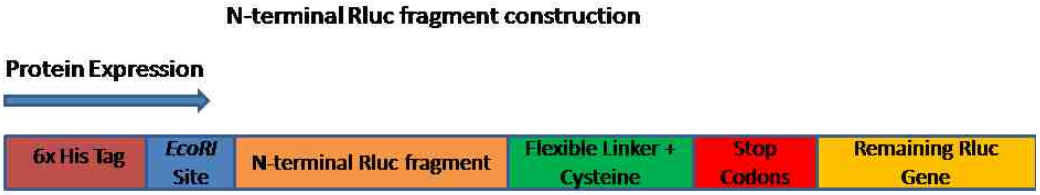

B

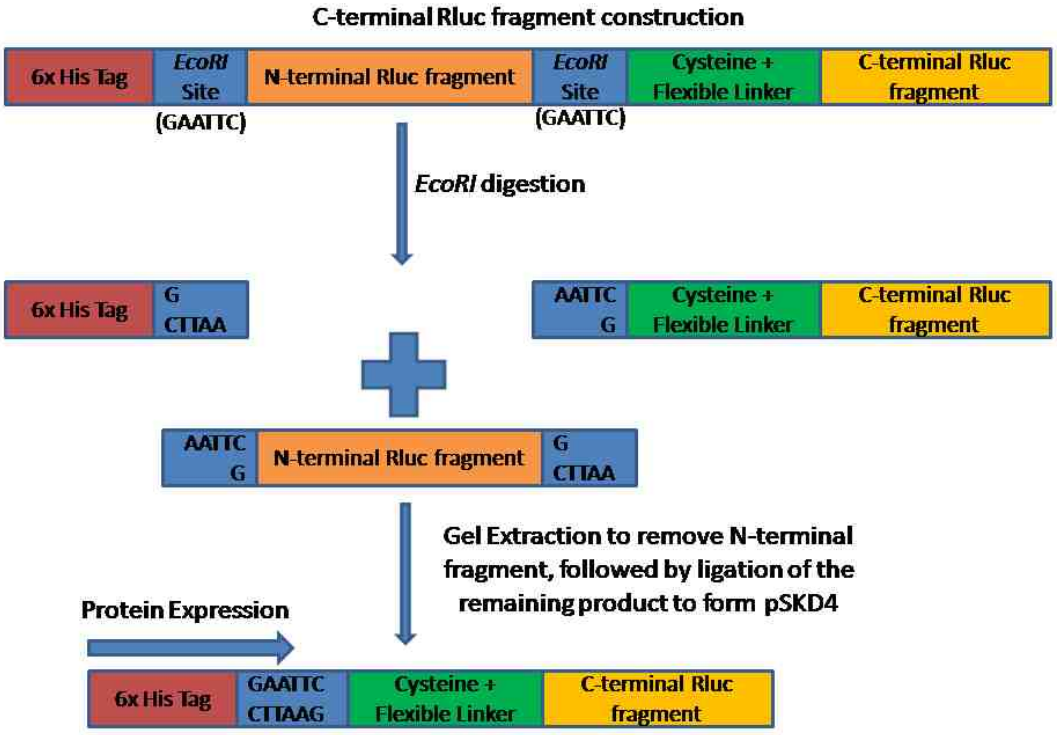

Figure 4.2 Split luciferase plasmid construction. A) The cloning site of the N-terminal split Rluc fragment plasmid. B) The cloning site of the C-terminal split Rluc fragment plasmid is shown after digesting with EcoRI to remove the N-terminal fragment gene, and after ligation. Reprinted with permission from Reference 90. Copyright 2009 American Chemical Society.

Expression of Rluc Fragments: Cells containing the C-terminal fragment and N-terminal fragment plasmids, were grown in Luria Bertani (LB)-broth containing

ampicillin (100 µg/mL) at 37°C to an optical density of 0.5 measured at 600 nm. Protein expression was induced using IPTG (1 mM final concentration) and the cells were grown for 24 h at room temperature. The cells were harvested by centrifugation at 16°C, 8600 x g for 15 min, resuspended in PBS buffer (50 mM sodium phosphate buffer, pH 8.0 containing 300 mM NaCl), and were sonicated for 3 min with a 20 s on and 15 s off cycle. The crude protein was obtained by centrifugation at room temperature, 3000 x g, for 15 min.

Purification of Rluc Fragments: The Hi-Trap copper chelating column precharged with $CuSO_4$ was prepared by washing with 5 mL of distilled water to remove the 20% ethanol storage solution. The column was equilibrated with 5 mL of binding buffer (50 mM sodium phosphate, pH 8.0 buffer containing 300 mM NaCl) before adding the samples of crude Rluc fragments. The column was then washed with 20 mL of binding buffer followed by a 10 mL of wash buffer (50 mM sodium phosphate, pH 8.0 containing 300 mM NaCl and 5 mM imidazole). The purified Rluc fragments were eluted with 2 mL of elution buffer (50 mM sodium phosphate, pH 8.0 containing 300 mM NaCl and 100 mM imidazole). The purity of eluted fractions was determined by SDS-PAGE (Appendix C). Protein concentration was determined via Bradford assay. A volume of 100 µL of each Rluc fragment was placed separately as well as mixed together into a microtiter plate, and the light intensity was measured after the addition of 0.5 µL of ctz (1 mg/mL).

Labeling of Rluc fragments: The conjugations for both the C-terminal fragment and N-terminal fragment consisted of a two step process. First, the crosslinker $BM(PEO)_2$ and

the Rluc fragments were linked through the cysteine thiol moiety which is adjacent to the SGGGGS flexible linker present on the fragments, followed by addition of the thiol-modified oligonucleotide probes (Figure 4.3). In order to conjugate the Rluc fragments to $BM(PEO)_2$, the fragments' disulfide bonds formed from the exposed cysteine residues were reduced by adding 10-fold mole excess of TCEP to the Rluc fragments, while stirring for 30 min at room temperature. Next, the $BM(PEO)_2$ was added to the Rluc fragments in a two-fold mole excess, while stirring for 2 h at room temp. Before adding the thiol-modified oligonucleotide probes, the disulfide bonds between the probes were reduced with 40 mM TCEP for 30 min at 37^{o}C. After reducing, the oligonucleotide probes were added dropwise to the stirring Rluc fragment-$BM(PEO)_2$ solution. The final mole ratio of Rluc fragment: crosslinker: oligonucleotide probe was 1:2:5. Upon linking the oligonucleotide probe to the Rluc fragment, extensive dialysis against PBS buffer (50 mM $NaHPO_4$, 300 mM NaCl, pH 7.2) was performed to remove unconjugated linker and probe. It is important to note that there are four possible products after conjugation: unmodified Rluc fragment; an Rluc fragment dimer linked by the $BM(PEO)_2$, an oligonucleotide dimer; and the correct Rluc fragment-oligonucleotide probe conjugate. Unreacted Rluc fragments and fragment dimers were not separated from labeled fragment since removal using dialysis will be a challenging task due to the small difference in molecular weight between oligo-labeled and unlabeled fragments. Additionally, since the fragments are inactive in isolation and cannot form functional Rluc by self-reassembly, non-conjugated Rluc fragments would not cause any interference or yield any background signal. The oligonucleotide dimers were separated in the dialysis step.

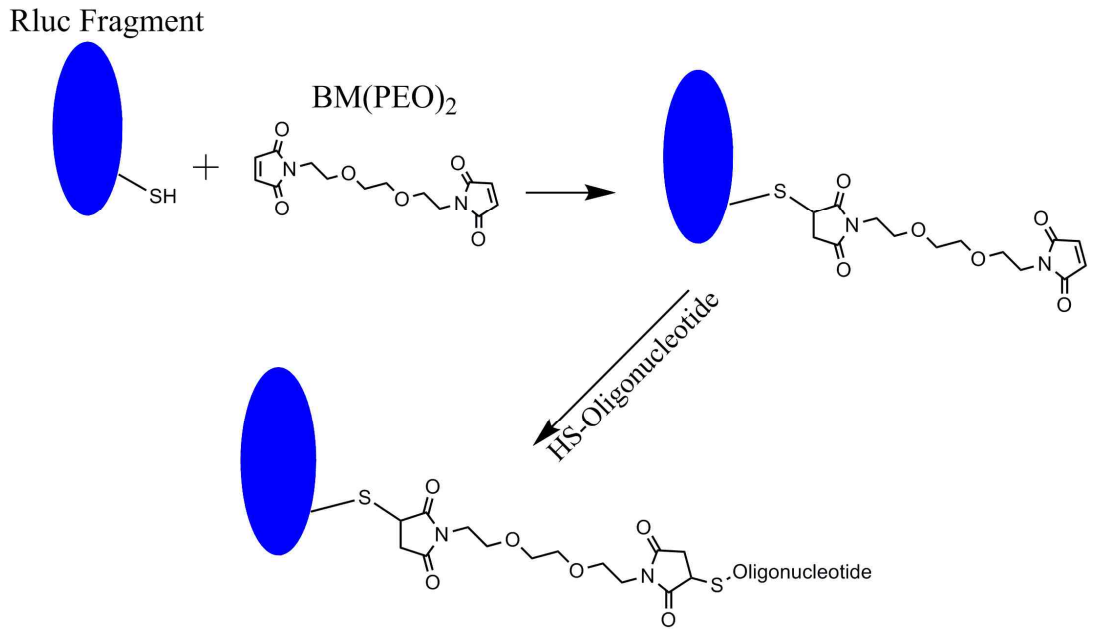

Figure 4.3 Split luciferase-DNA conjugation. A schematic representing the two-step Rluc fragment conjugation to the oligonucleotide probe in the presence of the crosslinker $BM(PEO)_2$. The fragment is first conjugated to the crosslinker, and next the reduced oligonucleotide probe is added to allow conjugation through the free maleimide group. Reprinted with permission from Reference 90. Copyright 2009 American Chemical Society.

Hybridization Study: A 1 x 10^{-11} M concentration of Rluc N-terminal fragment probe 2 conjugate and Rluc C-terminal fragment probe 1 conjugate was prepared in PBS buffer (100 mM sodium phosphate buffer containing 250 mM NaCl, 1 mM EDTA, and 0.1% BSA, pH 7.4). A volume of 100 µL of both fragment probe conjugates were mixed together and incubated at 37°C for 30 min. At the end of 30 min, the probe mixture was placed in a white, flat-bottom microtiter plate and 0.5 µL of coelenterazine (ctz) was added to the plate and luminescence measurement was performed with a 100 ms integration time. Control studies were performed using (1) buffer + ctz, (2) buffer + Rluc-N terminal fragment probe 1 conjugate + ctz, (3) buffer + Rluc-C terminal fragment probe 2 conjugate + ctz. Next, different concentrations of two Rluc fragment probe

conjugates were mixed together in equimole amounts and incubated at 37^{o}C for 30 min. Coelenterazine was added at the end of the incubation period and the luminescence intensity was measured.

Effect of free probe 1: A mixture of Rluc-N-terminal fragment probe 2 conjugate and Rluc-C-terminal fragment probe 1 conjugate, and 100 µL of two different concentrations (17 µM, 66 µM) of free probe 1 was incubated at 37^{o}C for 30 min in a microtiter plate. Next, 0.5 µL of ctz was added to the wells and luminescence measurement was performed.

4.3 Results and Discussion

The most critical issue in the success of protein reassembly from its split fragments is the selection of a cleavage site in the protein. Cleavage in regions inherent to interactions with the protein's substrate or catalytic residues which are not recovered through protein complementation will render the protein reassembly non-detectable. Availability of the three-dimensional structure can aid in the design of the protein fragments. Other considerations in the design of successful protein reassembly include small protein size, monomeric structure, and simplicity of the assay system. Reassembly of split *Renilla* luciferase from its fragments, driven by the interactions between the proteins myoD and Id *in vivo*, has been demonstrated [141], although the fragments were not isolated or purified. On the basis of this work a cleavage site of Gly229-Lys230 was chosen to dissect Rluc. The X-ray crystal structure of a mutant of Rluc was solved recently [142], however, the cleavage site was selected on the basis of prior work performed

in detecting protein-protein interactions using the native Rluc. The X-ray crystal structure of the Rluc mutant shows that it has a classic α/β-hydrolase fold at its core and contains a catalytic triad made from Asp120-Glu144-His285. The cleavage site selected in our study, Gly229-Lys230, would be such that the residue Asp120 and Glu144 of the catalytic triad will be in the N-terminal fragment whereas His285 will be in the C-terminal fragment (Figure 4.4). This suggests that although the substrate binding may occur in the N-terminal fragment, the catalytic triad is not completed until the two fragments come close for the generation of the bioluminescence signal. In the future, other cleavage sites could be evaluated on the basis of the X-ray crystal structure of Rluc. It would be interesting to cleave Rluc such that the triad is kept intact in one of the fragments while the substrate binding is disturbed in the absence of assembly of the two fragments. This type of fragmentation where the active site is maintained may reduce the overall time needed for reassembly of protein as observed in the case of split GFP work [134].

Using the gene for native Rluc from the plasmid phRL-CMV as the template, primers were designed to introduce a non-cleavable 6-histidine tag to allow purification of the Rluc fragments as well as codons for a flexible amino acid linker and a cysteine residue for nucleic acid conjugation. The Rluc N-terminal fragment was constructed by introducing two stop codons after the amino acid Gly229 using site-directed mutagenesis.

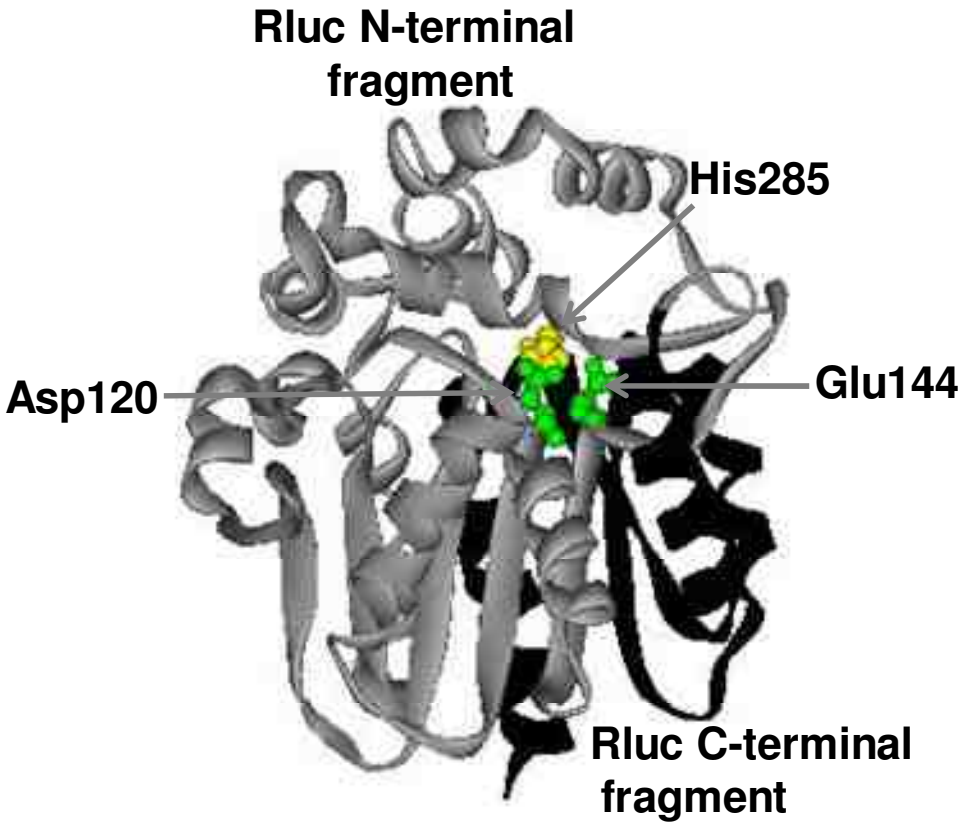

Figure 4.4 Rluc crystal structure. The X-ray crystal structure of Rluc8 a mutant of Rluc showing the three catalytic triads. The N-terminal Rluc fragment region is shown in grey and the C-terminal Rluc fragment region is shown in black. Reprinted with permission from Reference 90. Copyright 2009 American Chemical Society.

Similarly, primers were designed to obtain the gene sequence of the C-terminal fragment of Rluc (amino acid 230-311) with a unique cysteine near its N-terminus. Rluc fragments were expressed in *E. coli* cells and purified using a copper-immobilized Hi-Trap column. The purity of the two fragments was verified using SDS-PAGE and Coomassie staining (Appendix C). The SDS-PAGE shows that the two fragments, the N-terminal fragment (~30 kDa) and the C-terminal fragment (~16 kDa) were purified efficiently. The luminescence activity of the individual Rluc fragments (1 nmole) was monitored by

adding the substrate coelenterazine. As expected, no luminescence signal was observed in the presence of substrate, indicating the inability of fragments to process the coelenterazine (Figure 4.5). Next, the two fragments (1 nmole each) without the probe attached were mixed together followed by the addition of coelenterazine to check for any nonspecific binding between the fragments in the absence of oligonucleotide probes. The mixing of the two fragments did not result in the generation of any bioluminescence signal indicating that spontaneous reassembly between Rluc fragments does not occur (Figure 4.5).

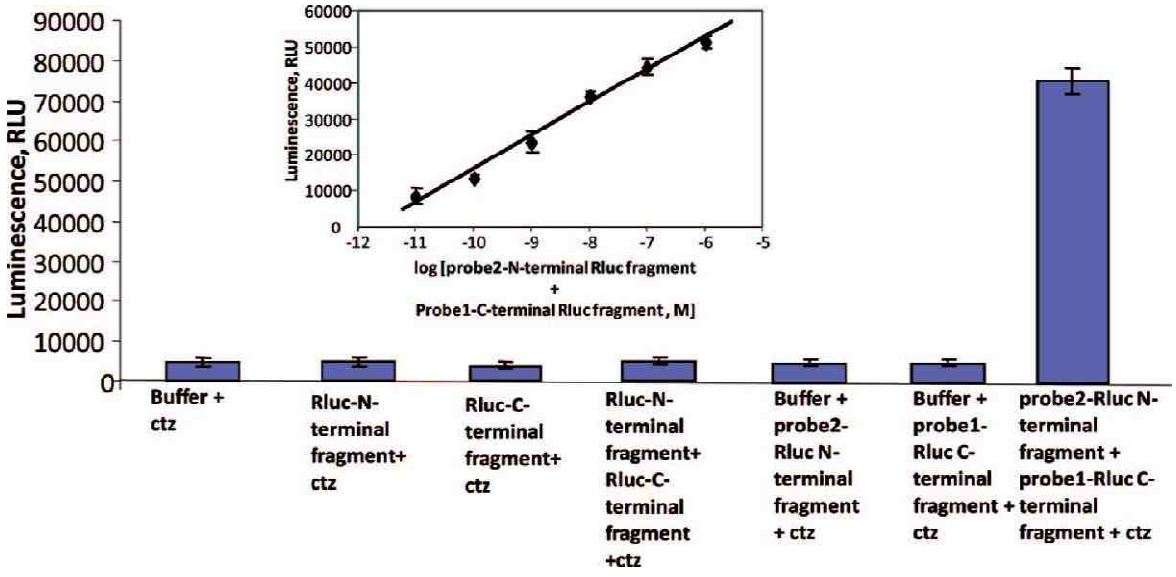

Figure 4.5 Bar graph showing the luminescence activity obtained in control and samples. The data arebased on an average response of three samples ± the standard deviation. The inset shows a plot of luminescence activity obtained after mixing different moles of the probe 1-Rluc N-terminal fragment conjugate and probe 2-Rluc C-terminal fragment conjugates and adding coelenterazine. The data are based on an average response of three samples ± the standard deviation. Reprinted with permission from Reference 90. Copyright 2009 American Chemical Society.

Thiol-modified oligonucleotide probes were conjugated to the split Rluc fragment using maleimide-sulfhydryl chemistry through the homobifunctional crosslinker $BM(PEO)_2$ (1,8-bis-Maleimidotriethylene glycol). The Rluc N-terminal fragment contains three cysteine residues with limited accessibility. Therefore, it is hypothesized that a cysteine introduced at the C-terminus during the construction of the fragment will be the major target site for oligonucleotide conjugation through the thiol moiety. The Rluc C-terminal fragment does not contain a cysteine residue, therefore, the cysteine introduced near the N-terminus of the C-terminal fragment via site-directed mutagenesis was targeted for the oligonucleotide conjugation. In order to perform the conjugation Rluc fragments were first reduced using tricholroethyl phospine, TCEP. Rluc fragments were then reacted with $BM(PEO)_2$ using the manufacturer's protocol in a 1:2 ratio of fragments to linker. Both oligonucleotide probes (Probe 1- 5'-SH-TAGCTTATCAGACTGATGTTGA3' and Probe 2- 5'TCAACATCAGTCTGATAAGCTA-SH-3') were reduced using 40 mM TCEP at 37°C and were added at a 5 times mole excess to the Rluc-$BM(PEO)_2$ conjugate. Probe 2 was conjugated to the N-terminal fragment and probe 1 was fused to the C-terminal fragment. Unreacted probes and crosslinker were then separated using dialysis in sodium phosphate buffer (50 mM sodium phosphate, pH 7.2 containing 300 mM NaCl). Removal of any unreacted Rluc fragments using dialysis is not possible due to the larger size of the fragments. However this should not be problematic for our study because the fragments either alone or mixed together do not yield any luminescence signal in the presence of coelenterazine.

Initially, a control study was performed to determine any background signal from fragment-probe conjugates. The bioluminescence measurements were performed by adding coelenterazine to Rluc-N-terminal fragment-probe 2 and to Rluc-C-terminal fragment-probe 1 separately. The luminescence signal obtained using probe-fragment conjugates was comparable to that obtained using buffer mixed with coelenterazine. Next, nanomoles of each of the two probe-fragment conjugates were mixed together at 37^{o}C for 30 min and bioluminescence intensity was measured after the addition of coelenterazine. Figure 4.5 depicts a bar graph of luminescence intensity obtained upon mixing the two complementary probe-fragments and the intensity obtained in the control study. The control resulted in a minimal background luminescence representative of the luminescnece of coelenterazine alone. In comparison, a strong bioluminescence signal was observed upon formation of an active Rluc driven through probe hybridization. In another study, various concentrations of probe-Rluc fragment conjugates were mixed and bioluminescence signal measured after incubation. A linear increase in luminescence with increasing concentrations of the two probe-fragment conjugates was obtained (Figure 4.5 inset). A detection limit of 5 fmoles (2.5 x 10-^{11} M) of probe-Rluc fragment conjugates. This detection limit was calculated corresponding to the signal obtained using the formula: signal of the blank + 3 times the standard deviation of the reagent blank. In a study performed using GFP as the reporter for fragment reassembly driven through DNA hybridization, the concentrations of probe-GFP fragment conjugates employed were 200 nM [134]. Results indicate that oligonucleotide probe hybridization using Rluc reassembly was detected approximately 4 orders of magnitude lower than that with split GFP.

A bioluminescence emission profile of the reassembled Rluc compared to the native Rluc (Figure 4.6) was obtained. The reassembled protein showed an emission maximum of 495 nm, while the native Rluc showed a 485 nm emission peak. This red shift of reassembled protein vs. native protein has been observed previously with GFP [134]. It is thought that the shift in emission wavelength may be explained by the change in proximity of the amino acids around the chromophore compared to the native Rluc, as well as the presence of the negatively charged DNA molecules driving the reassembly.

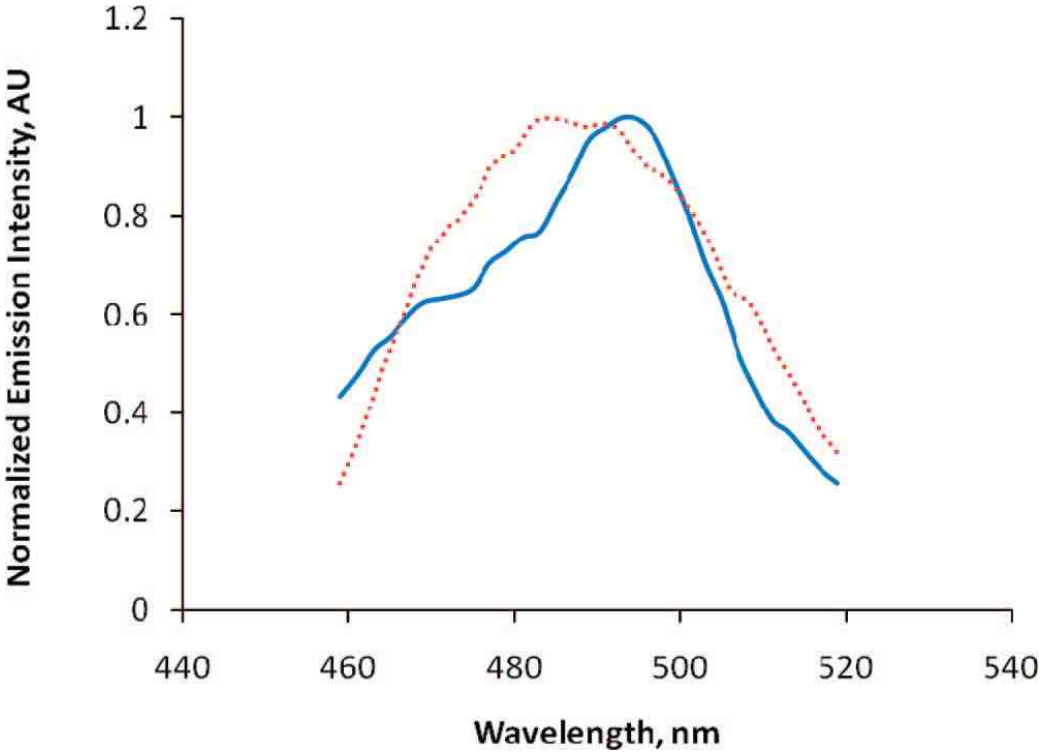

Figure 4.6 Luminescence emission scan of native Rluc and reassembled Rluc. Bioluminescence emission scan obtained using a Cary Eclipse fluorometer of reassembled Rluc (solid line) and intact Rluc (dotted line) after adding coelenterazine. Reprinted with permission from Reference 90. Copyright 2009 American Chemical Society.

Next, the potential application of hybridization-driven Rluc reassembly for target miRNA detection was studied using a synthetic DNA oligonucleotide as a target, mimicking the microRNA miR21. This was evaluated by examining whether the fragment reassembly driven through oligonucleotide hybridization can be competitively inhibited by a free complementary probe. When an excess of free oligonucleotide probe (13.2 nmoles) (5'-TAGCTTATCAGACTGATGTTGA-3') was added to the reassembled Rluc fragment-probe complex (1 nmole) a reduction in the bioluminescence signal was observed. Approximately 45% reduction in the bioluminescence intensity in the presence of free probe compared to the control without the free probe was observed. Although excess free probe was used, complete quenching of the bioluminescence was not observed. A possible reason for this is when the free probe is added to the fragment-probe hybridized complex, a higher temperature than 37^{o}C may be needed to separate hybridized strands. A similar phenomenon was observed in the study performed using GFP split fragments in oligonucleotide hybridization [134]. To further validate this result, when 3.4 nmoles of free probe was added to the probe-directed reassembled Rluc (1 nmole each), a 25% reduction in the bioluminescence intensity was observed. This result indicates that the free probe can prevent DNA-directed reassembly of Rluc in a concentration-dependent manner.

Ideally, a competitive assay can be performed such that the free probe is allowed to hybridize with the complementary probe-Rluc fragment followed by the addition of the second probe-Rluc fragment. An alternative method would be to simultaneously mix probe-fragment conjugates and the free probe. Another strategy to perform target nucleic acid quantitation can be based on designing the probes such that they bind adjacently to

the target. Here, the Rluc fragments can be conjugated to the probes and directly added to the target to be detected. This would allow reassembly of fragments and generation of active Rluc in the presence of the target, yielding an increase in the signal rather than a decrease.

Finally, the reassembly of probe-Rluc fragments was performed in a cellular extract to evaluate whether the Rluc assembly strategy would work in a more complex matrix. Another objective that was fulfilled by this experiment was to evaluate whether any nonspecific nucleic acid present in the sample will interfere with the hybridization of probes and hence the subsequent reassembly of Rluc fragments. For this study, *E. coli* strain ER2566 cell extract was utilized. To obtain the extract, sonication was performed, which also is employed for genomic DNA isolation [143]. After sonicating the cells in PBS buffer, 1 nmole of the probe 2-N-terminal Rluc fragment and probe 1-C-terminal Rluc fragment were mixed with the cell extract and hybridized. The luminescence intensity obtained was comparable to that obtained in the *in vitro* study (Figure 4.7). A comparison of the light intensity in the buffer matrix and in the *E. coli* cell matrix showed an approximately 4.1% decrease from buffer matrix to cell extract matrix. Therefore, reassembly of Rluc driven through DNA hybridization is not significantly affected by the cell extract matrix.

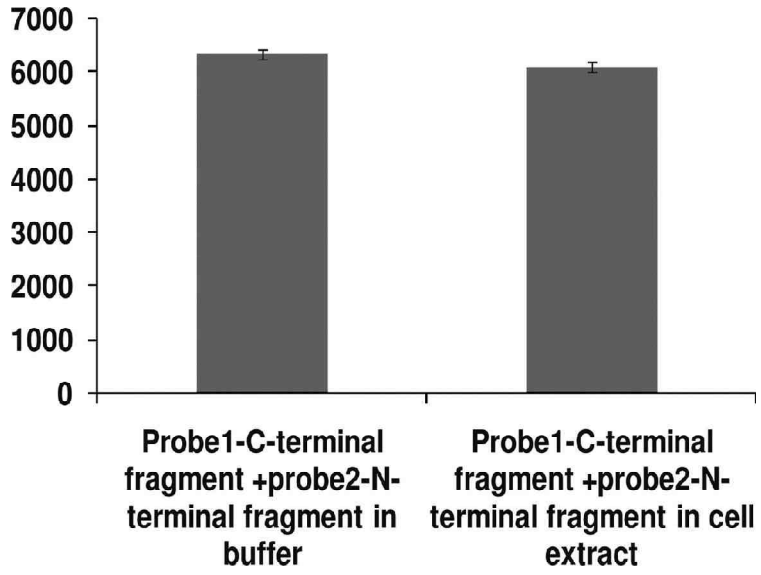

Figure 4.7 Reassembled Rluc luminescence intensity in buffer vs. cell extract. Luminescence intensity obtained after adding coelenterazine to the samples containing probe-fragment conjugates in buffer and *E. coli* cell extract. The data are based on an average response of three samples ± the standard deviation. Reprinted with permission from Reference 90. Copyright 2009 American Chemical Society.

4.4 Conclusions

This work demonstrates that Rluc reassembly can be performed *in vitro* driven through oligonucleotide hybridization. The detection limit for Rluc reassembly was 5 fmoles (2.5 x 10^{-11} M) of probe-Rluc fragment conjugates, which is approximately 4 orders of magnitude lower than that reported using probe-GFP fragment conjugates. These studies also show that the reassembly can be inhibited in the presence of a complementary oligonucleotide mimicking the sequence of the microRNA miR-21, indicating that this strategy can be useful in the quantitative detection of target miRNA. The bioluminescence emission, small size, and monomeric structure make Rluc an efficient label for the development of complementation assays. Furthermore, the method developed offers the advantage of parallel analysis in a 96-well microplate format,

allowing for high throughput capabilities. Hybridization in a complex cell extract matrix did not significantly affect hybridization as evidenced by no significant change in light output upon addition of coelenterazine.

CHAPTER 5: FLUORESCENCE-BASED MICRORNA DETECTION

5.1 Introduction

The three methods employing *Renilla* luciferase described previously, while powerful in their applications to miRNA detection, have only reported the detection of a single target, miR21. It is of interest to expand the miRNA detection methods available to include analysis of multiple miRNAs. A simple method to detect more than one miRNA target can involve the incorporation of fluorescent dyes. Fluorescent dyes, when attached to nucleic acids, can be effective labels for the detection of hybridization [144-146]. Fluorescent dyes, approximately 0.5 nm in diameter, are advantageous to bioluminescent proteins, fluorescent proteins, and quantum dots due to their small size [147]. Quantum dots vary in size from 2-10 nm in diameter, while luminescent proteins are approximately 5 nm in diameter [148]. Fluorescent dyes are also commercially available with multiple functional groups, including succinimidyl esters, iodoacetamides, and maleimides, allowing for ease of conjugation to thiol and amine-modified oligonucleotides. Fluorescent dyes also have the advantage of a wide array of excitation and emission wavelengths, and can be paired with numerous fluorescent molecules for FRET-based assays [149, 150]. Due to their small size, brightness, variety of excitation/emission wavelengths, and ability to conjugate to nucleic acids, fluorophores will be employed as a label to detect hybridization of miRNA oligonucleotide targets in a quantitative manner.

As a proof of concept, two synthetic oligonucleotides mimicking microRNAs miR155 and miR103, were employed to demonstrate that more than one miRNA can be detected in the same assay, in a solution-phase format. In addition to reporting the detection of dual targets in a single assay, it is also important to employ hybridization conditions which result in maximal specificity (the ability to differentiate between single nucleotide mismatches) and sensitivity. Therefore, hybridization optimization is discussed in the following chapter as well.

Several microRNAs have been implicated in pancreatic cancer. Two of them, miR155 and miR103, are the focus of this chapter. It has been found that upregulation of miR103 and the downregulation of miR155 can differentiate pancreatic tumor cells from normal pancreatic cells [151, 152]. To detect the miRNAs, two sets of oligonucleotide probes were designed, one set containing a fluorophore (miR155-T1 and miR103-T2), and the other set consisting of a complementary probe containing a quencher (miR155-CT1 and miR103-CT2). In the absence of target, the two complementary probes hybridize, resulting in a quenching of fluorescence upon excitation. In the presence of target, the target hybridizes with the quencher probe, inhibiting hybridization between the quencher-probe and fluorophore-probe (Figure 5.1). Therefore, as target concentration increases, the fluorescence increases until saturation is reached.

This assay design, although similar to a molecular beacon (MB) with the fluorophore and quencher, is advantageous compared to the MB. MBs contain a short stem of approximately 6 base pairs, and a single-stranded loop containing 15-40 bases [153]. This short stem can often separate, resulting in inadequate quenching of the fluorophore. With the current assay design, the quencher and fluorophore probes are 22 and 23

nucleotides for the miR103 and miR155, respectively. These longer length probes can prevent separation of the two probes through increasing the melting temperature of the hybridization complex, resulting in less background signal than molecular beacons. While the concept of two complementary oligonucleotide probes containing a fluorophore and quencher has been employed previously for hybridization studies involving truncated probe sequences [154, 155], fluorophore and quencher oligonucleotide probe pairs have not been utilized in this manner for microRNA detection.

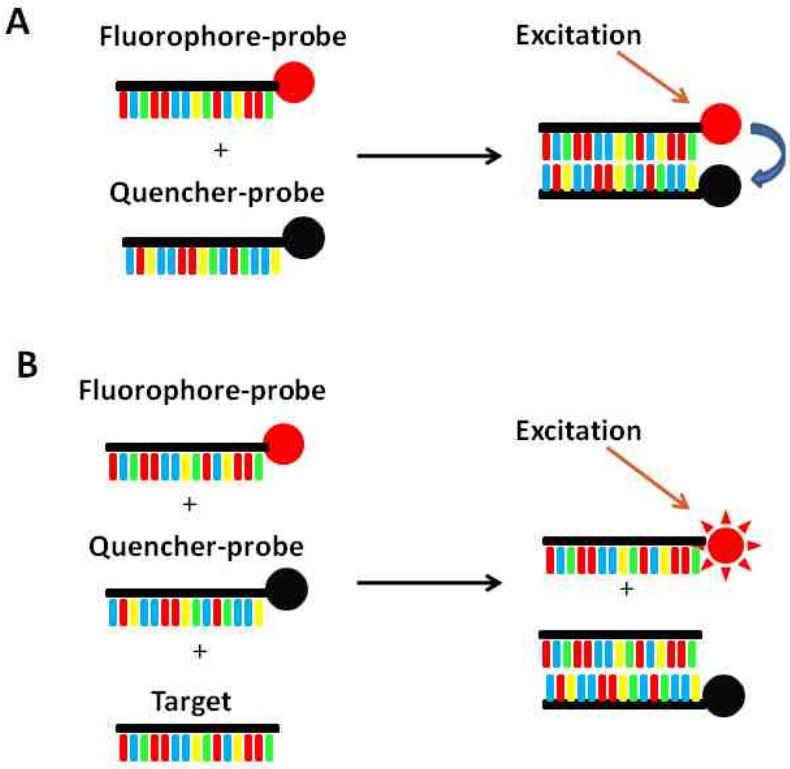

Figure 5.1 Fluorophore/quencher-based miRNA detection assay. A) In the absence of target, the fluorophore-probe and quencher-probe hybridize, resulting in a quenching of the fluorescence upon excitation. B) In the presence of target, the quencher-probe hybridizes with the target, inhibiting the fluorophore-probe from hybridizing with the quencher-probe, resulting in an increase in fluorescence upon excitation.

Quantum dots, although having desirable properties including enhanced resistance to photobleaching, face problems with toxicity due to leakage from their metal core [147, 156, 157]. The small size of the fluorophores also presents an advantage over the use of quantum dots as well as fluorescent and bioluminescent proteins. This assay design is also desirable due to its solution-phase capability. Another important advantage to the detection method described here is its ability to detect two targets in the same solution. Simply selecting the fluorophores such that non-specific emission does not occur due to spectral overlap between the two fluorophores will allow for the dual-detection capabilities. Here, a dual miRNA target detection method is reported, while also displaying target specificity and compatibility in more complex matrices.

5.2 Materials and Methods

Reagents: Sodium chloride, sodium tetraborate, boric acid, sodium phosphate, and white flat-bottom 96 well plates were all obtained from Thermofisher Scientific (Pittsburgh, PA). *E. coli* strain ER2566 was obtained from New England Biolabs (Ipswich, MA). Modified oligonucleotide probes were all obtained from Integrated DNA Technologies (Iowa City, Iowa). Synthetic DNA targets were obtained from Operon Biotechnologies (Huntsville, AL). Synthetic RNA targets were obtained from Invitrogen (Carlsbad, CA). All buffers were made with ultrapure milli-Q water (18 MΩ). Diethyl pyrocarbonate (DEPC) was purchased from Acros Organics (Geel, Belgium). RNAsin RNAse inhibitor was purchased from Promega (Madison, WI). Fluroescence measurements were performed on a Varian Cary Eclipse fluorescence spectrophotometer with a photomultiplier tube voltage of 600 V.

Oligonucleotide Probe Design: DNA oligonucleotide probes were designed depending on their target. Each oligonucleotide probe was synthesized either with a fluorophore at the 5' end or a quencher at the 3'end. Fluorophore-probes were designed to be the same sequence as target, and quencher-probes were designed to be complementary to their respective targets. Oligonucleotide probes and their targets are seen in Table 5.1. Both DNA and RNA targets were designed based on the hsa-miRNA sequences of miR155 and miR103. The miR155 T1 and CT1 probes were modified with 6-carboxy fluorescein and Iowa Black FQ quencher, respectively. The miR103 T2 and CT2 probes were modified with Texas Red and Iowa Black RQ quencher, respectively.

Table 5.1 Fluorophore/quencher oligonucleotide probe design

Strand Name	Sequence
FAM-T1 miR155	5'-FAM-TTAATGCTAATCGTGATAGGGGT-3'
IowaBlack-CT1 miR155	5'-ACCCCTATCACGATTAGCATTAA-IowaBlack-3'
miR155 Target	5'-UUAAUGCUAAUCGUGAUAGGGGU-3'
TEX615-T1 miR103	5'-tex615-AGCAGCATTGTACAGGGCTATGA-3'
IowaBlack-CT1 miR103	5'-TCATAGCCCTGTACAATGCTGCT-IowaBlack-3'
miR103 Target	5'-AGCAGCAUUGUACAGGGCUAUGA-3'

Optimization of probe hybridization: Hybridization time was optimized. Hybridization times between 10 min and 60 min were performed for detection of synthetic DNA mimicking miR155. Well plates were covered with parafilm and aluminum foil to prevent evaporation and quenching of the fluorophores due to light exposure. The hybridization order of quencher-CT1 + target, followed by a five minute wait time, and addition of fluorophore-T1 probe was employed for the time and temperature

hybridization optimization. Varying amounts of miR155 DNA target were employed (0.1-60 pmoles), with 20 pmoles of each fluorophore-probe and quencher-probe.

Assay Specificity: To measure the specificity of the assay, one, two and three nucleotide mismatch target DNA oligonucleotides were designed for detection of miR155. Mismatches were selected at three different locations on the oligonucleotide. The sequences of the mismatch target DNA can be seen in Table 5.2, with nucleotide mismatches displayed as lowercase with red font. The hybridization buffer of 10 mM borate pH 7.4 was employed for all optimization assays. Equimole amounts (20 pmoles) of miR155-T1 and miR155-CT1 and increasing amounts of target (1 pmole-60 pmoles) were mixed. Hybridization took place for 30 minutes at room temperature. To optimize hybridization temperature, the one, two, and three nucleotide mismatch targets were hybridized in 10 mM borate buffer at 50^{o}C, 42^{o}C, 37^{o}C, and room temperature. Triplicate samples were performed for each data point.

Table 5.2 miR155 DNA target mismatch sequences

Target	Sequence
miR155 perfect match	5'-TTAATGCTAATCGTGATAGGGGT-3'
miR155 1 nt mismatch	5'-TTAATGCTAATCGcGATAGGGGT-3'
miR155 2 nt mismatch	5'-TTAATGCgAATCGcGATAGGGGT-3'
miR155 3 nt mismatch	5'-TTtATGCgAATCGcGATAGGGGT-3'

DNA target detection: Both the miR155 and miR103 DNA targets were detected both independently and simultaneously in 10 mM borate buffer pH 7.4. Equimole amounts (20

pmoles) of fluorophore-probe and quencher-probe were employed, along with varying amounts of target (0.1 pmoles-60 pmoles). For the miR103 DNA target detection excitation and emission wavelengths of 596 nm and 613 nm, respectively, were employed. For dual detection, multi-wavelength mode was utilized on the fluorescence spectrophotometer. Samples were prepared by mixing target and quencher-probe, hybridizing for 5 minutes at room temperature, followed by addition of fluorophore-probe and hybridization for 30 min at 42^{o}C. Triplicate samples were prepared for each data point. Reagent blanks for both the miR155 and miR103 DNA target detection were determined by measuring the fluorescence of the fluorophore-probe and quencher-probe with no target present, once hybridization reached equilibrium. New reagent blanks were performed for each assay.

Complex matrix hybridization: In order to employ this method in more complex matrices, mouse serum and cellular extract from *E. coli* ER2566 cells was utilized. For the mouse serum, 25% serum, 75% buffer mixture was employed for the data collection. *E. coli* extract was prepared by growing *E. coli* ER2566 cells overnight, followed by resuspension in 10 mM borate buffer pH 7.4 and sonication to open the ER2566 cells. Cells were pelleted, and the supernatant was employed further for the assay. Samples were prepared by mixing target and quencher-probe, hybridizing for 5 minutes, followed by addition of fluorophore-probe, mixing, and taking the measurements 30 min after hybridization at 37^{o}C. Total sample volumes were 150 µL. Each sample was performed in triplicate. Concentration of target, fluorophore-probe and quencher-probe were identical to those utilized for the DNA target detection in borate buffer.

RNA target detection: To apply the assay to microRNA detection, synthetic microRNAs were employed. The assays performed for the RNA detection were all performed in nuclease-free water. To make the nuclease-free water, DEPC was added to 10 mM borate buffer, followed by incubation at 37^{o}C, and autoclaving to deactivate free DEPC. RNA detection was performed in multiple matrices, as with the DNA detection. Matrices utilized were buffer, cell extract, and serum. Both single probe detection and dual probe detection were performed as with the DNA detection. Equimoles of quencher-probe and fluorophore-probe (20 pmoles) were utilized, along with varying amounts of RNA target (0.1 pmoles-60 pmoles). Synthetic RNA detection in serum required addition of RNAsin RNAse inhibitor to the serum. To prepare the RNAsin-treated serum, 2.5 μL of RNAsin per 37.5 μL of serum was added, followed by incubation for three hours at 37^{o}C. All samples were performed in triplicate.

5.3 Results and Discussion

MicroRNA detection is vital to the understanding of cancer and disease progression. In order to develop a method for miRNA detection, a solution-phase approach has been utilized based on the design of fluorophore and quencher-labeled DNA oligonucleotide probes. Both probes were designed complementary to one another, with the fluorophore-probe (T1 or T2) consisting of the same nucleotide sequence as the target. Upon addition of target, quencher-probe and target hybridize. This prevents the fluorophore-probe from hybridizing to the quencher-probe, resulting in an increase in fluorescence.

In order to employ a method which is capable of detecting dual microRNAs in solution, fluorophores were chosen which were spectrally distinct, and would not result in cross excitation. With this in mind, FAM (6-carboxyfluorescein) fluorophore and TEX 615 (Texas Red) were chosen. FAM has a 495 nm excitation and a 520 nm emission wavelength, while TEX 615 has a 596 nm excitation and a 613 nm emission wavelength. These two fluorophores were examined for cross-excitation. It was found that 613 nm emission was insignificant with an excitation of 495 nm, and 520 nm emission was not detectable with an excitation of 596 nm. To effectively quench the fluorophores, quenchers were chosen based on manufacturer's recommendations (IowaBlackFQ for the FAM, and IowaBlackRQ for the TEX615). The order of reagents employed was quencher-probe + target, followed by addition of fluorophore-probe. When adding the fluorophore-probe and quencher-probe, followed by picomole amounts of target, the target is unlikely to displace the fluorophore-probe from the quencher-probe, resulting in quenching of the FAM fluorescence. In order for target to displace the fluorophore-probe, a truncated fluorophore-probe or quencher-probe can be designed with a sticky end [154, 155]; however, this method increases hybridization time due to the complex kinetics involved in initial hybridization and strand displacement, which is caused by the competing reaction of rehybridization of the displaced probe. The sequence of fluorophore-T1 probe + quencher-CT1 probe, followed by addition of target could be accomplished with the addition of an extremely large excess of target, as observed with the split luciferase assay, although it is optimal to detect lower amounts of target.

The buffer chosen for hybridization was 10 mM Sodium tetraborate buffer pH 7.4. A low buffer capacity buffer was chosen due to its low sodium concentration.

Sodium chloride was also not added to the hybridization buffer, as this may decrease hybridization stringency. The presence of sodium chloride minimizes charge repulsion among the negatively charged phosphate backbone of the hybridized complex, further stabilizing mismatches. Therefore, the buffer should not contain any sodium chloride in order to increase hybridization stringency. The hybridization time performed for the assay was determined to be 30 minutes. At all hybridization temperatures (room temperature, 37^{o}C, 42^{o}C, and 50^{o}C), the fluorescence intensity had leveled off by 30 minutes.

The placement of nucleotide mismatches is very important when studying the specificity of a hybridization assay. Each of the three mismatches shown in Table 5.2 was chosen carefully based on its neighboring bases. The first mismatch is flanked on the 5' side by 5'-CG-3', which according to the nearest neighbor model of melting temperature determination, will stabilize a mismatch duplex the greatest of any two base combination (ΔH^{o}=11.9 kcal/mole) [158]. Therefore, if the assay was capable of differentiating the single mismatch target, it should be capable of differentiating between miRNAs differing in one nucleotide, such as the *let-7* family of miRNAs. The second nucleotide mismatch is flanked on the 5' side by 5'-GC-3', which, compared to the ten possible two base combinations, has the second highest enthalpy (ΔH^{o}=11.1 kcal/mole) [158]. Taken together, the combination of these two mismatches and their placement, will present difficulties in terms of specificity. The final mismatch is flanked at the 5' by TT, which is does not possess the stabilizing effect that 5'-GC-3' will have (ΔH^{o}=9.1 kcal/mole); however, placing the mismatch very near the end of the probe sequence also presents difficulties in specificity, simply because nearly the entire length of the quencher-probe can still

hybridize with the target, resulting in an increase in fluorescence intensity. Based on this information, when designing mismatches, it is crucial to examine the bases flanking the mismatch placement.

Hybridization temperature was optimized by monitoring nucleotide specificity and varying the temperature in 10 mM Borate buffer pH 7.4 (Figure 5.2). From the data, it is evident that 42^{o}C hybridization is optimal, due to the enhanced specificity compared to the other hybridization temperatures (Figure 5.2C). The 42^{o}C hybridization still possesses high signal intensities for the perfect match target. The two nucleotide mismatch target fluorescence intensity is baseline, along with the three nucleotide mismatch target (data not shown). The one nucleotide mismatch target still hybridizes non-specifically with the CT1 probe; however, hybridization efficiency is greatly reduced compared to room temperature hybridization (Figure 5.2A). At 50^{o}C, fluorescence intensity of the fluorescein was greatly reduced due to the instability of the fluorophore at high temperatures (Figure 5.2D). The 37^{o}C hybridization temperature is more stringent; however, this method only selects for the three nucleotide mismatch target, with the two nucleotide mismatch target still hybridizing with the quencher-probe (Figure 5.2B). The room temperature hybridization does not allow for discrimination of even the three nucleotide mismatch. Therefore, the 42^{o}C hybridization temperature in 10 mM borate buffer pH 7.4 was the optimal hybridization buffer for target specificity. The results of the temperature study are indicative of the importance of the melting temperature of the duplex. For the DNA duplex, the miR155 DNA oligonucleotide has a melting temperature of 48^{o}C according to the following equation, where [Na^{+}] is the sodium

concentration and G+C represents the number of guanine and cytosine bases in the oligonucleotide.

$$T_m = 81.6 + 16.6 \times \log[Na^+] + (41 \times G+C / \text{oligonucleotide length}) - (500 / \text{oligo length})$$

It is important to perform hybridization at least 5 degrees below the melting temperature in order to allow for annealing of the two nucleic acid probes. At a temperature greater than the melting temperature, the quencher probe and fluorophore probe should all be separate, thus resulting in a nonspecific increase in signal. The studies performed show the opposite. The reasoning behind this is the thermal instability of the fluorescein label.

Calibration curves were obtained for the DNA targets of both the miR155 and miR103 to determine the detection limit of each. DNA targets were chosen first to evaluate the viability of the assay for the detection of RNA sequences. Hybridization was performed at 42^{o}C for 30 minutes in 10 mM Borate buffer pH 7.4 (Figure 5.3A). The limit of detection, calculated from the equation $S_{LOD}=S_{Blank} + 3*s$, where S_{Blank} is the signal of the reagent blank and s is the standard deviation of the reagent blank, was found to be 7.02 pmoles (46.8 nM) and 12.1 pmoles (80.8 nM) for the miR155 and miR103 DNA targets, respectively. Hybridization was also performed at 37^{o}C (Figure 5.3B) and room temperature (Figure 5.3C) as a comparison. The detection limits obtained for miR155 and miR103 DNA targets at room temperature hybridization were 1.81 pmoles (12.1 nM) and 0.280 pmoles (1.87 nM), respectively. For 37^{o}C hybridization, detection limits for miR155 and miR103 DNA detection were 2.90 pmoles (19.4 nM) and 4.36 pmoles (29.1 nM), respectively. The detection limits become gradually less favorable at

higher temperatures. This result is most likely due to the fact that due to the higher stringency, lower concentration targets cannot hybridize with the CT1 as efficiently. Also, it should be noted that the fluorescence intensity decreased from lower temperature to higher temperature hybridization, owed to the instability of the fluorophore at rising temperatures. Therefore, when optimizing specificity based on hybridization temperature, the detection limit of the assay may suffer slightly.

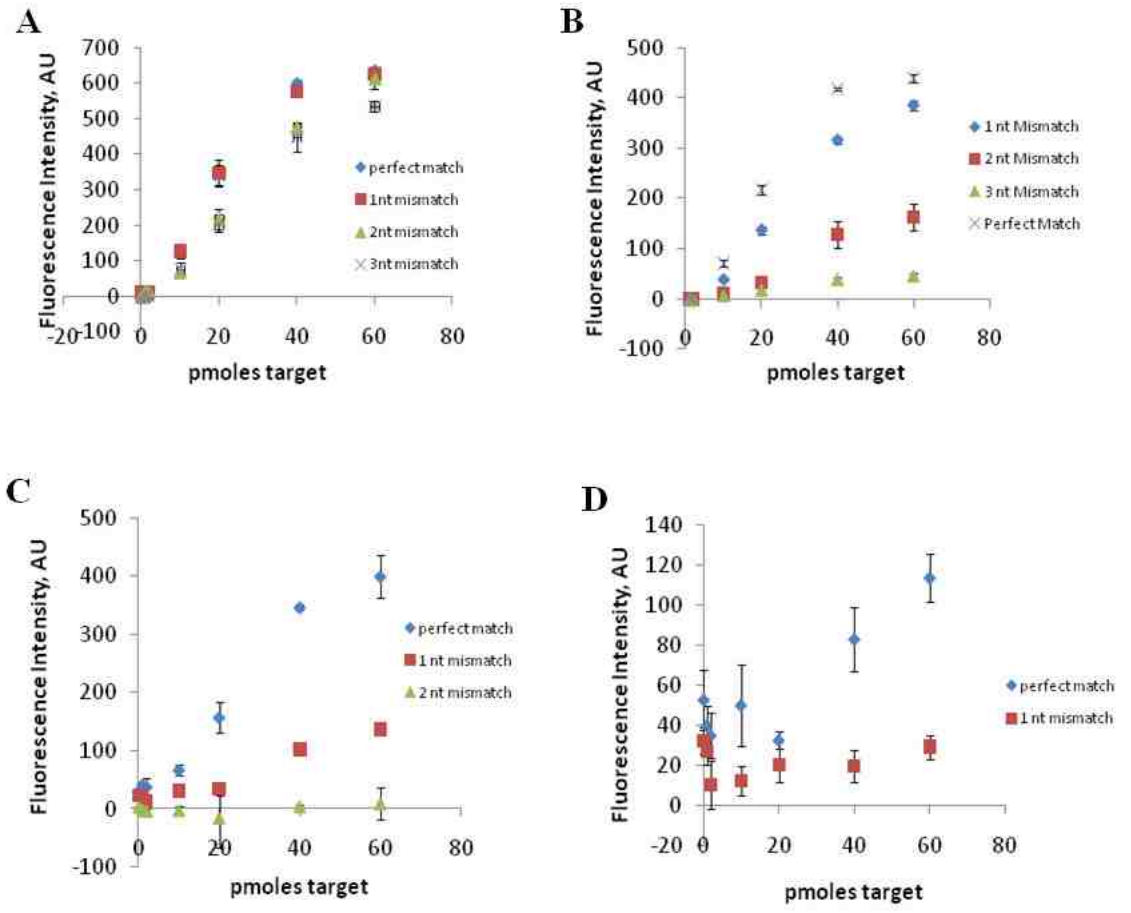

Figure 5.2 Effect of hybridization temperature on miR155 DNA target specificity. A) miR155 DNA specificity at 23°C in 10 mM Borate buffer pH 7.4. B) Specificity at 37°C in 10 mM Borate pH 7.4. C) Specificity at 42°C in 10 mM Borate pH 7.4. D) Specificity at 50°C in 10 mM Borate pH 7.4.

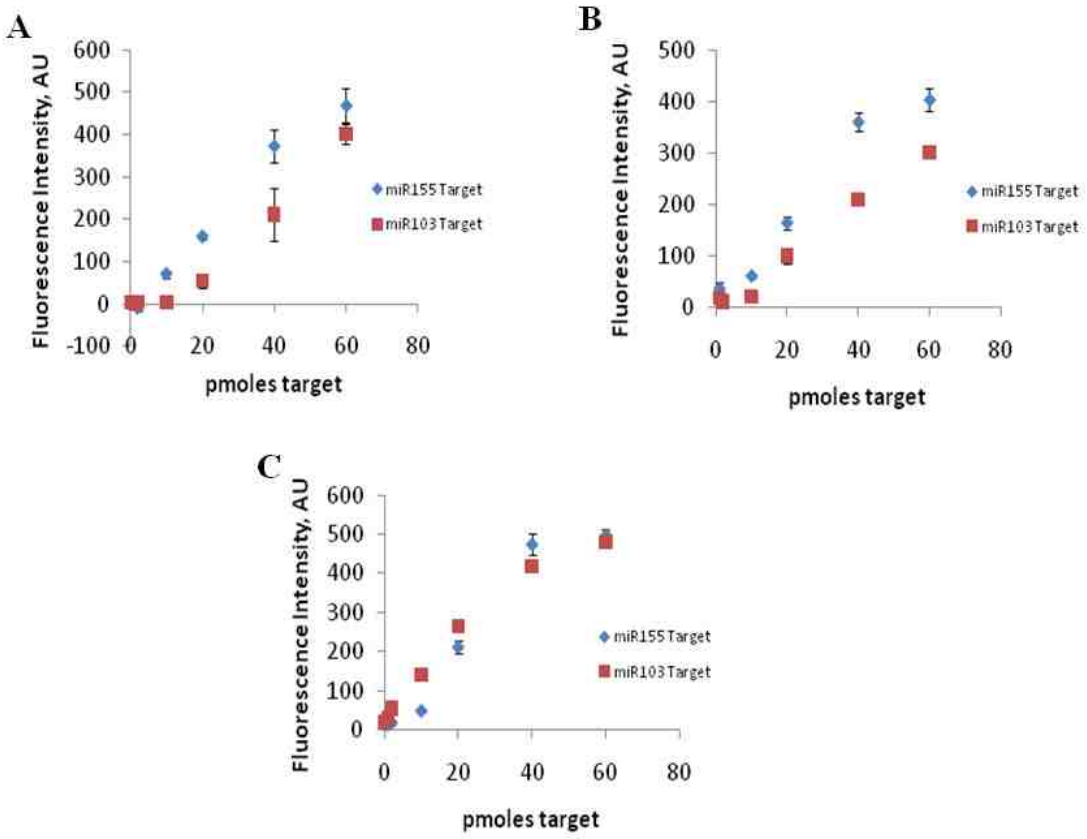

Figure 5.3 Effect of hybridization temperature on miR155 and miR103 dual DNA detection in 10 mM borate buffer. A) Dose-response curve of miR155 and miR103 in 10 mM borate buffer 1 mM EDTA at 42°C hybridization. B) Dose-Response curve at 37°C hybridization C) Dose-response curve at room temperature.

It is important in the development of miRNA detection methods that hybridization can be performed efficiently in more complex matrices. In order to display the robustness of the assay, cellular extract and serum matrices were employed. For the cellular extract matrix, *E. coli* strain ER2566 was utilized. Dual-probe DNA detection was performed in the cellular extract as with the buffer matrix (Figure 5.4A). It is important to note, however, that nuclease activity was quite high in the cellular extract. This high nuclease activity ultimately resulted in the degradation of target, as well as fluorophore-probe and

quencher-probe, resulting in inefficiency of the quencher due to the inability of the fluorophore-probe and quencher-probe to hybridize. The result of this was seen with an increase in fluorescence upon excitation, even in the blank. In order to combat this, cellular extract was heated to deactivate the DNAses, and 2 mM EDTA was added as well. The inactivation of the DNAses through these two steps allowed the assay to be compatible in the cellular extract. The detection limits of miR155 DNA target and miR103 DNA target in the cellular matrix were calculated to be 3.58 pmoles (23.8 nM) and 11.8 pmoles (79.0 nM), respectively. While the optimal hybridization temperature for the miR155 target was 42^{o}C, even with the pretreatment of the cell extract, performing the hybridization at this temperature gave poor results, likely due to heightened nuclease activity. Therefore, the lower temperature of 37^{o}C was employed for hybridization.

In order to perform the assay in serum, first the optimal serum concentration was determined by diluting the serum samples with 10 mM borate buffer, and adding miR155-T1 probe to the solution. Concentrations varied from 100% serum to 0% serum at 25% intervals. It was found that 100% serum completely masks the fluorescence of the FAM fluorophore. As the serum concentration decreases, the FAM fluorescence intensity increases. A serum concentration of 25% was chosen for the assays. For the dual DNA target detection in serum samples, the detection limits were calculated to be 8.89 pmoles (59.3 nM) and 8.38 pmoles (55.9 nM) for the miR155 and miR103 DNA targets, respectively (Figure 5.4B).

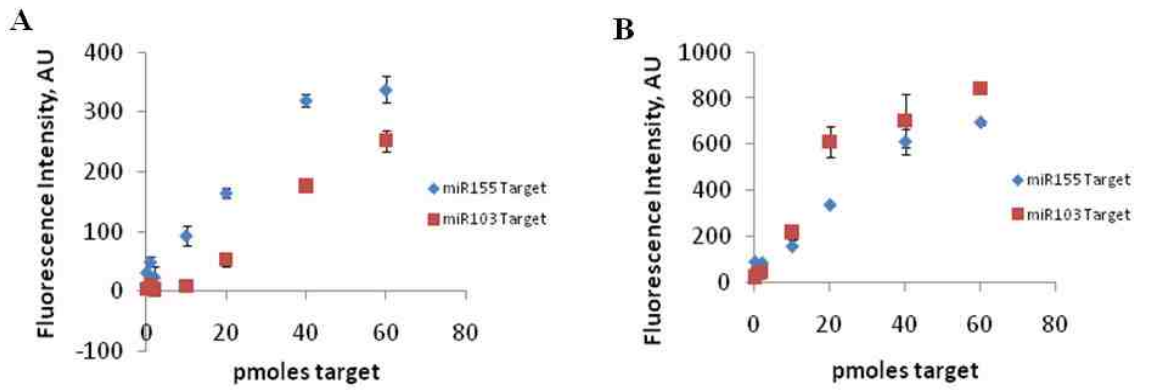

Figure 5.4 miR155 and miR103 dual DNA target detection in cell extract and serum. A) Dose-response curve in *E. coli* ER2566 cell extract 37°C hybridization. B) Dose-response curve in 25% serum.

To apply this assay to the detection of miRNA, synthetic RNAs were employed. Both miR155 and miR103 RNAs were detected simultaneously in solution. One of the challenges with studying RNAs is the presence of RNAses, which can rapidly degrade RNAs. Therefore, nuclease-free DEPC-treated buffers were employed in all RNA detection assays. Dual-probe detection was first performed in solution. The RNA detection resulted in detection limits of 6.03 pmoles (40.2 nM) for the miR155 target, and 17.2 pmoles (115 nM) for the miR103 target (Figure 5.5A). Compared to the DNA targets, the miR155 detection limits were quite similar; however, the miR103 differed substantially, which may be due to trace levels of RNAses in the buffers. The compatibility of the synthetic miRNA detection in cellular extract was tested as well. As with the DNA target detection, the cellular extract was treated before use by heating to 90°C for 5 min and adding EDTA. Observed detection limits for miR155 and miR103 were 6.78 pmoles (45.2 nM) and 29.7 pmoles (198 nM), respectively (Figure 5.5B). The slope of the calibration curves for the miR155 and miR103 were quite different, however.

The miR155 displayed the same fluorescence intensity profile that the DNA target did, while the miR103 intensities were quite low compared to the DNA. To determine whether the received stock RNA oligo was already degraded, the concentration of miR103 RNA was tested along with imaging the RNA on an agarose gel. Both were validated in the presence of the RNA. While the assay was compatible in cellular extract for RNA detection, the RNAs immediately degraded in the presence of serum, resulting in a rapid decrease in fluorescence. Attempts to heat the serum and add EDTA did not improve the detection. It was therefore necessary to treat the serum with an RNAse inhibitor prior to addition of synthetic RNA. RNAsin is a solution containing a 56 kDa protein which functions by binding to RNAses in a 1:1 ratio, inhibiting RNAse activity. RNAsin was added to the serum in a 1:10 ratio of inhibitor (64 U/ μL) to serum, followed by incubation for 3 h at 37^{o}C and normal assay preparation. The addition of the RNAsin greatly increased RNA stability for the miR103, displaying detection limits of 20.4 pmoles (136 nM); however the miR155 still degraded (Figure 5.5C). It should be noted that naturally occurring miRNA is stable in serum compared to synthetic RNA [159]. RNAsin is a solution containing a 56 kDa protein which functions by binding to RNAses in a 1:1 ratio, inhibiting RNAse activity. RNAsin was added to the serum in a 1:10 ratio of inhibitor (64 U/ μL) to serum, followed by incubation for 3 h at 37^{o}C and normal assay preparation. The addition of the RNAsin greatly increased RNA stability for the miR103, displaying detection limits of 20.4 pmoles (136 nM); however the miR155 still degraded (Figure 5.5C). It should be noted that naturally occurring miRNA is stable in serum compared to synthetic RNA [159]. This suggests that serum miRNAs must be protected from RNAses in a way that is not possible for synthetic RNA. The reason behind RNA

protection in serum has been attributed to its packaging in vesicles [32], whereas unprotected spiked RNA is highly unstable. Since microRNA has been found to be present in serum, this method could allow for microRNA detection directly in serum after concentration of the samples.

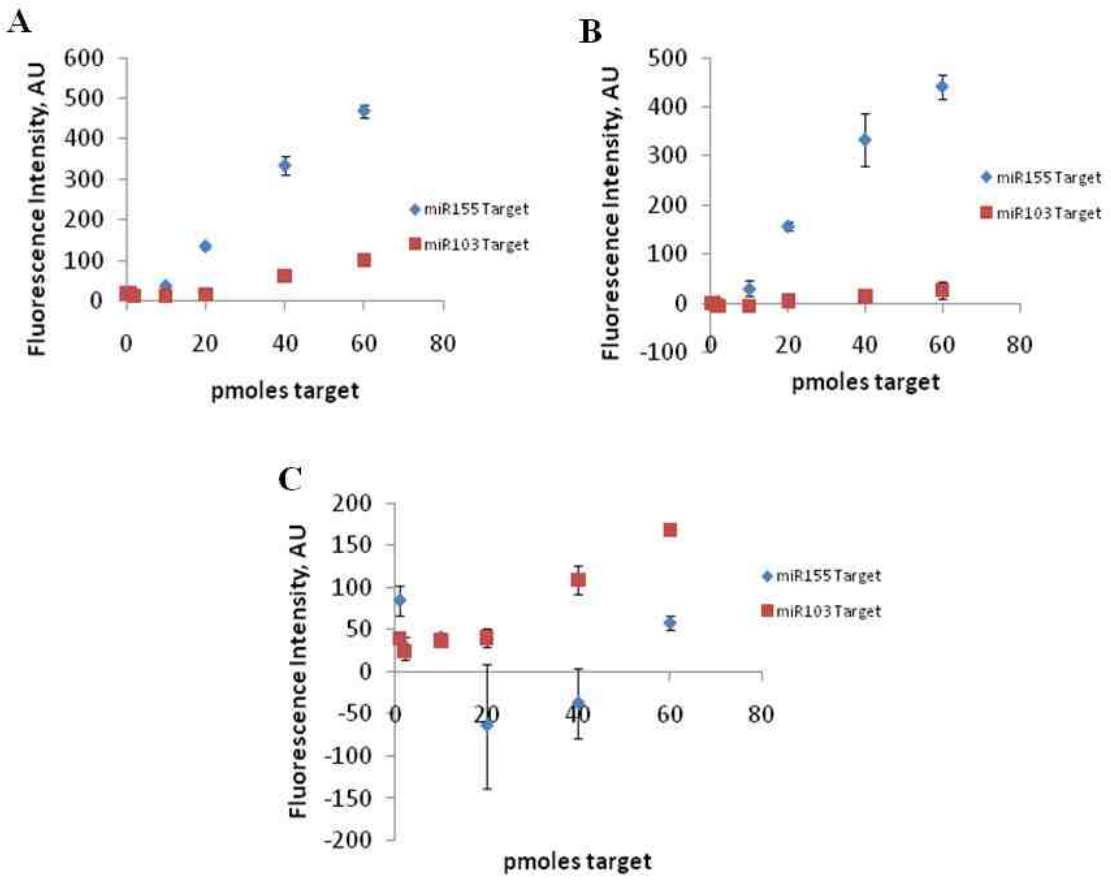

Figure 5.5 miR155 and miR103 dual RNA target detection. A) Dual detection in 10 mM Borate buffer 0.1%DEPC with 37°C hybridization. B) Dual detection in E. coli ER2566 cell extract with 37°C hybridization. C) Dual detection in 25% serum with 37°C hybridization.

5.4 Conclusions

This method was capable of detecting dual target nucleic acid in a wide variety of matrices with detection limits in the nanomolar range with two nucleotide specificity. The specificity can be further optimized through the incorporation of LNAs in the CT1/2

or T1/2 probe sequences. Also, additives such as formamide may increase specificity to discriminate single nucleotide mismatches. This method was very rapid, performed in only 30 minutes. Dual targets were able to be detected simultaneously through measuring the fluorescence intensities of the two fluorophore emission wavelengths. This method also displayed the ability to detect synthetic microRNA in the nanomolar range. Although the synthetic RNA is not stable in untreated serum, addition of RNAse inhibitors to buffer allowed for miR103 target detection. Due to the fact that native serum miRNAs are stable, this method can be applied to the direct detection of miRNA in serum. This method represents a simple, rapid, sensitive detection method for the quantitation of dual microRNAs in solution, which can ultimately serve as a screening method for microRNA expression profiles.

CHAPTER 6: CONCLUSION

6.1 Summary of Developed Methods

With the recent implication of miRNA levels and their role in disease progression, it is extremely important to be able to detect this small, 18-24 nucleotide length RNA molecule. While multiple methods of miRNA detection have been developed previously, each method suffers at least one drawback, whether lacking specificity, sensitivity, a lengthy assay, or requiring expensive equipment. In order to overcome these drawbacks, three novel miRNA detection methods were developed based on employing *Renilla* luciferase as a label and also one method employing fluorophores as labels. All four methods are rapid, simple, and do not require highly expensive equipment. The following is a summary of each of the four detection methods, along with future directions which can be applied to expand these four methods' utilitity to miRNA detection. A table summarizing the attributes and specifics of each of the four methods is found in this section (Table 6.1).

First, a solid-phase miRNA detection method employing *Renilla* luciferase as a label was developed. The advantages of this assay are its application in a microplate format and thus high-throughput screening capability, along with its high sensitivity. This method produced a detection limit of synthetic miR21 RNA in phosphate buffered saline of 5 femtomoles (25 pM). This method was also applied to detection of real miR21 in

two mammalian cell lines. A drawback of this method is that it relies on a decrease in bioluminescence intensity upon increasing amounts of target, rather than an increase in bioluminescence intensity. Another drawback for this assay is that multiple wash steps to remove unbound oligonucleotide probes are required, thus increasing the total assay time. For this method, the total assay time after blocking the well-plate with bovine serum albumin was 90 minutes. Although the assay is 90 minutes in length, it is still advantageous over Northern blotting. It is advantageous to microarrays and qRT-PCR in terms of cost.

To expand the utility of this miRNA detection method, and apply it to diagnostics, serum extract samples from patients with and without breast cancer have been collected and are being analyzed in the lab based on their miR21 expression levels. The solid-phase method is being employed to analyze the samples, and a modified *Renilla* luciferase protein containing eight mutations (RL8) is being employed which possesses enhanced light output compared to the native *Renilla* luciferase employed for the work in this dissertation [160]. In the future, this method should be optimized to selectively detect perfect match target miRNA from single nucleotide mismatch RNA.

Second, a BRET-based detection method was employed to detect a DNA oligonucleotide corresponding to miR21. The BRET donor was Rluc, while the BRET acceptor was a quantum dot. The advantages of this assay were that it can be performed in the solution-phase, and thus does not require the washing steps as with solid-phase assays. Also, this method is very rapid, with a total assay time of only 30 minutes. The BRET-based assay was shown to detect as little as 4 picomoles of target (20 nM). The disadvantages of this assay are that it also relies on a decrease in BRET signal (quantum

dot emission) upon increasing the amount of target present in the sample. Another disadvantage is the detection limit is not as desirable as with the solid-phase method. The reasoning behind this is that resonance energy transfer-based assays are not as sensitive as standard luminescence assays involving a single label. Smaller diameter quantum dots can be employed to combat this sensitivity issue in order to decrease the distance between donor and acceptor. Despite the drawback of limited sensitivity, the total assay time is a substantial advantage over the solid-phase assay.

In the future, this method can be applied to the detection of the breast cancer patient sera samples that are being employed for the solid-phase assay. Along with the miR21 detection, probes can be employed along with spectrally distinct quantum dots, such that multiple miRNAs can be detected in a multiplex format.

Third, a protein complementation-based detection method was employed for the analysis of a synthetic DNA oligonucleotide mimicking miR21 microRNA. This method was developed based on previous reports that proteins, when genetically engineered to form two inactive fragments, may reform an active enzyme when coming into close proximity with one another. As with the BRET-based method, an advantage of this method is that the total assay time is 30 minutes. Another advantage of this assay is that the background signal is insignificant, unlike the high background associated with fluorophore-based applications. A disadvantage of the assay is that in order to detect miRNA, a decrease in signal is observed.

In the future, the split luciferase method should be employed to detect real miRNA samples such as the serum extract samples. Differing split sites should also be tested to determine if luminescence recovery increases compared to the current split site.

Also, the split luciferase method should be applied to the detection of larger, precursor miRNA, such that the oligonucleotides bound to the two fragments will hybridize adjacently to one another, resulting in an increase in signal upon target detection, rather than a decrease.

Fourth, a fluorescence-based miRNA detection method was developed in which fluorophore-labeled oligonucleotides hybridize with quencher-labeled oligonucleotides in the absence of target. In the presence of target, however, the target hybridizes with the quencher-probe, thus preventing the fluorophore-probe from hybridizing with the quencher-probe. Therefore, in the presence of target, the fluorescence intensity will increase. This method was very rapid, with the ability to be performed in 30 minutes. Another advantage was the ability to detect dual targets in the same solution due to the incorporation of spectrally distinct fluorophores on separate oligonucleotide probe sets. The detection limit of this assay was approximately 2-80 nM for both independent and dual target detection. A limitation to this assay is that the detection limit is not as desirable as with the solid-phase method. Another limitation is the stability of the fluorophores at high temperatures. Hybridization temperatures above 50^{o}C cannot be used due to a loss of fluorescence of the fluorophore. Despite the drawbacks, the total assay time, as with the other solution-phase assays developed, and also the need for only a fluorescence microplate reader, make the fluorophore/quencher method desirable for miRNA quantitation. In the future, this method should be applied to the detection of patient samples containing miR155 and miR103.

Comparing each of the four detection methods, the solid-phase method is the most desirable for diagnostic applications due to its high sensitivity and low cost. The

remaining three methods should be tested for their diagnostic value in the analysis of patient samples.

Table 6.1 Description of miRNA detection methods developed in this dissertation

Detection Method	Description	Detection Limit
Solid-phase	Oligonucleotide probe with the same sequence as target miR21 is labeled with Rluc. Target and Rluc-DNA conjugate compete to hybridize with a biotinylated capture probe. Rluc signal decreases upon increasing concentration	5 fmoles (25 pM)
BRET-based	Solution-phase method where oligonucleotide probe with the same sequence as target is labeled with Rluc. Oligo probe complementary to target is labeled with QD. In absence of target, BRET from Rluc to QD occurs. In presence of target, less QD-probe and Rluc-probe will hybridize, resulting in less energy transfer between the Rluc and QD.	4 pmoles (20 nM)
Protein reassembly-based	Solution-phase method where oligonucleotide probe with the same sequence as target is labeled with C-terminal fragment. An oligo probe with the complementary sequence to target is labeled with N-terminal fragment. In absence of target, reassembly of Rluc occurs, resulting in generation of luminescence upon addition of coelenterazine. In the presence of target, less reassembly occurs, resulting in a decrease in luminescence intensity upon addition of coelenterazine.	3.4 nmoles (17 µM)
Fluorophore/ quencher-based	Solution-phase method where oligo probe with the same sequence as target is labeled with fluorophore. An oligo probe with a complementary sequence to the target is labeled with a quencher probe. In the absence of target, the fluorophore-probe and quencher-probe hybridize, resulting in a quenching of fluorescence upon excitation. In the presence of target, less fluorophore-probe hybridizes with quencher-probe, resulting in an increase in fluorescence intensity upon excitation.	~0.3-10 pmoles (~2-80 nM)

6.2 Comparison of Developed miRNA Detection Methods to Prior Methods

Comparing the developed methods in this dissertation to the methods outlined in the introduction, the detection limit of the solid-phase method rivals that of the new and emerging miRNA detection methods. What separates the solid-phase method in this work from the other methods is assay simplicity as well as assay cost. None of the prior methods have employed bioluminescent proteins which can be reproducibly produced,

thus lowering costs. On the basis of cost and simplicity, the solid-phase method is an improvement over all previous miRNA detection methods.

The BRET-based method, while lacking in sensitivity, is superior to all the previous methods in that the total assay time is very rapid, and only a microplate reader is needed for detection. The BRET-based method is also superior to the electrochemical and optical methods in that multiplex detection can be performed, although not outlined in the work presented here.

The protein reassembly-based method, like the BRET-based method, is inferior to the previous methods in terms of sensitivity. While lacking in sensitivity this method is very rapid, simple, and requires only a microplate reader for detection of target. This assay is also very cost-effective, in that the two Rluc fragments can be reproducibly produced. Considering the previous methods require costly labels, costly solid-supports, as well as costly instrumentation, this method is very advantageous compared to previous methods.

The fluorophore/quencher-based method also has the drawback of low sensitivity compared to the previous methods; however, this method is very rapid, taking only 30 minutes to detect target. This method is superior to the electrochemical and optical methods in that detection of multiple targets can be performed in a single well.

6.3 Concluding Remarks

The methods developed in this dissertation all have the ability to be applied to miRNA diagnostics. Therefore, it would be beneficial to further develop these methods in order to discover their full diagnostic potential. Due to the heightened understanding of

miRNA expression levels, and their implications in disease progression, it would be beneficial to the medical world to have diagnostic devices with technological components allowing for miRNA quantitation. Already, miRNA expression levels are capable of successfully identifying tumor types in cancer patients. It is possible that one day, miRNA expression levels may be able to diagnose cancer in the early stages of development. Therefore, it is highly important that scientists continue to pursue methods for miRNA detection which are capable of translating into the clinical setting. Perhaps in the future, the component technologies developed in this dissertation may be applied to clinical diagnostic screening devices.

LIST OF REFERENCES

LIST OF REFERENCES

(1) Lee, R. C.; Feinbaum, R. L.; Ambros, V. Cell 1993, 75, 843-854.
(2) Boehm, M.; Slack, F. Science 2005, 310, 1954-1957.
(3) Reinhart, B. J.; Slack, F. J.; Basson, M.; Pasquinelli, A. E.; Bettinger, J. C.; Rougvie, A. E.; Horvitz, H. R.; Ruvkun, G. Nature 2000, 403, 901-906.
(4) Lau, N. C.; Lim, L. P.; Weinstein, E. G.; Bartel, D. P. Science 2001, 294, 858-862.
(5) Lee, R. C.; Ambros, V. Science 2001, 294, 862-864.
(6) Lagos-Quintana, M.; Rauhut, R.; Lendeckel, W.; Tuschl, T. Science 2001, 294, 853-858.
(7) Hwang, H. W.; Mendell, J. T. British Journal of Cancer 2006, 94, 776-780.
(8) Grishok, A.; Pasquinelli, A. E.; Conte, D.; Li, N.; Parrish, S.; Ha, I.; Baillie, D. L.; Fire, A.; Ruvkun, G.; Mello, C. C. Cell 2001, 106, 23-34.
(9) Griffiths-Jones, S. Nucleic Acids Research 2004, 32, D109-D111.
(10) Griffiths-Jones, S.; Grocock, R. J.; van Dongen, S.; Bateman, A.; Enright, A. J. Nucleic Acids Research 2006, 34, D140-D144.

(11) Carninci, P.; Kasukawa, T.; Katayama, S.; Gough, J.; Frith, M. C.; Maeda, N.; Oyama, R.; Ravasi, T.; Lenhard, B.; Wells, C.; Kodzius, R.; Shimokawa, K.; Bajic, V. B.; Brenner, S. E.; Batalov, S.; Forrest, A. R.; Zavolan, M.; Davis, M. J.; Wilming, L. G.; Aidinis, V.; Allen, J. E.; Ambesi-Impiombato, A.; Apweiler, R.; Aturaliya, R. N.; Bailey, T. L.; Bansal, M.; Baxter, L.; Beisel, K. W.; Bersano, T.; Bono, H.; Chalk, A. M.; Chiu, K. P.; Choudhary, V.; Christoffels, A.; Clutterbuck, D. R.; Crowe, M. L.; Dalla, E.; Dalrymple, B. P.; de Bono, B.; Della Gatta, G.; di Bernardo, D.; Down, T.; Engstrom, P.; Fagiolini, M.; Faulkner, G.; Fletcher, C. F.; Fukushima, T.; Furuno, M.; Futaki, S.; Gariboldi, M.; Georgii-Hemming, P.; Gingeras, T. R.; Gojobori, T.; Green, R. E.; Gustincich, S.; Harbers, M.; Hayashi, Y.; Hensch, T. K.; Hirokawa, N.; Hill, D.; Huminiecki, L.; Iacono, M.; Ikeo, K.; Iwama, A.; Ishikawa, T.; Jakt, M.; Kanapin, A.; Katoh, M.; Kawasawa, Y.; Kelso, J.; Kitamura, H.; Kitano, H.; Kollias, G.; Krishnan, S. P.; Kruger, A.; Kummerfeld, S. K.; Kurochkin, I. V.; Lareau, L. F.; Lazarevic, D.; Lipovich, L.; Liu, J.; Liuni, S.; McWilliam, S.; Madan Babu, M.; Madera, M.; Marchionni, L.; Matsuda, H.; Matsuzawa, S.; Miki, H.; Mignone, F.; Miyake, S.; Morris, K.; Mottagui-Tabar, S.; Mulder, N.; Nakano, N.; Nakauchi, H.; Ng, P.; Nilsson, R.; Nishiguchi, S.; Nishikawa, S.; Nori, F.; Ohara, O.; Okazaki, Y.; Orlando, V.; Pang, K. C.; Pavan, W. J.; Pavesi, G.; Pesole, G.; Petrovsky, N.; Piazza, S.; Reed, J.; Reid, J. F.; Ring, B. Z.; Ringwald, M.; Rost, B.; Ruan, Y.; Salzberg, S. L.; Sandelin, A.; Schneider, C.; Schonbach, C.; Sekiguchi, K.; Semple, C. A.; Seno, S.; Sessa, L.; Sheng, Y.; Shibata, Y.; Shimada, H.; Shimada, K.; Silva, D.; Sinclair, B.; Sperling, S.; Stupka, E.; Sugiura, K.; Sultana, R.; Takenaka, Y.; Taki, K.; Tammoja, K.; Tan, S. L.; Tang, S.; Taylor, M. S.; Tegner, J.; Teichmann, S. A.; Ueda, H. R.; van Nimwegen, E.; Verardo, R.; Wei, C. L.; Yagi, K.; Yamanishi, H.; Zabarovsky, E.; Zhu, S.; Zimmer, A.; Hide, W.; Bult, C.; Grimmond, S. M.; Teasdale, R. D.; Liu, E. T.; Brusic, V.; Quackenbush, J.; Wahlestedt, C.; Mattick, J. S.; Hume, D. A.; Kai, C.; Sasaki, D.; Tomaru, Y.; Fukuda, S.; Kanamori-Katayama, M.; Suzuki, M.; Aoki, J.; Arakawa, T.; Iida, J.; Imamura, K.; Itoh, M.; Kato, T.; Kawaji, H.; Kawagashira, N.; Kawashima, T.; Kojima, M.; Kondo, S.; Konno, H.; Nakano, K.; Ninomiya, N.; Nishio, T.; Okada, M.; Plessy, C.; Shibata, K.; Shiraki, T.; Suzuki, S.; Tagami, M.; Waki, K.; Watahiki, A.; Okamura-Oho, Y.; Suzuki, H.; Kawai, J.; Hayashizaki, Y. Science 2005, 309, 1559-1563.

(12) Katayama, S.; Tomaru, Y.; Kasukawa, T.; Waki, K.; Nakanishi, M.; Nakamura, M.; Nishida, H.; Yap, C. C.; Suzuki, M.; Kawai, J.; Suzuki, H.; Carninci, P.; Hayashizaki, Y.; Wells, C.; Frith, M.; Ravasi, T.; Pang, K. C.; Hallinan, J.; Mattick, J.; Hume, D. A.; Lipovich, L.; Batalov, S.; Engstrom, P. G.; Mizuno, Y.; Faghihi, M. A.; Sandelin, A.; Chalk, A. M.; Mottagui-Tabar, S.; Liang, Z.; Lenhard, B.; Wahlestedt, C. Science 2005, 309, 1564-1566.

(13) Lee, Y.; Jeon, K.; Lee, J. T.; Kim, S.; Kim, V. N. Embo J 2002, 21, 4663-4670.

(14) Lee, Y.; Ahn, C.; Han, J.; Choi, H.; Kim, J.; Yim, J.; Lee, J.; Provost, P.; Radmark, O.; Kim, S.; Kim, V. N. Nature 2003, 425, 415-419.

(15) Lund, E.; Guttinger, S.; Calado, A.; Dahlberg, J. E.; Kutay, U. Science 2004, 303, 95-98.

(16) Bohnsack, M. T.; Czaplinski, K.; Gorlich, D. Rna 2004, 10, 185-191.
(17) Zeng, Y.; Cullen, B. R. Nucleic Acids Res 2004, 32, 4776-4785.
(18) Yi, R.; Qin, Y.; Macara, I. G.; Cullen, B. R. Genes Dev 2003, 17, 3011-3016.
(19) Hammond, S. M.; Boettcher, S.; Caudy, A. A.; Kobayashi, R.; Hannon, G. J. Science 2001, 293, 1146-1150.
(20) Bartel, D. P. Cell 2004, 116, 281-297.
(21) Hammond, S. M. FEBS Lett 2005, 579, 5822-5829.
(22) Kim, V. N. Genes Dev 2006, 20, 1993-1997.
(23) Jinek, M.; Doudna, J. A. Nature 2009, 457, 405-412.
(24) Halder, J.; Kamat, A. A.; Landen, C. N., Jr.; Han, L. Y.; Lutgendorf, S. K.; Lin, Y. G.; Merritt, W. M.; Jennings, N. B.; Chavez-Reyes, A.; Coleman, R. L.; Gershenson, D. M.; Schmandt, R.; Cole, S. W.; Lopez-Berestein, G.; Sood, A. K. Clin Cancer Res 2006, 12, 4916-4924.
(25) Peer, D.; Park, E. J.; Morishita, Y.; Carman, C. V.; Shimaoka, M. Science 2008, 319, 627-630.
(26) Liu, Z.; Winters, M.; Holodniy, M.; Dai, H. Angew Chem Int Ed Engl 2007, 46, 2023-2027.
(27) Qin, X. F.; An, D. S.; Chen, I. S.; Baltimore, D. Proc Natl Acad Sci U S A 2003, 100, 183-188.
(28) Gilad, S.; Meiri, E.; Yogev, Y.; Benjamin, S.; Lebanony, D.; Yerushalmi, N.; Benjamin, H.; Kushnir, M.; Cholakh, H.; Melamed, N.; Bentwich, Z.; Hod, M.; Goren, Y.; Chajut, A. PLoS One 2008, 3, e3148.
(29) Hanke, M.; Hoefig, K.; Merz, H.; Feller, A. C.; Kausch, I.; Jocham, D.; Warnecke, J. M.; Sczakiel, G. Urol Oncol 2009.
(30) Xie, Y.; Todd, N. W.; Liu, Z.; Zhan, M.; Fang, H.; Peng, H.; Alattar, M.; Deepak, J.; Stass, S. A.; Jiang, F. Lung Cancer 2010, 67, 170-176.
(31) Park, N. J.; Zhou, H.; Elashoff, D.; Henson, B. S.; Kastratovic, D. A.; Abemayor, E.; Wong, D. T. Clin Cancer Res 2009, 15, 5473-5477.
(32) El-Hefnawy, T.; Raja, S.; Kelly, L.; Bigbee, W. L.; Kirkwood, J. M.; Luketich, J. D.; Godfrey, T. E. Clin Chem 2004, 50, 564-573.
(33) Sassen, S.; Miska, E. A.; Caldas, C. Virchows Arch 2008, 452, 1-10.
(34) Calin, G. A.; Dumitru, C. D.; Shimizu, M.; Bichi, R.; Zupo, S.; Noch, E.; Aldler, H.; Rattan, S.; Keating, M.; Rai, K.; Rassenti, L.; Kipps, T.; Negrini, M.; Bullrich, F.; Croce, C. M. Proc Natl Acad Sci U S A 2002, 99, 15524-15529.
(35) Iorio, M. V.; Ferracin, M.; Liu, C. G.; Veronese, A.; Spizzo, R.; Sabbioni, S.; Magri, E.; Pedriali, M.; Fabbri, M.; Campiglio, M.; Menard, S.; Palazzo, J. P.; Rosenberg, A.; Musiani, P.; Volinia, S.; Nenci, I.; Calin, G. A.; Querzoli, P.; Negrini, M.; Croce, C. M. Cancer Res 2005, 65, 7065-7070.
(36) Chan, J. A.; Krichevsky, A. M.; Kosik, K. S. Cancer Res 2005, 65, 6029-6033.
(37) Huang, Q.; Gumireddy, K.; Schrier, M.; le Sage, C.; Nagel, R.; Nair, S.; Egan, D. A.; Li, A.; Huang, G.; Klein-Szanto, A. J.; Gimotty, P. A.; Katsaros, D.; Coukos, G.; Zhang, L.; Pure, E.; Agami, R. Nat Cell Biol 2008, 10, 202-210.
(38) Jagla, M.; Feve, M.; Kessler, P.; Lapouge, G.; Erdmann, E.; Serra, S.; Bergerat, J. P.; Ceraline, J. Endocrinology 2007, 148, 4334-4343.

(39) Chen, J. F.; Murchison, E. P.; Tang, R.; Callis, T. E.; Tatsuguchi, M.; Deng, Z.; Rojas, M.; Hammond, S. M.; Schneider, M. D.; Selzman, C. H.; Meissner, G.; Patterson, C.; Hannon, G. J.; Wang, D. Z. Proc Natl Acad Sci U S A 2008, 105, 2111-2116.
(40) Lukiw, W. J.; Zhao, Y.; Cui, J. G. J Biol Chem 2008, 283, 31315-31322.
(41) Thum, T.; Gross, C.; Fiedler, J.; Fischer, T.; Kissler, S.; Bussen, M.; Galuppo, P.; Just, S.; Rottbauer, W.; Frantz, S.; Castoldi, M.; Soutschek, J.; Koteliansky, V.; Rosenwald, A.; Basson, M. A.; Licht, J. D.; Pena, J. T.; Rouhanifard, S. H.; Muckenthaler, M. U.; Tuschl, T.; Martin, G. R.; Bauersachs, J.; Engelhardt, S. Nature 2008, 456, 980-984.
(42) Xiao, C.; Rajewsky, K. Cell 2009, 136, 26-36.
(43) Krutzfeldt, J.; Rajewsky, N.; Braich, R.; Rajeev, K. G.; Tuschl, T.; Manoharan, M.; Stoffel, M. Nature 2005, 438, 685-689.
(44) Scherr, M.; Venturini, L.; Battmer, K.; Schaller-Schoenitz, M.; Schaefer, D.; Dallmann, I.; Ganser, A.; Eder, M. Nucleic Acids Res 2007, 35, e149.
(45) Ovcharenko, D.; Kelnar, K.; Johnson, C.; Leng, N.; Brown, D. Cancer Res 2007, 67, 10782-10788.
(46) Esquela-Kerscher, A.; Trang, P.; Wiggins, J. F.; Patrawala, L.; Cheng, A.; Ford, L.; Weidhaas, J. B.; Brown, D.; Bader, A. G.; Slack, F. J. Cell Cycle 2008, 7, 759-764.
(47) Trang, P.; Medina, P. P.; Wiggins, J. F.; Ruffino, L.; Kelnar, K.; Omotola, M.; Homer, R.; Brown, D.; Bader, A. G.; Weidhaas, J. B.; Slack, F. J. Oncogene 2010, 29, 1580-1587.
(48) Takeshita, F.; Patrawala, L.; Osaki, M.; Takahashi, R. U.; Yamamoto, Y.; Kosaka, N.; Kawamata, M.; Kelnar, K.; Bader, A. G.; Brown, D.; Ochiya, T. Mol Ther 2010, 18, 181-187.
(49) Liu, Z.; Chen, K.; Davis, C.; Sherlock, S.; Cao, Q.; Chen, X.; Dai, H. Cancer Res 2008, 68, 6652-6660.
(50) Wang, X.; Ren, J.; Qu, X. ChemMedChem 2008, 3, 940-945.
(51) Kam, N. W.; Liu, Z.; Dai, H. J Am Chem Soc 2005, 127, 12492-12493.
(52) Singh, R.; Pantarotto, D.; Lacerda, L.; Pastorin, G.; Klumpp, C.; Prato, M.; Bianco, A.; Kostarelos, K. Proc Natl Acad Sci U S A 2006, 103, 3357-3362.
(53) Driskell, J. D.; Seto, A. G.; Jones, L. P.; Jokela, S.; Dluhy, R. A.; Zhao, Y. P.; Tripp, R. A. Biosens Bioelectron 2008, 24, 923-928.
(54) Cissell, K. A.; Shrestha, S.; Deo, S. K. Analytical Chemistry 2007, 79, 4754-4761.
(55) Wark, A. W.; Lee, H. J.; Corn, R. M. Angew Chem Int Ed Engl 2008, 47, 644-652.
(56) Schmittgen, T. D.; Jiang, J.; Liu, Q.; Yang, L. Nucleic Acids Res 2004, 32, e43.
(57) Cummins, J. M.; He, Y.; Leary, R. J.; Pagliarini, R.; Diaz, L. A., Jr.; Sjoblom, T.; Barad, O.; Bentwich, Z.; Szafranska, A. E.; Labourier, E.; Raymond, C. K.; Roberts, B. S.; Juhl, H.; Kinzler, K. W.; Vogelstein, B.; Velculescu, V. E. Proc Natl Acad Sci U S A 2006, 103, 3687-3692.
(58) Lagos-Quintana, M.; Rauhut, R.; Lendeckel, W.; Tuschl, T. Science 2001, 294, 853-858.

(59) Valoczi, A.; Hornyik, C.; Varga, N.; Burgyan, J.; Kauppinen, S.; Havelda, Z. Nucleic Acids Res 2004, 32, e175.
(60) Mattie, M. D.; Benz, C. C.; Bowers, J.; Sensinger, K.; Wong, L.; Scott, G. K.; Fedele, V.; Ginzinger, D.; Getts, R.; Haqq, C. Mol Cancer 2006, 5, 24.
(61) Miska, E. A.; Alvarez-Saavedra, E.; Townsend, M.; Yoshii, A.; Sestan, N.; Rakic, P.; Constantine-Paton, M.; Horvitz, H. R. Genome Biol 2004, 5, R68.
(62) Yeung, M. L.; Bennasser, Y.; Myers, T. G.; Jiang, G.; Benkirane, M.; Jeang, K. T. Retrovirology 2005, 2, 81.
(63) Yang, H.; Kong, W.; He, L.; Zhao, J. J.; O'Donnell, J. D.; Wang, J.; Wenham, R. M.; Coppola, D.; Kruk, P. A.; Nicosia, S. V.; Cheng, J. Q. Cancer Res 2008, 68, 425-433.
(64) Thomson, J. M.; Parker, J.; Perou, C. M.; Hammond, S. M. Nat Methods 2004, 1, 47-53.
(65) Nelson, P. T.; Baldwin, D. A.; Scearce, L. M.; Oberholtzer, J. C.; Tobias, J. W.; Mourelatos, Z. Nat Methods 2004, 1, 155-161.
(66) Babak, T.; Zhang, W.; Morris, Q.; Blencowe, B. J.; Hughes, T. R. RNA 2004, 10, 1813-1819.
(67) Sun, Y.; Koo, S.; White, N.; Peralta, E.; Esau, C.; Dean, N. M.; Perera, R. J. Nucleic Acids Res 2004, 32, e188.
(68) Liu, C. G.; Calin, G. A.; Meloon, B.; Gamliel, N.; Sevignani, C.; Ferracin, M.; Dumitru, C. D.; Shimizu, M.; Zupo, S.; Dono, M.; Alder, H.; Bullrich, F.; Negrini, M.; Croce, C. M. Proc Natl Acad Sci U S A 2004, 101, 9740-9744.
(69) Lu, J.; Getz, G.; Miska, E. A.; Alvarez-Saavedra, E.; Lamb, J.; Peck, D.; Sweet-Cordero, A.; Ebert, B. L.; Mak, R. H.; Ferrando, A. A.; Downing, J. R.; Jacks, T.; Horvitz, H. R.; Golub, T. R. Nature 2005, 435, 834-838.
(70) Liang, R. Q.; Li, W.; Li, Y.; Tan, C. Y.; Li, J. X.; Jin, Y. X.; Ruan, K. C. Nucleic Acids Res 2005, 33, e17.
(71) Gao, Z.; Yang, Z. Anal Chem 2006, 78, 1470-1477.
(72) Tan, W.; Fang, X.; Li, J.; Liu, X. Chemistry 2000, 6, 1107-1111.
(73) Hartig, J. S.; Grune, I.; Najafi-Shoushtari, S. H.; Famulok, M. J Am Chem Soc 2004, 126, 722-723.
(74) Neely, L. A.; Patel, S.; Garver, J.; Gallo, M.; Hackett, M.; McLaughlin, S.; Nadel, M.; Harris, J.; Gullans, S.; Rooke, J. Nat Methods 2006, 3, 41-46.
(75) Li, J.; Schachermeyer, S.; Wang, Y.; Yin, Y.; Zhong, W. Anal Chem 2009, 81, 9723-9729.
(76) Fang, S.; Lee, H. J.; Wark, A. W.; Corn, R. M. J Am Chem Soc 2006, 128, 14044-14046.
(77) Allawi, H. T.; Dahlberg, J. E.; Olson, S.; Lund, E.; Olson, M.; Ma, W. P.; Takova, T.; Neri, B. P.; Lyamichev, V. I. RNA 2004, 10, 1153-1161.
(78) Prescher, J. A.; Bertozzi, C. R. Nat Chem Biol 2005, 1, 13-21.
(79) Rusinov, V.; Baev, V.; Minkov, I. N.; Tabler, M. Nucleic Acids Res 2005, 33, W696-700.
(80) Adai, A.; Johnson, C.; Mlotshwa, S.; Archer-Evans, S.; Manocha, V.; Vance, V.; Sundaresan, V. Genome Res 2005, 15, 78-91.

(81) Lai, E. C.; Tomancak, P.; Williams, R. W.; Rubin, G. M. Genome Biol 2003, 4, R42.
(82) Zaytseva, N. V.; Goral, V. N.; Montagna, R. A.; Baeumner, A. J. Lab Chip 2005, 5, 805-811.
(83) Curry, E.; Ellis, S. E.; Pratt, S. L. Mol Reprod Dev 2009, 76, 218-219.
(84) Ruby, J. G.; Jan, C. H.; Bartel, D. P. Nature 2007, 448, 83-86.
(85) Orom, U. A.; Kauppinen, S.; Lund, A. H. Gene 2006, 372, 137-141.
(86) Matthews, J. C.; Hori, K.; Cormier, M. J. Biochemistry 1977, 16, 85-91.
(87) Kricka, L. J. Clin Chem 1991, 37, 1472-1481.
(88) Cissell, K. A.; Rahimi, Y.; Shrestha, S.; Hunt, E. A.; Deo, S. K. Anal Chem 2008, 80, 2319-2325.
(89) Cissell, K. A.; Campbell, S.; Deo, S. K. Anal Bioanal Chem 2008, 391, 2577-2581.
(90) Cissell, K. A.; Rahimi, Y.; Shrestha, S.; Deo, S. K. Bioconjug Chem 2009, 20, 15-19.
(91) Hammond, S. M. Nat Methods 2006, 3, 12-13.
(92) Srikantha, T.; Klapach, A.; Lorenz, W. W.; Tsai, L. K.; Laughlin, L. A.; Gorman, J. A.; Soll, D. R. J Bacteriol 1996, 178, 121-129.
(93) Matthews, J. C.; Hori, K.; Cormier, M. J. Biochemistry 1977, 16, 5217-5220.
(94) Hart, R. C.; Matthews, J. C.; Hori, K.; Cormier, M. J. Biochemistry 1979, 18, 2204-2210.
(95) D. J. Squirrell, R. L. Price and M. J. Murphy Analytica Chimica Acta 2002, 457, 109-114
(96) Zhu, S.; Si, M. L.; Wu, H.; Mo, Y. Y. J Biol Chem 2007, 282, 14328-14336.
(97) Si, M. L.; Zhu, S.; Wu, H.; Lu, Z.; Wu, F.; Mo, Y. Y. Oncogene 2007, 26, 2799-2803.
(98) Pan, Q.; Luo, X.; Toloubeydokhti, T.; Chegini, N. Mol Hum Reprod 2007.
(99) Kutay, H.; Bai, S.; Datta, J.; Motiwala, T.; Pogribny, I.; Frankel, W.; Jacob, S. T.; Ghoshal, K. J Cell Biochem 2006, 99, 671-678.
(100) Sambrook, J.; Maniatis, T.; Fritsch, E. F. Molecular cloning : a laboratory manual, 3rd ed.; Cold Spring Harbor Laboratory Press: Cold Spring Harbor, N.Y., 2001.
(101) Osborn, L.; Kunkel, S.; Nabel, G. J. Proc Natl Acad Sci U S A 1989, 86, 2336-2340.
(102) Dignam, J. D.; Lebovitz, R. M.; Roeder, R. G. Nucleic Acids Res 1983, 11, 1475-1489.
(103) Tricoli, J. V.; Jacobson, J. W. Cancer Res 2007, 67, 4553-4555.
(104) Mirasoli, M.; Deo, S. K.; Lewis, J. C.; Roda, A.; Daunert, S. Anal Biochem 2002, 306, 204-211.
(105) Desai, U. A.; Deo, S. K.; Hyland, K. V.; Poon, M.; Daunert, S. Anal Chem 2002, 74, 3892-3898.
(106) Xu, Y.; Piston, D. W.; Johnson, C. H. Proc Natl Acad Sci U S A 1999, 96, 151-156.
(107) Medintz, I. L.; Uyeda, H. T.; Goldman, E. R.; Mattoussi, H. Nat Mater 2005, 4, 435-446.

(108) Michalet, X.; Pinaud, F. F.; Bentolila, L. A.; Tsay, J. M.; Doose, S.; Li, J. J.; Sundaresan, G.; Wu, A. M.; Gambhir, S. S.; Weiss, S. Science 2005, 307, 538-544.
(109) Gill, R.; Zayats, M.; Willner, I. Angew Chem Int Ed Engl 2008, 47, 7602-7625.
(110) So, M. K.; Xu, C.; Loening, A. M.; Gambhir, S. S.; Rao, J. Nat Biotechnol 2006, 24, 339-343.
(111) Xu, X.; Soutto, M.; Xie, Q.; Servick, S.; Subramanian, C.; von Arnim, A. G.; Johnson, C. H. Proc Natl Acad Sci U S A 2007, 104, 10264-10269.
(112) Angers, S.; Salahpour, A.; Joly, E.; Hilairet, S.; Chelsky, D.; Dennis, M.; Bouvier, M. Proc Natl Acad Sci U S A 2000, 97, 3684-3689.
(113) Walls, Z. F.; Gambhir, S. S. Bioconjug Chem 2008, 19, 178-184.
(114) James, J. R.; Oliveira, M. I.; Carmo, A. M.; Iaboni, A.; Davis, S. J. Nat Methods 2006, 3, 1001-1006.
(115) Jares-Erijman, E. A.; Jovin, T. M. Nat Biotechnol 2003, 21, 1387-1395.
(116) Paulmurugan, R.; Gambhir, S. S. Anal Chem 2005, 77, 1295-1302.
(117) Paulmurugan, R.; Gambhir, S. S. Anal Chem 2007, 79, 2346-2353.
(118) Paulmurugan, R.; Umezawa, Y.; Gambhir, S. S. Proc Natl Acad Sci U S A 2002, 99, 15608-15613.
(119) Ooi, A. T.; Stains, C. I.; Ghosh, I.; Segal, D. J. Biochemistry 2006, 45, 3620-3625.
(120) Magliery, T. J.; Wilson, C. G.; Pan, W.; Mishler, D.; Ghosh, I.; Hamilton, A. D.; Regan, L. J Am Chem Soc 2005, 127, 146-157.
(121) Stains, C. I.; Porter, J. R.; Ooi, A. T.; Segal, D. J.; Ghosh, I. J Am Chem Soc 2005, 127, 10782-10783.
(122) Kim, S. B.; Otani, Y.; Umezawa, Y.; Tao, H. Anal Chem 2007, 79, 4820-4826.
(123) Deo, S. K. Anal Bioanal Chem 2004, 379, 383-390.
(124) Ozawa, T.; Kaihara, A.; Sato, M.; Tachihara, K.; Umezawa, Y. Anal Chem 2001, 73, 2516-2521.
(125) Gangopadhyay, J. P.; Jiang, S. Q.; Paulus, H. Anal Chem 2003, 75, 2456-2462.
(126) Galarneau, A.; Primeau, M.; Trudeau, L. E.; Michnick, S. W. Nat Biotechnol 2002, 20, 619-622.
(127) Johnsson, N.; Varshavsky, A. Proc Natl Acad Sci U S A 1994, 91, 10340-10344.
(128) Rossi, F.; Charlton, C. A.; Blau, H. M. Proc Natl Acad Sci U S A 1997, 94, 8405-8410.
(129) Pelletier, J. N.; Campbell-Valois, F. X.; Michnick, S. W. Proc Natl Acad Sci U S A 1998, 95, 12141-12146.
(130) MacDonald, M. L.; Lamerdin, J.; Owens, S.; Keon, B. H.; Bilter, G. K.; Shang, Z.; Huang, Z.; Yu, H.; Dias, J.; Minami, T.; Michnick, S. W.; Westwick, J. K. Nat Chem Biol 2006, 2, 329-337.
(131) Hu, C. D.; Kerppola, T. K. Nat Biotechnol 2003, 21, 539-545.
(132) Jach, G.; Pesch, M.; Richter, K.; Frings, S.; Uhrig, J. F. Nat Methods 2006, 3, 597-600.
(133) Remy, I.; Michnick, S. W. Nat Methods 2006, 3, 977-979.

(134) Demidov, V. V.; Dokholyan, N. V.; Witte-Hoffmann, C.; Chalasani, P.; Yiu, H. W.; Ding, F.; Yu, Y.; Cantor, C. R.; Broude, N. E. Proc Natl Acad Sci U S A 2006, 103, 2052-2056.
(135) Whitehead, T. P.; Kricka, L. J.; Carter, T. J.; Thorpe, G. H. Clin Chem 1979, 25, 1531-1546.
(136) Thore, A. Ann Clin Biochem 1979, 16, 359-369.
(137) Shrestha, S.; Paeng, I. R.; Deo, S. K.; Daunert, S. Bioconjug Chem 2002, 13, 269-275.
(138) Contag, C. H.; Bachmann, M. H. Annu Rev Biomed Eng 2002, 4, 235-260.
(139) Porter, J. R.; Stains, C. I.; Jester, B. W.; Ghosh, I. J Am Chem Soc 2008, 130, 6488-6497.
(140) Shekhawat, S. S.; Porter, J. R.; Sriprasad, A.; Ghosh, I. J Am Chem Soc 2009, 131, 15284-15290.
(141) Paulmurugan, R.; Gambhir, S. S. Anal Chem 2003, 75, 1584-1589.
(142) Loening, A. M.; Fenn, T. D.; Gambhir, S. S. J Mol Biol 2007, 374, 1017-1028.
(143) Zhang, L.; Foxman, B.; Gilsdorf, J. R.; Marrs, C. F. Biotechniques 2005, 39, 640, 642, 644.
(144) Jo, J. J.; Kim, M. J.; Son, J. T.; Kim, J.; Shin, J. S. Biochem Biophys Res Commun 2009, 385, 88-93.
(145) Wang, X.; Lou, X.; Wang, Y.; Guo, Q.; Fang, Z.; Zhong, X.; Mao, H.; Jin, Q.; Wu, L.; Zhao, H.; Zhao, J. Biosens Bioelectron 2010, 25, 1934-1940.
(146) Huber, D. E.; Markel, M. L.; Pennathur, S.; Patel, K. D. Lab Chip 2009, 9, 2933-2940.
(147) Resch-Genger, U.; Grabolle, M.; Cavaliere-Jaricot, S.; Nitschke, R.; Nann, T. Nat Methods 2008, 5, 763-775.
(148) Medintz, I. L.; Mattoussi, H.; Clapp, A. R. Int J Nanomedicine 2008, 3, 151-167.
(149) Hohng, S.; Ha, T. Chemphyschem 2005, 6, 956-960.
(150) Sapsford, K. E.; Berti, L.; Medintz, I. L. Angew Chem Int Ed Engl 2006, 45, 4562-4589.
(151) Roldo, C.; Missiaglia, E.; Hagan, J. P.; Falconi, M.; Capelli, P.; Bersani, S.; Calin, G. A.; Volinia, S.; Liu, C. G.; Scarpa, A.; Croce, C. M. J Clin Oncol 2006, 24, 4677-4684.
(152) Gironella, M.; Seux, M.; Xie, M. J.; Cano, C.; Tomasini, R.; Gommeaux, J.; Garcia, S.; Nowak, J.; Yeung, M. L.; Jeang, K. T.; Chaix, A.; Fazli, L.; Motoo, Y.; Wang, Q.; Rocchi, P.; Russo, A.; Gleave, M.; Dagorn, J. C.; Iovanna, J. L.; Carrier, A.; Pebusque, M. J.; Dusetti, N. J. Proc Natl Acad Sci U S A 2007, 104, 16170-16175.
(153) Tan, W.; Wang, K.; Drake, T. J. Curr Opin Chem Biol 2004, 8, 547-553.
(154) Gidwani, V.; Riahi, R.; Zhang, D. D.; Wong, P. K. Analyst 2009, 134, 1675-1681.
(155) Meserve, D.; Wang, Z. H.; Zhang, D. D.; Wong, P. K. Analyst 2008, 133, 1013-1019.
(156) Derfus, A. M.; Chan, W. C. W.; Bhatia, S. N. Nano Letters 2004, 4, 11-18.
(157) Kirchner, C.; Liedl, T.; Kudera, S.; Pellegrino, T.; Munoz Javier, A.; Gaub, H. E.; Stolzle, S.; Fertig, N.; Parak, W. J. Nano Lett 2005, 5, 331-338.

(158) Breslauer, K. J.; Frank, R.; Blocker, H.; Marky, L. A. Proc Natl Acad Sci U S A 1986, 83, 3746-3750.
(159) Mitchell, P. S.; Parkin, R. K.; Kroh, E. M.; Fritz, B. R.; Wyman, S. K.; Pogosova-Agadjanyan, E. L.; Peterson, A.; Noteboom, J.; O'Briant, K. C.; Allen, A.; Lin, D. W.; Urban, N.; Drescher, C. W.; Knudsen, B. S.; Stirewalt, D. L.; Gentleman, R.; Vessella, R. L.; Nelson, P. S.; Martin, D. B.; Tewari, M. Proc Natl Acad Sci U S A 2008, 105, 10513-10518.
(160) Loening, A. M.; Fenn, T. D.; Wu, A. M.; Gambhir, S. S. Protein Eng Des Sel 2006, 19, 391-400.

APPENDICES

Appendix A

The gene sequence of Rluc cloned into pRSetB is shown in this section. In order to clone the Rluc gene into pRSetB, BamHI and EcoRI restriction sites were employed based on the pRSetB plasmid sequence. The Rluc gene was amplified by PCR via primers that added a BamHI site through the forward primer, and an EcoRI site through the reverse primer (See chapter 2, section 2 for details). The N-terminal histidine tag is highlighted in green, the BamHI site in yellow, the added base to correct for the reading frame in red, and the Rluc gene in grey. A T-7 promoter-specific forward primer was employed for the sequencing, which was performed by an Applied Biosystems 3100 Genetic Analyzer. The EcoRI site cannot be seen from the sequence below due to limitations in detectable sequence length. Sequencing employing a T-7 reverse priming site reveals the presence of the EcoRI site (data not shown).

5'ANGGTTTCCTCTGAATATTTTGTTTACTTTAAGAAGGAGATATACATATGCG
GGGTTCTCATCATCATCATCATCATGGTATGGCTAGCATGACTGGTGGACAGC
AAATGGGTCGGGATCTGTACGACGATGACGATAAGGATCCGATGGCTTCCAA
GGTGTACGACCCCGAGCAACGCAAACGCATGATCACTGGGCCTCAGTGGTGG
GCTCGCTGCAAGCAAATGAACGTGCTGGACTCCTTCATCAACTACTATGATTC
CGAGAAGCACGCCGAGAACGCCGTGATTTTTCTGCATGGTAACGCTGCCTCC
AGCTACCTGTGGAGGCACGTCGTGCCTCACATCGAGCCCGTGGCTAGATGCA
TCATCCCTGATCTGATCGGAATGGGTAAGTCCGGCAAGAGCGGGAATGGCTC
ATATCGCCTCCTGGATCACTACAAGTACCTCACCGCTTGGTTCGAGCTGCTGA
ACCTTCCAAAGAAAATCANGTNNGTGGGCCACNACTGGGGGGCTTGTCTGGC
CTTTCACTACTCCTACNAGCACCAAGACAAGATCCAGGCCATCGTCCATGCT
GAGAGTGTCGTGGACNTGATCGAGTCCTGGGACGAGTGGCCTGACATCNAGG
AGGATATCGCCCTGATCAANAGCGAAAAGGGCNAGAAAATGGTGCTTGAGA

Appendix B

The gene sequence of Rluc + 6x histidine tag are found in this section. The native phRL-CMV plasmid containing the Rluc gene does not have a histidine tag for purification purposes; therefore, site-directed mutagenesis was performed in order to introduce the histidine tag at the N-terminus of the Rluc protein, as well as add an EcoRI site for genetic engineering purposes. The histidine tag is highlighted in red, the EcoRI site in green, and the Rluc sequence in grey. There are only four codons for the histidine tag present, which is due to the fact that the histidine tag sequence is too close in proximity to the primer annealing site. An Rluc-specific forward primer was employed for the sequencing, which was performed by an Applied Biosystems 3100 Genetic Analyzer.

5’TGCTNCCATCACCATCACGAATTCGCTTCCAGGTGTACGACCCCGAGCAAC
GCAAACGCATGATCACTGGGCCTCAGTGGTGGGCTCGCTGCAAGCAAATGAA
CGTGCTGGACTCCTTCATCAACTACTATGATTCCGAGAAGCACGCCGAGAAC
GCCGTGATTTTTCTGCATGGTAACGCTGCCTCCAGCTACCTGTGGAGGCACGT
CGTGCCTCACATCGAGCCCGTGGCTAGATGCATCATCCCTGATCTGATCGGA
ATGGGTAAGTCCGGCAAGAGCGGGAATGGCTCATATCGCCTCCTGGATCACT
ACAAGTACCTCACCGCTTGGTTCGAGCTGCTGAACCTTCCAAAGAAAATCAT
CTTTGTGGGCCACGACTGGGGGGCTTGTCTGGCCTTTCACTACTCCTACGAGC
ACCAAGACAAGATCAAGGCCATCGTCCATGCTGAGAGTGTCGTGGACGTGAT
CGAGTCCTGGGACGAGTGGCCTGACATCGAGGAGGATATCGCCCTGATCAAG
AGCGAAGAGGGCGAGAAAATGGTGCTTGAGAATAACTTCTTCGTCGAGACCA
TGCTCCCAAGCAAGATCATGCGGAAACTGGAGCCTGAGGAGTTCGCTGCCTA
CCTGGAGCCATTCAAGGAGAAGGGCGAGGTTAGACGGCCTACCCTCTCCTGG
CCTCGCGAGATCCCTCTCGTTAAGGGAGGCAAGCCCGACGTCGTCCAGATTG
TCCGCAACTACAACGCCTACCTTCGGGCCAGCGACGATCTGCCTAAGA-3’

Appendix C

The Rluc His Tag template plasmid sequence for the engineering of the Rluc split plasmids has been reported in Appendix B. The following information in this section relates to the genetic engineering of the split *Renilla* luciferase fragments. The gene sequence of the N-terminal fragment, identified as Big Lux, is seen in the following sequence data, where the highlighted red sequence represents the first four residues of the 6x histidine tag (The first two histidine tag codons are present; however, the sequencer was not able to detect the adenine bases due to close proximity to the annealing primer), the green highlighted sequence represents the EcoRI restriction enzyme site, the blue highlighted sequence represents the N-terminal Rluc, and the gold highlighted sequence represents the flexible linker, cysteine residues, and stop codons. A T7 promoter-specific forward primer was employed.

5’CNTGCTCCCATCACCATCACGAATTCGCTTCCAGGTGTACGACCCCGAGCA
ACGCAAACGCATGATCACTGGGCCTCAGTGGTGGGCTCGCTGCAAGCAAATG
AACGTGCTGGACTCCTTCATCAACTACTATGATTCCGAGAAGCACGCCGAGA
ACGCCGTGATTTTTCTGCATGGTAACGCTGCCTCCAGCTACCTGTGGAGGCAC
GTCGTGCCTCACATCGAGCCCGTGGCTAGATGCATCATCCCTGATCTGATCGG
AATGGGTAAGTCCGGCAAGAGCGGGAATGGCTCATATCGCCTCCTGGATCAC
TACAAGTACCTCACCGCTTGGTTCGAGCTGCTGAACCTTCCAAAGAAAATCAT
CTTTGTGGGCCACGACTGGGGGGCTTGTCTGGCCTTTCACTACTCCTACGAGC
ACCAAGACAAGATCAAGGCCATCGTCCATGCTGAGAGTGTCGTGGACGTGAT
CGAGTCCTGGGACGAGTGGCCTGACATCGAGGAGGATATCGCCCTGATCAAG
AGCGAAGAGGGCGAGAAAATGGTGCTTGAGAATAACTTCTTCGTCGAGACCA
TGCTCCCAAGCAAGATCATGCGGAAACTGGAGCCTGAGGAGTTCGCTGCCTA
CCTGGAGCCATTCAAGGAGAAGGGCGAGGTTAGACGGCCTACCCTCTCCTGG
CCTCGCGAGATCCCTCTCGTTAAGGGAGGCAGTGGAGGTGGAGGTAGTTGTT
AGTAAAAGCCCGACGTCGTCCAGATTGTCCGCAACTACANCGCCTACCTTCG
GGCCAGCGACGATCTGCCTAAGATGTTCATCGAGTCCGACCCTGGGTTCTTTT
CCAACGCTATTGTCGAGGGAGCTAANAAGTTCCNTAACACCGAGTTCGTGAA
GGTGAAGGCCTCCCTTCACCAGGAGGACCCTCCANATGAAATGGGTAAGTAC
ATCAANAGCTTCNTGGANCGCGTGCTGAAAACGANCAGTATTCTAAGCGNCC
CT-3’

The C-terminal fragment sequencing result after digestion with EcoRI to remove the N-terminal gene sequence, followed by ligation, is seen in the following sequencing data. The red highlighted sequence represents the histidine tag. The green highlighted sequence represents the EcoRI site. The gold highlighted sequence represents the flexible linker and cysteine residue. The grey highlighted sequence represents the C-terminal Rluc fragment (Small Lux). The stop codon is highlighted in purple. The remaining sequence represents the phRL-CMV non-coding DNA. The same T7 promotor-specific forward primer was used as with the Big Lux.

5’CNTGCTCCCATCACCATCACGAATTCTGTAGTGGAGGTGGAGGTAGTAAGC
CCGACGTCGTCCAGATTGTCCGCAACTACAACGCCTACCTTCGGGCCAGCGA
CGATCTGCCTAAGATGTTCATCGAGTCCGACCCTGGGTTCTTTTCCAACGCTA
TTGTCGAGGGAGCTAAGAAGTTCCCTAACACCGAGTTCGTGAAGGTGAAGGG
CCTCCACTTCAGCCAGGAGGACGCTCCAGATGAAATGGGTAAGTACATCAAG
AGCTTCGTGGAGCGCGTGCTGAAGAACGAGCAGTAATTCTAGAGCGGCCGCT
TCGAGCAGACATGATAAGATACATTGATGAGTTTGGACAAACCACAACTAGA
ATGCAGTGAAAAAAATGCTTTATTTGTGAAATTTGTGATGCTATTGCTTTATT
TGTAACCATTATAAGCTGCAATAAACAAGTTAACAACAACAATTGCATTCAT
TTTATGTTTCAGGTTCAGGGGGAGGTGTGGGAGGTTTTTTAAAGCAAGTAAA
ACCTCTACAAATGTGGTAAAATCGATAAGGATCCAGGTGGCACTTTTCGGGG
AAATGTGCGCGGAACCCCTATTTGTTTATTTTTCTAAATACATTCAAATATGT
ATCCGCTCATGAGACAATAACCCTGATAAATGCTTCAATAATATTGAAAAAG
GAAGAGTATGAGTATTCAACATTTCCGTGTCGCCCTTATTCCCTTTTTTGCGG
CATTTTGCCTTCCTGTTTTTGCTCACCCAGAAACGCTGGTGAAAGTAAAA-3’

The purified Rluc split fragments are shown in the 12% SDS-PAGE gel photo (Figure A.1). Lanes 1 and 4 contain EZ-run protein marker. Lanes 2 and 3 contain purified N-terminal fragment and C-terminal fragment, respectively. The predicted molecular weight of the N-terminal fragment is 31 kDa, while the C-terminal fragment’s predicted molecular weight is 15 kDa.

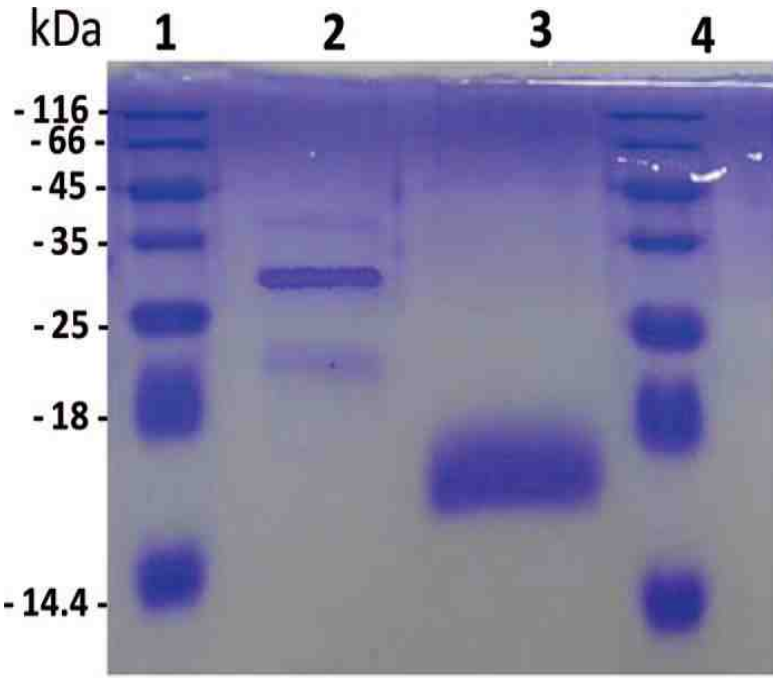

Figure A.1 SDS-PAGE gel picture of split Rluc fragment purification. Lane 1-EZ-run protein marker. Lane 2-N-terminal Rluc. Lane 3-C-terminal Rluc. Lane 4-EZ-run protein marker. Reprinted with permission from Reference 90. Copyright 2009 American Chemical Society.

VITA

VITA

Kyle A. Cissell

Industry Experience
January 2010-present: UltraPid Nanodiagnostics; Research Scientist
- Developing point-of-care technologies for the detection of viral infections
- Leading a team of three scientist in the development of new products
- Expanding intellectual property through filing of provisional patents

Education
- 2010: PhD, Analytical Chemistry, Purdue University (Indianapolis) Thesis title: "Luminescence-Based MicroRNA Detection Methods"
  Advisor: Professor Sapna K. Deo
- 2005: BA, Chemistry, DePauw University, Greencastle IN

Academic Research Experience
2005-2010:Purdue University, Indianapolis; Professor Sapna K. Deo, advisor
- Broadened the scope of microRNA detection to include bioluminescent technology
- Improved microRNA detection limits to the femtomole level utilizing bioluminescence techniques
- Developed bioluminescent protein complementation assay for nucleic acid detection
- Extensive bioconjugation experience employing various crosslinkers
- Developed BRET assays to detect bacterial signature sequences
- Developed fluorescence-based assays for dual microRNA target detection
- Developed a biosensing system based on binding-induced conformational changes of disordered peptides

2004:DePauw University, Greencastle IN; Professor David Harvey, advisor
- Optimized metal extraction procedure for soil analysis to detect trace metals utilizing atomic absorption spectroscopy

Awards and Honors
- National Institutes of Health Graduate Research Festival Invitee (2009)
- Pfizer Graduate Travel Award Winner, ACS Analytical Chemistry Division (2007)
- IUPUI Department of Chemistry and Chemical Biology Poster Presentation 1st Place (2007)

- Sigma Xi Research Award Competition Prize Winner (2006)
- Purdue School of Science Research Fellowship (8/2005 to 8/2006)
- Percy L. Julian Science Scholar, DePauw University (2002-2005)

Publications

1. Cissell, Kyle A., Yasmeen Rahimi, Suresh Shrestha, Sapna K. Deo, "Reassembly of a Bioluminescent Protein *Renilla* luciferase Directed Through DNA Hybridization", Bioconjugate Chemistry Vol. 20 (2009) 15-19
2. Cissell, Kyle A., Sapna K. Deo, "Trends in microRNA Detection", Analytical and Bioanalytical Chemistry Vol. 394 (2009) 1109-1116
3. Cissell, Kyle A., Eric A. Hunt, Sapna K. Deo, "Resonance Energy Transfer Methods of RNA Detection", Analytical and Bioanalytical Chemistry Vol. 393 (2008) 125-135
4. Cissell, Kyle A., Sean Campbell, Sapna K. Deo, "Rapid, Single-Step Nucleic Acid Detection", Analytical and Bioanalytical Chemistry, Vol. 391 (2008) 2577-2581
5. Cissell, Kyle A., Suresh Shrestha, Jennifer Purdie, Derrick Kroodsma, Sapna K. Deo, "Molecular Biosensing System Based on Intrinsically Disordered Proteins", Analytical and Bioanalytical Chemistry,Vol. 391 (2008) 1721-1729
6. Cissell, Kyle A., Yasmeen Rahimi, Suresh Shrestha, Eric A. Hunt, Sapna K. Deo, "Bioluminescence-Based Detection of MicroRNA, miR21 in Breast Cancer Cells", Analytical Chemistry, Vol. 80 (2008) 2319-2325 (Featured in Research Focus Section)
7. Cissell, Kyle A., Suresh Shrestha, Sapna K. Deo, "microRNA Detection: Challenges for the Analytical Chemist", Analytical Chemistry, Vol. 79 (2007) 4754-4761 (Featured on the cover page)

Book Chapter

Deo, Sapna K., Kyle A. Cissell, Ann Goulding, Yasmeen Rahimi, Suresh Shrestha, Biochemistry, structure, and engineering of red fluorescent proteins, Chapter 6, in: "Luciferases and Fluorescent Proteins Technology: Principles and Advances in Biotechnology and Bioimaging," V. R. Viviani and Y. Ohmiya, Eds., Research Signpost Press, (2007)

Presentations

1. Cissell, Kyle A., David Broyles, and Sapna K. Deo, "Fluorescence-Based Detection of MicroRNAs Expressed in Pancreatic Cancer", 62nd Pittsburgh Conference February 28-March 4, 2010, Orlando FL
2. Cissell, Kyle A. and Sapna K. Deo, "Bioluminescence Resonance Energy Transfer-Based Detection of E. coli 16srRNA", 61st Pittsburgh Conference March 10-13, 2009, Chicago IL
3. Cissell, Kyle A. and Sapna K. Deo, "Detection of Nucleic Acids Based on Bioluminescence Resonance Energy Transfer between Renilla Luciferase and Quantum Dots", 60th Pittsburgh Conference March 3-6, 2008, New Orleans LA

4. Cissell, Kyle A., Yasmeen Rahimi, and Sapna K. Deo, "MicroRNA Detection Based on Protein Reassembly", 234th ACS National Meeting, September 9-14, 2007, Boston MA
5. Cissell, Kyle A., Suresh Shrestha, Derrick Kroodsma, and Sapna K. Deo, "Design of a Biosensing System Based on an Intrinsically Unstructured Protein as a Biological Recognition Element", 59th Pittsburgh Conference on Analytical Chemistry and Applied Spectrocsopy February 25-March 2, 2007, Chicago IL